WELDING Journal

February 2003

AWS

Plasma Arc Cutting Update

Avoid Weld Distortion in Aluminum

Welding Metallurgy: Know the Basics

PUBLISHED BY THE AMERICAN WELDING SOCIETY TO ADVANCE THE SCIENCE, TECHNOLOGY AND APPLICATION OF WELDING

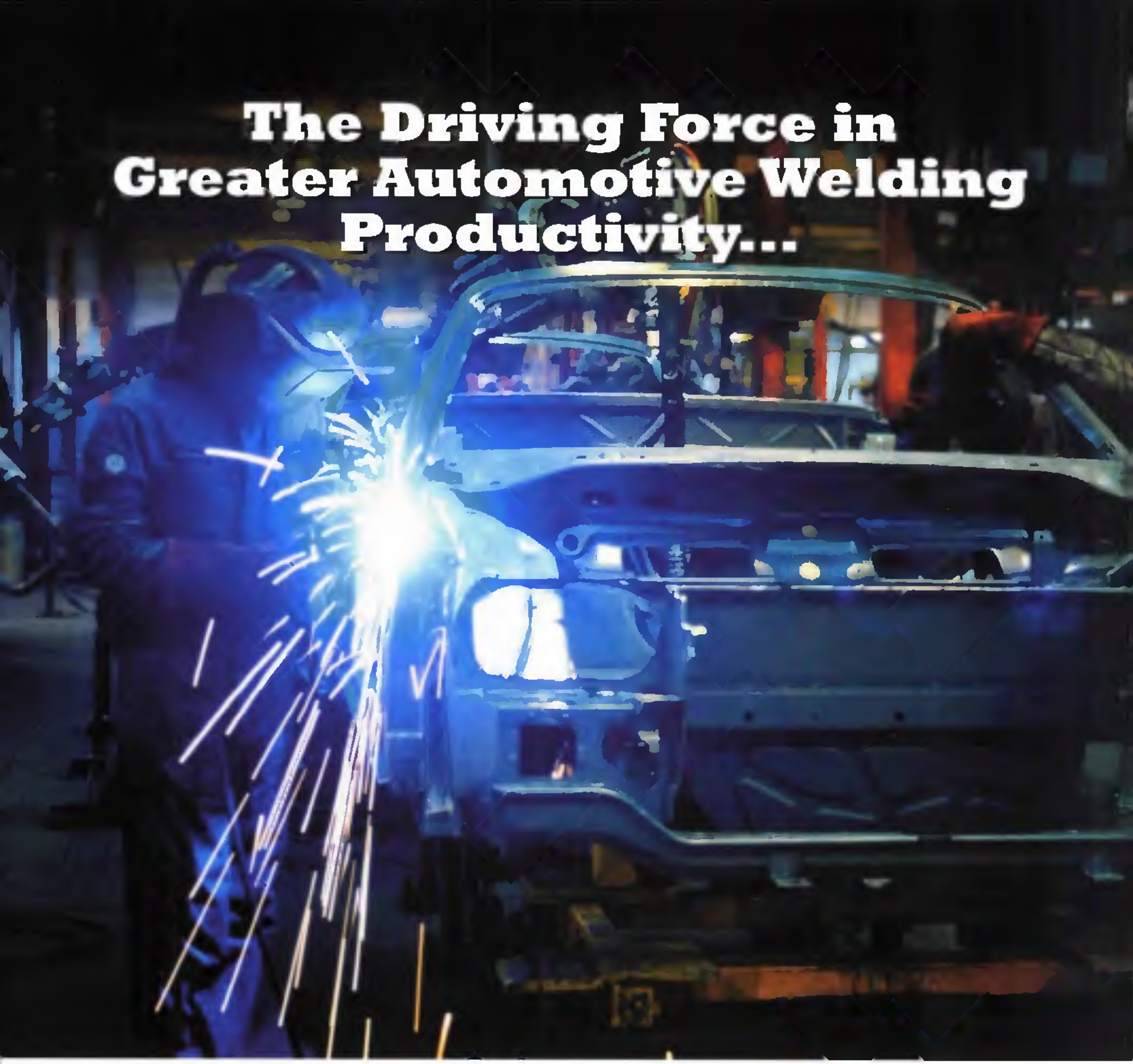
The Driving Force in
Greater Automotive Welding
Productivity...

GOOD NEWS FOR THE POWER HUNGRY

The new **Invertec V350-PRO** power source from Lincoln Electric pours out the highest welding output in its class for superior MIG, TIG, flux-cored, or stick welding performance. See for yourself at your local Lincoln distributor.

- Superior MIG welding performance on steel, stainless steel, or aluminum.
- Touch Start™ TIG for outstanding arc starts without high frequency.
- Variable hot start and arc force control for maximum stick welding performance.
- Inverter-based versatility handles most DC welding applications from 5 to 425 amps.
- Simple control panel design makes set-up a breeze.
- Select from the energy-efficient Factory Model, the portable Construction Model, or the dynamic Pulsing Model.

You can depend on Lincoln Electric:

- ISO 9001.
- 3-year warranty and the unmatched support of Lincoln Electric.

Invertec V350-PRO Multi-process Power Source

The Lincoln Electric Company
Cleveland, Ohio U.S.A.
216-481-8100
www.lincolnelectric.com

LINCOLN ELECTRIC
THE WELDING EXPERTS

Circle No. 29 on Reader Info-Card

AR03-11

CONTENTS

February 2003 • Volume 82 • Number 2

AWS Web site http://www.aws.org

Features

24 Plasma Arc Cutting Machine Selection and Techniques
Modern plasma arc cutting machines come in small packages, but they can tackle the big jobs
B. Schmidt

28 Thermal Distortion in Aluminum Welded Structures
Good welding techniques are the key to minimizing thermal distortion with aluminum
T. Anderson

31 The ABCs of Steel Metallurgy
A basic knowledge of metallurgy goes a long way in understanding the effect welding has on carbon steel
D. McGowan

Welding Research Supplement

25-S The Mechanism of Stress-Relief Cracking in a Ferritic Alloy Steel
The mechanism of stress-relief cracking is investigated through stress relaxation testing and microstructural characterization
J. G. Nawrocki et al.

36-S Influence of Reflected Arc Light on Vision Sensors for Automatic GTAW Systems
Arc sensors have reliability problems because of light reflectance, but a model developed to predict arc noise offers greater design flexibility
J.-Y. Yu et al.

43-S Improved Ferrite Number Prediction Model that Accounts for Cooling Rate Effects — Part 2: Model Results
A ferrite prediction model based on neural networks is valid for both austenitic stainless steel and duplex stain less steel under conditions of conventional or high cooling rates
J. M. Vitek et al.

Departments

Washington Watchword 4
Press-Time News 6
Editorial 8
News of the Industry 10
Technology 12
Aluminum Q&A 14
Brazing Q&A 16
New Products 18
Coming Events 38
Society News 41
Guide to AWS Services 58
Navy Joining Center 60
New Literature 62
Personnel 64
Red Hot 66
Classifieds 69
Advertiser Index 71

Welding Journal (ISSN 0043-2296) is published monthly by the American Welding Society for $90.00 per year in the United States and possessions, $130 per year in foreign countries: $6.00 per single issue for AWS members and $8.00 per single issue for nonmembers. American Welding Society is located at 550 NW LeJeune Rd., Miami, FL 33126-5671; telephone (305) 443-9353. Periodicals postage paid in Miami, Fla., and additional mailing offices. **POSTMASTER:** Send address changes to Welding Journal, 550 NW LeJeune Rd., Miami, FL 33126-5671.

BY HUGH K. WEBSTER
AWS WASHINGTON GOVERNMENT AFFAIRS OFFICE

OSHA Proposing Rule on Hexavalent Chromium

The Occupational Safety and Health Administration (OSHA) is moving forward with a proposed rulemaking on occupational exposure to hexavalent chromium.

OSHA published a request for information in the *Federal Register* last year, asking for public comments relating to hexavalent chromium, most commonly used as a structural and anticorrosive element in the production of stainless steel, iron, and steel and in electroplating, welding, and painting. OSHA's request for information included health effects; risk assessment; methods of analyzing exposure levels; investigations into occupational exposures, control measures, and technological and economic impact feasibility; use of personal protective equipment and respirators; current employee training and medical screening programs; and environmental and small business impacts.

OSHA's current general industry standard sets a permissible exposure limit for hexavalent chromium compounds at 100 $\mu g/m^3$ as a ceiling concentration; the standard for construction is 100 $\mu g/m^3$ as an 8-hour time-weighted average.

In a related development, the U.S. Court of Appeals for the Third Circuit issued an order mandating OSHA prepare a hexavalent chromium standard. The plaintiff in that lawsuit, Public Citizen, the consumer advocacy organization founded by Ralph Nader, had asked the court to require OSHA to issue a proposed standard by the end of March 2003 and a final standard 12 months after that. OSHA argued that such a timetable is unrealistic. The court ordered OSHA and Public Citizen to mediate the issue, and if the mediation does not produce an agreement on a schedule, the court will establish one.

Standard Proposed on Shipyard Fire Protection

OSHA has issued a proposed standard on fire protection in shipyards. The proposal closely follows the recommendation of a Negotiated Rulemaking Advisory Committee with representatives from industry, trade associations, labor organizations, the International Association of Fire Fighters, the National Fire Protection Association, and the National Institute of Occupational Safety and Health. Covering an estimated 98,000 shipyard workers at more than 700 establishments involved in shipbuilding, ship conversion, ship repairing, or shipbreaking, the standard would also provide safety measures for workers in fire brigades and shipyard fire departments. "The basic tasks of shipyard workers — welding, grinding, or cutting metal, often in confined spaces — expose them to the risk of fire from many combustible sources," said OSHA administrator John Henshaw.

OSHA's proposal addresses fire safety plans, training, multi-employer work sites, hot work precautions, fire watches, fire response, employee evacuation, medical requirements for shipyard fire response, hazards of fixed extinguishing systems aboard vessels, shoreside fire protection systems, and training. The proposal also includes a model fire safety plan.

E-Government Bill Becomes Law

President George W. Bush signed legislation at the end of 2002 enacting the Electronic Government Act, which is designed to improve access to government information and services. Among other things, this law is designed to establish an office of electronic government and an on-line directory of federal Web sites. It will also require federal courts to post opinions on-line and authorizes $345 million over four years for interagency "e-government" projects. The law contains a variety of other provisions that require agencies to establish on-line rulemaking, encourage compatibility of electronic signatures, and provide strong privacy protections.

On-Line Rulemaking Portal to Be Established

The Office of Management and Budget has created a Web site, *www.regulations.gov*, designed to allow any person to review and submit comments with respect to any proposed federal regulation. The goal is to make the distribution of proposed regulations much more widespread, to encourage public comments, and to make the public comment process simpler and easier. The federal rulemaking process has often been viewed as the exclusive province of government bureaucrats and Washington insiders. Whether or not this view is entirely accurate, a goal of this new Web site is to change both the perception and the reality.

Supreme Court Considers Constitutionality of Punitive Damages

In one of the most closely watched cases of its current term, the U.S. Supreme Court is considering the constitutional restrictions on punitive damages awards. The case, *State Farm Mutual Automobile Insurance Company v. Campbell*, involves a punitive damages award that was 145 times greater than the compensatory award. State Farm is arguing such an award effectively deprived the company of due process of law and, therefore, is unconstitutional. The U.S. Supreme Court has addressed constitutional guidelines for punitive damages in seven prior cases over the past 15 years. But while the court has stated the Constitution does impose limits on punitive damages under certain circumstances, the court has yet to establish any "bright line" tests. A decision from the court is expected later this year.

White House Receives Comments on Proposed Regulatory Changes

For the second year in a row, the White House has solicited comments from the general public regarding regulations that should be modified or changed. More than 1700 companies, associations, consumer advocacy groups, labor unions, and environmental organizations submitted suggestions. This process is perceived as a method for interested persons to make their views known directly to the White House and particularly to the Office of Management and Budget (OMB), rather than to the specific agencies that traditionally are reluctant to modify their own regulations in response to requests from the public. While OMB itself does not issue regulations, it does pass the suggestions along to the relevant agencies, often with a strong recommendation. In fact, last year, several of the proposals submitted resulted in specific agency action. This resulted in a sharp increase in the number of comments submitted this year.

Contact the AWS Washington Government Affairs Office at 1747 Pennsylvania Ave. NW, Washington, DC 20006; e-mail hwebster@wc-b.com; *FAX (202) 835-0243.*

Böhler
WELDING

Bohler Stainless Steel Flux-Cored Wires Save You Money...

...in the cost of shielding gas.

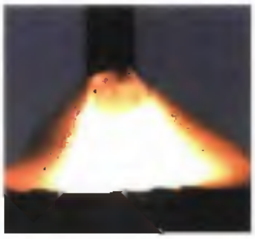

Excellent arc characteristics with 100% CO_2, or 75% Ar + 25% CO_2

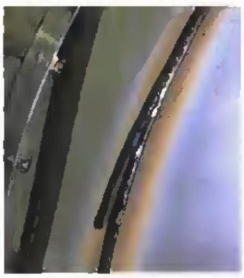

...in the cost of fabrication.

The self peeling slag and smooth weld finish minimize time of post weld clean-up.

...in the cost of rework.

The wide arc provides uniform, deep penetration with good side wall fusion and a smooth weld profile.

To ensure weld metal chemistry, all wires are made utilizing austenitic stainless steel sheaths and agglomerated flux infills. The wire reels are vacuum shrink-packed to preserve product freshness during shipping and storage.

Save Time and Money With BOHLER Flux-Cored Wires For Stainless Steel

BOHLER flux-cored wires are proven for production welding world wide.

Bohler stainless steel flux-cored wires are ideal for both heavy wall components and thin sheet metal fabrication applications. They produce excellent results with either 100% CO_2 or mixed shielding gas. And, for positional welding our T1 wires provide excellent operating characteristics as well as help reduce operator fatigue.

Our flux-cored wires provide a powerful, penetrating arc that deposits a smooth spatter free weld that is cost effective, with excellent overall wire performance, reliably and consistently.

Little post weld cleaning is required and temper coloration is minimized. There are also fewer defects caused by porosity, slag inclusions or lack of fusion.

7 Reasons To Specify Bohler FCAW Stainless Wire

- Reliable and Consistent Weld Quality
- Smooth Welding Characteristics
- Minimum Post Weld Clean Up
- Excellent Operator Appeal
- Significantly Reduced Welding Costs
- Bohler Welding Manufactures to ISO 9001 Quality Standards
- World Wide Leader in Welding Technology for Over 75 Years

Circle No. 15 on Reader Info-Card

Bohler Thyssen Welding USA, Inc.
P.O. Box 721678
Houston, Texas 77272-1678
Phone: (281) 499-1212
Fax: (281) 499-4347
www.btwusa.com • custsvc@btwusa.com

Bohler Thyssen Welding Canada, Ltd.
22 LePage Court
Downsview, ON M3J 1Z9
Phone: (416) 638-3253
Fax: (416) 638-4632
www.btwcan.com • custsvc.cdn@btw

BÖHLER

PRESS TIME NEWS

Alcoa to Cut 8000 Jobs; Sell Some Businesses

Alcoa Inc., the world's largest aluminum producer, recently announced it will cut 8000 jobs at more than 70 locations worldwide, as well as sell some of its noncore businesses as part of a continuing restructuring effort.

"Global manufacturing weakness has persisted longer than we anticipated," said Alain Belda, Alcoa chairman and CEO. "In particular, aerospace, industrial gas turbine, and telecommunication markets remained soft, reinforcing the need to increase the scope of our cost savings and restructuring initiatives."

The company announced a net loss of $223 million, or 27 cents a share, for the fourth quarter of 2002. This compared to a net loss of $142 million, or 17 cents a share, for the same period a year ago.

The fourth quarter losses include a special after-tax charge of $95 million to restructure operations of businesses serving the aerospace, automotive, and industrial gas turbine markets and in the U.S. smelting system. It includes operations that have experienced negligible growth, particularly in Europe and South America. Businesses to be sold include specialty chemicals, specialty packaging equipment, and agricultural products. While the restructuring actions will take place in 2003, the majority of the economic benefits will be realized in 2004.

Alcoa began 2002 with 129,000 employees throughout the world. It now has 127,000 employees.

ICA Fluor Daniel to Build Power Plant in Mexico

ICA Fluor Daniel recently signed a contract to construct a 498-MW, combined-cycle power plant in Gomez Palacios, Durango, Mexico. The $250 million plant will provide electricity to the northern industrial zone of Mexico and stabilize the electrical grid in the area.

The contract, which was awarded by Iberdrola Energia, S.A., a subsidiary of Spain's Grupo Iberdrola, is a 30-month, lump-sum, turnkey project that involves engineering, procurement, construction, and start-up services. The project is expected to be completed in April 2005.

"This plant will be a clean, combined-cycle, gas-fired plant designed to have minimal environmental impact," said Jorge Borja, general director of ICA Fluor Daniel. "It will meet the highest atmospheric emissions standards and have low water consumption by means of an air-cooled condenser. Additionally, the plant will conserve fresh water by recycling residential waste water."

ICA Fluor Daniel is the industrial engineering company jointly owned by Fluor Corp. and Empresas ICA Sociedad Controladora. The project is the second power plant Iberdrola has awarded to the company.

Gunderson Rail Services Announces Orders for 200 Cars; Will Add New Workers

Gunderson Rail Services, the repair, refurbishment, and wheel services group of The Greenbriar Companies, Inc., recently received orders for 100 new-generation and 106 modified mechanical refrigeration boxcars. Cryo-Trans, a leasing company that specializes in the development and leasing of state-of-the-art frozen product railcars, placed the $20 million orders.

Shells for the 100 new railcars will be built at Gunderson Inc. in Portland, Oreg., then completed at Gunderson Rail Services' facility in Springfield, Oreg. In addition, 106 existing cryogenic boxcars will be modified to mechanically refrigerated boxcars at Gunderson Rail Services' Tri-Cities, Wash., plant.

As a result of these and other recent orders, the company will hire 100 additional workers at the Portland facility and the other two plants will add 30 employees each.

FANUC Robotics Makes Name Change

FANUC Robotics North America, Inc., Rochester Hills, Mich., recently changed its name to FANUC Robotics America, Inc. According to the company, the new name more accurately reflects what its business focus has been for 20 years — meeting the needs of customers in North and South America.

FANUC Robotics began in 1982 as a joint venture between FANUC Ltd. and General Motors Corp. It became a wholly owned subsidiary of FANUC Ltd., Oshinomura, Japan, in 1992. Today, it provides robotic systems for a wide variety of industries and offers 175 robot model variations.

WELDING Journal

Publisher *Jeff Weber*
Assistant Publisher *Christine Tarafa*

Editorial
Editor/Editorial Director *Andrew Cullison*
Senior Editor *Mary Ruth Johnsen*
Associate Editor *Susan Campbell*
Associate Editor *Ross Hancock*
Peer Review Coordinator *Doreen Kubish*
Contributing Editor *Bob Irving*

Graphics and Production
Creative Director *Jose Lopez*
Production Editor *Zaida Chavez*

Advertising
National Sales Director *Rob Saltzstein*
National Sales Representative *Sheila Tait*
Advertising Sales Promotion Coordinator *Lea Garrigan*
Advertising Production *Frank Wilson*

Subscriptions
Orlando Collado
American Welding Society
550 NW LeJeune Rd., Miami, FL 33126
(800) 443-9353, ext. 290

New Beginnings

As I reflect on my tenure as a member of the AWS Board of Directors during the past nine years, I am more excited today about the future of the American Welding Society than I have ever been. As many of you know, AWS has seen some substantial changes in staff leadership during the last year and a half. I believe those changes have had and will continue to have a positive impact on the future of our Society. Those changes would not have been possible without the strong commitment and diligent oversight of the volunteer leadership that you as members, through your District Directors, elected as officers and directors at large.

Since I had the honor of serving as AWS president during the year those changes began, I would like to take this opportunity to thank the many officers, board members, and Finance Committee members who gave their time and resources during this difficult period. They are the ones who helped shape the new positive direction the American Welding Society is taking. While it took the efforts of the entire Executive Committee and the full board to institute the many changes that will help ensure the Society's success, I would like to personally thank several individuals who fully and thoughtfully supported the process that made those changes possible. Ernest Levert, president; Earl Lipphardt, treasurer; Rusty Franklin, director at large; Tom Mustaleski, vice president; Damian Kotecki, vice president; Dave Nangle, vice chair, Finance Committee; and Bob Pali, Finance Committee member. Without the wise counsel, countless hours, and unswerving support these people gave to the Society, the outcome would not have been as successful and positive as it has been. It is because AWS can attract talented people such as these to serve on our board of directors and Finance Committee that our Society is and will remain one of the premier technical societies in existence anywhere in the world today.

I would also like to thank our dedicated staff who have weathered and accepted the staff leadership changes. Remember, it is the work of the volunteers through our staff personnel that makes all of the benefits and programs offered by AWS possible. It is with warm regards that I offer thanks to Bill Rice. Bill agreed to take time off from his much deserved retirement as president of Airgas to steer the AWS staff as our interim executive director while the National Executive Director Selection Committee found a well-qualified and permanent one. They did an exceptionally good job as they found and hired Ray Shook to fill that position. I believe Ray will do an excellent job as our executive director and wish him all the best in moving AWS forward into the future.

My time as a member of the AWS Board of Directors is fast coming to a close. It is with deep respect and appreciation that I thank the membership for allowing me to serve our Society as a national board member. I hope the Society continues attracting officers, board members, committee members, and professional staff personnel such as those I have mentioned. The continued success of our Society depends on it.

Richard L. Arn
AWS Past President (2001–2002)

Genesis Systems Group Awarded Patent

Genesis Systems Group, Davenport, Iowa, recently was awarded a U.S. patent on its Quick Change Tooling. The design offers a one-step process to release the tool from the positioner, making it ready for changeover. A repeatable, self-alignment system helps reduce unnecessary wear and eliminates the need for precision alignment due to moving, bumping, or initial work cell setup. The design also includes a self-engaging latch to hold the fixture in place for safety.

The Quick Change Tooling design is suited for any industry that has a medium-to-high mix of parts and/or high changeover applications.

MTS Systems to Build Friction Stir Welding System for U.S. Space Program

MTS Systems Corp., Eden Prairie, Minn., was recently awarded several contracts totaling more than $4 million to manufacture a universal friction stir welding system for the National Center for Advanced Manufacturing (NCAM)-Louisiana Partnership, which is located at NASA's Michoud Assembly Facility in New Orleans, La. NCAM is a partnership between NASA, the state of Louisiana, the University of New Orleans, and Lockheed Martin Corp. that focuses on next-generation manufacturing technologies.

One of the initial programs the equipment will be used for is the Complex Curvature Friction Stir Welding Risk Reduction Program for NASA's Next-Generation Launch Technologies Program. Lockheed will use the system to weld full-size test panels representative of a dome section for a reusable cryogenic tank.

"Friction stir welding is a relatively new process that is rapidly maturing, and the MTS technology is advancing the state of the art," said Paula Hartley, manager, Large Metallic Structures, Lockheed Martin. "The universal friction stir welding system will provide an accurate, consistent means for implementing conventional friction stir welding on complex curvature components."

TRUMPF and EOS to Develop a Direct Metal Laser Melting System

The TRUMPF Group and EOS recently signed an agreement to develop a production system for direct metal laser melting, a variation of EOS's direct metal laser sintering process, in which a scanning laser beam completely melts metal powder that is free of binders or fluxing agents to build up three-dimensional objects with the same properties as the original material. The process gives designers the potential to build parts of almost any complexity in a wide range of metal materials.

TRUMPF, headquartered in Ditzingen, Germany, manufactures industrial lasers and laser systems. EOS, headquartered in Munich, is a leader in laser sintering and manufactures systems for rapid prototyping and manufacturing. The two companies have a cross-licensing agreement for direct metal laser melting.

The direct metal laser melting method is based on process developments carried out by the Fraunhofer Institute for Laser Technology, Aachen, Germany, which will continue to be involved in further developments. To date, parts have been produced from tool steel, titanium, and stainless steel. Other materials are being investigated.

First Nine Months of 2002 Sees Rise in North American Robot Orders

North American robot orders rose 11% in the first nine months of 2002, according to statistics from Robotic Industries Association (RIA), the industry's trade group. The biggest gains came in the third quarter, when orders by North American companies jumped 41% in units and 47% in dollars.

Through September, North American customers ordered 7511 robots valued at $596.4 million, an increase of 11% in units and 15% in dollars over the same period in 2001. With sales to customers outside North America added in, North American robot suppliers sold 7766 robots valued at $618.6 million in the first nine months of 2002, a 5% gain in units and 11% increase in dollars.

The biggest gains in 2002, according to RIA Executive Vice President Donald A. Vincent, were in orders for arc welding, dispensing/coating, spot welding, and higher payload material handling and assembly robots. The only major application areas that declined in the first nine months were lower payload assembly and material handling applications, material removal, and inspection, which, as a group, account for only 15% of the robotics market.

Praxair, CONCOA, and Chart Form Alliance

Praxair, Inc., Controls Corporation of American (CONCOA), and Chart Industries, Inc., recently formed an alliance that brings the companies' products together to serve as a single source for laser applications.

In addition to technical expertise and experience, the alliance brings together the following: Praxair's line of LaserStar™ pure gases and gas blends of helium, nitrogen, carbon dioxide, and carbon monoxide; CONCOA's gas control equipment; and Chart's Trifecta™ line of continuous-flow, gas delivery systems for laser assist gases.

"Metal fabricators make a substantial financial commitment when they buy a laser system," said Janet Coffman, vice president of marketing, Praxair Distribution. "To help them maximize their return on investment, Praxair, CONCOA, and Chart's laser specialists will work with our customers to choose the right gas type, supply mode, and gas regulation and distribution equipment for their individual applications."

Multiquip Celebrates 30th Anniversary

This year marks the 30th anniversary of Multiquip, Carson, Calif. The company was founded in 1973 in Long Beach, Calif., by the recently retired Irv Levine. It now has annual sales of more than $200 million and employs more than 500 employees in its offices in the United States, England, Mexico, Canada, and Brazil.

The company built its success by becoming the exclusive U.S. distributor for Mikasa's compaction equipment. In 1985, it formed MQ Power to distribute sound-attenuated portable generators. It acquired Whiteman in 1988, and a variety of other acquisitions followed. It is now a supplier of soil and asphalt compaction equipment; concrete and masonry placing, finishing, and cutting products; portable power generation equipment; dewatering pumps; welding machines; and light towers.

Universal Plasma Arc Torch: New to the Market

The metalworking world has long been confronted with a plasma cutting dilemma. To keep up with changing needs, users have incorporated incompatible plasma cutting system brands and models as they've adapted their metal fabrication shops and manufacturing and maintenance operations to new products, materials, technologies, productivity, and growth goals.

Keeping all the parts and pieces managed can be difficult. For example, a large East Coast manufacturer has more than 100 plasma arc cutting systems consisting of more than ten different models from three manufacturers. The equipment ranges from 40 to 80 A in capacity, with eight different torch models requiring more than 50 different consumable parts. Problems the company faces include trying to keep track of what system uses what torch and what consumables go into the torch. If the wrong consumables are used, such as placing a 60-A tip in an 80-A system, parts life, cutting performance, and productivity all suffer. When parts are mixed from one model to another, a major torch or unit failure can occur, resulting in significant repair costs.

A universal torch could adapt to the needs of end users. The major hurdle faced trying to develop such a universal torch is the nonuniversal technology being used with plasma arc cutting equipment. Technology was needed to integrate all torch start methods — high-frequency start, touch start, and internal moving parts. Other differences include varying air pressures, varying gas flow rate requirements, and internal gas management designs within each torch.

It is difficult trying to come up with a truly "universal" plasma torch that can be adapted to the many plasma cutting systems in the market. The "fit" needed to include feel, look, size, ergonomics, simplicity of use, safety, and performance. Performance includes cutting characteristics, parts life, ruggedness, durability, accessibility, versatility, and adaptability.

After three years of research and development, Thermal Dynamics developed such a product — 1Torch™.

The heart of this technology is a component known as the "start cartridge." Until the development of the start cartridge, plasma cutting torches relied on incompatible start processes and components. With high frequency (blow-apart) and start pilot torch designs (touch and lift/scratch), the electrode or tip must mechanically move within the torch to allow the pilot arc to start. This can require springs or moving parts in the torch head itself. During the starting of the pilot arc, high-pressure air passes around the consumable parts, inducing the separation of these parts. These parts are constantly being moved, and consumable parts life is often reduced because of repeated, wear-related misalignment.

The new torch starts the pilot arc by moving the start cartridge, not the tip or electrode. This device contains a moving element that initiates the pilot arc with or without high frequency. This technology allows the SureLok™ electrode to remain locked in place, which aids heat transfer and cooling of the consumable parts.

A fixed electrode maintains a constant electrode-to-tip orifice relationship. In traditional blow-apart designs, the electrode is not fixed but must move to provide the spark to initiate the plasma arc. Gas passing around the electrode during cutting can cause the moving electrode to wobble. This results in short tip life as the plasma arc erodes the tip orifice, creating a wider, less precise plasma arc. Maintaining tip-to-electrode alignment and eliminating vulnerable moving parts from the torch head itself result in a well-defined cutting arc and longer parts life.

A tip-based way of managing gas flow to deliver precision gas management is part of the system. Most plasma torches require a gas distributor or swirl rings for each amperage level. In the new torch, gas management is integral to the tip and does not depend on a specific gas distributor. The tip is tuned to optimize cut performance at its rated cutting current, which enhances consumable life and cutting performance.

One of the benefits of torch standardization for a multisystem end user is a reduction in the number of consumables that must be inventoried. There are 20 consumable parts for this system. Of those 20 consumables, 12 are tips, including 30- and 40-A drag tips; 40-, 50/55-, 60, 70-, 80-, and 90/100-A standard tips; and 40-, 60-, 80-, and 100-A gouging tips. Additional consumables include a MaximumLife™ electrode, start cartridge, and a half-dozen shield-related components: cup, retainer, drag cap, machine cap, gouging cap, and deflector cap.

Field-testing demonstrated the system's day-in, day-out cutting capability and also identified it as a reliable gouging tool. The torch was found to be suited for both drag shield (current levels of above 40 A), where the tip is kept from contacting the material, and drag tip cutting (current levels 40 A and above), where the tip is allowed to protrude beyond the end of the shield cup for direct contact with the material. Results were good on thinner material.

Many plasma operators use the same plasma system to cut by hand as well as with a pipe beveler or a mechanized positioning device. The universal torch is available with a quick-disconnect device that allows torch installation or removal with less than one turn of the locking nut. Electrical connectors inside the device disengage in a specific sequence to eliminate the possibility of accidental torch activation or a shock to the operator.

Thermal Dynamics is a division of Thermadyne™ Holdings, a global welding and cutting products company with headquarters in St. Louis, Mo. For more information, visit the Thermal Dynamics Web site at *www.thermal-dynamics.com* or call Mike Linehan at (800) 752-7621.

BY TONY ANDERSON

Q: I have recently changed from using the gas metal arc welding (GMAW) process on steel to welding aluminum with the same process. I am finding it difficult to feed the aluminum wire through my feeding system. I often experience equipment problems such as fusion of the aluminum welding wire to the contact tip, which requires the breakdown of the feeding system and replacement of the contact tip. These problems are time consuming and costly. Is there any way I can improve this situation? I am using 0.047-in.-diameter ER4043 filler metal.

A: Feedability — the ability to consistently feed the spooled welding wire without interruption during welding — is probably the most common problem experienced when moving from welding steel to welding aluminum using GMAW. Feedability is a far more significant issue with aluminum than steel, primarily because of the differences in the materials' mechanical properties. Steel welding wire is rigid, can be fed more easily over a greater distance, and can withstand far more mechanical abuse than aluminum wire. Aluminum is softer, more susceptible to being deformed or shaved during the feeding operation, and, consequently, requires far more attention when selecting and setting up a feeding system for gas metal arc welding. Feedability problems can be increased when using smaller diameter wires and softer aluminum alloys, such as 1100 and 4043, rather than harder alloys such as 5356. Feedability problems often express themselves in the form of irregular wire feed or as burnbacks (the fusion of the welding wire to the inside of the contact tip).

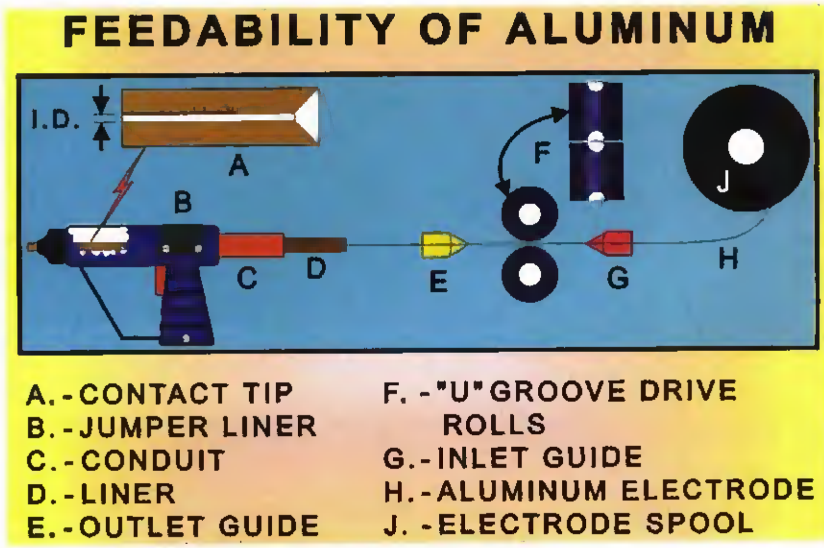

Fig. 1 — A wire feeding system for gas metal arc welding of aluminum.

How the System Affects Feedability

To prevent excessive problems with feedability, it is important to understand the entire feeding system and its effect on aluminum welding wire — Fig. 1. If we start with the spool end of the feeding system, we must first consider the brake settings. Brake setting tension should be backed off to a minimum. Only sufficient brake pressure to prevent the spool from free-wheeling when stopping welding is required. Any pressure over and above this will increase the potential for feeding problems and burnbacks. Electronic braking systems and electronic and mechanical combinations have been developed to provide more sensitivity within the braking system and are particularly useful for improved feeding of aluminum wire.

Inlet and outlet guides, as well as liners, which are typically made from metallic material for steel welding, must be made from a nonmetallic material such as Teflon or nylon to prevent abrasion and shaving of the aluminum wire.

Drive rolls designed specifically for feeding aluminum should be used. These often have U-type contours with edges that are chamfered and not sharp. They should be smooth, aligned, and provide correct drive roll pressure. Drive rolls with sharp edges can shave the soft aluminum wire. These shavings can collect inside the feeding system and cause burnbacks from blockages within the liner. Excessive drive roll pressure and/or drive roll misalignment can deform the aluminum wire and increase friction drag through the liner and contact tip.

Contact tip dimensions and quality are of great importance. You should only use contact tips made specifically for aluminum wire welding, with smooth internal bores and the absence of sharp burrs on the inlet and outlet ends of the tips. Contact tip bore diameter should be approximately 10 to 15% larger than the electrode diameter.

The quality of the welding wire used for GMAW can influence feedability characteristics. Such characteristics as surface smoothness, wire diameter control, and final treatment of the wire during the spooling operation can assist or detract from the ability to easily deliver the wire through the feeding system. Consistent quality characteristics of the aluminum welding wire should be considered in order to minimize feedability problems.

Feeding Systems

In terms of aluminum wire feeding, four feeding systems are used: push feeders, pull feeders, push-pull feeders, and spool-on-gun feeding systems. For aluminum welding with the push and the pull feeders, limitations are recognized dependent on application and feeding distance. These systems are generally limited to a practical length of about 12 ft. With push feeders, feeding distance limit is a result of the flexibility of the aluminum wire and its tendency to buckle and bend in the liner; with pull feeders the limit results from a rapid increase in friction drag in the liner, particularly if there are bends in the conduit. Push-pull feeders, were developed to overcome wire feeding problems experienced by the other systems and are the most positive method of feeding aluminum welding wire. Push-pull systems can improve feedability in many applications and are often essential for more critical/specialized operations such as robotic and automated applications to ensure consistent feedability. Spool-on-gun feeding systems are usually designed to use 1-lb spools of wire mounted in the gun. These guns are usually air cooled and are generally limited to smaller wire sizes and light-duty service. Because of their relatively low current rating, they are not perfectly suited to heavy-duty continual production welding, but are often quite effective for tack welding and other light-duty applications. The choice of the most suitable feeding system for each application is based on such factors as the type of welding (light or heavy duty), the electrode size and alloy (large or small diameter/hard or soft filler metal), the need for a long flexible conduit, and the importance of minimizing electrode cost (larger-diameter wire is generally lower priced than smaller diameter).

The demands of welding applications vary extensively, as does the cost of each feeding system. The cost of downtime from feeding problems and replacement parts can also be significant. For these reasons, you should choose the feeding system best suited to your application and set it up to optimize its feeding capability. ◆

TONY ANDERSON is Technical Services Manager for AlcoTec Wire Corp., Traverse City, Mich. He is Chairman of the AWS D10H Subcommittee on Aluminum Piping and D8G Subcommittee on Automotive Arc Welding — Aluminum, Vice Chairman of the AWS D1G Subcommittee 7 on Aluminum Structures, and Chairman of the Aluminum Association Technical Advisory Committee for Welding and Joining. Questions may be sent to Mr. Anderson c/o Welding Journal, *550 NW LeJeune Rd., Miami, FL 33126 or via e-mail at* tanderson@alcotec.com.

BY R. L. PEASLEE

Q. Can you help locate a suitable steel to make a brazing fixture? The braze alloy is AMS 4777, the brazing temperature is approximately 1925°F (1066°C), and the base material of the part is AM 350. I am looking for something that will not size the part. Currently, a graphite fixture, which is getting damaged due to loading/unloading of the part, is being used.

A. Graphite is the best fixture material as it does not warp when cycling from room temperature to the brazing temperature many times. The fixture must be designed for the specific assembly and fixture at the brazing temperature. Since graphite has a lower rate of expansion than AM 350, it is necessary to calculate the rate of expansion of both materials at the brazing temperature. Unfortunately, AM 350 is not listed in the *Brazing Handbook*, and graphite data are only given up to 1200°F. We have found it is not always possible to extrapolate and come up with the correct answer. Often, trials are required.

Although 304 is often used as a fixture material, it also has its problems. If a part is run through the furnace while sitting on a 1-in. 304 circular plate, the plate will distort. The faster the assembly and fixture are heated and cooled, the faster the fixture (and assembly) will potentially distort. If a hole can be put in the center of the 304 plate, there will be less distortion per run. The bigger the hole, the slower the distortion per run. However, 304 has a high rate of expansion and fixture maintenance will be required, depending on the number of runs and the brazing temperature. As has often been said, "Generally, distortion is the result of the differential temperature." In this case, from the inside diameter to the outside diameter.

Alloy 600 is a better fixture than 304 because 600 has a lower rate of expansion and there will be less distortion for each run. In time, 600 has the same problems as 304, but not as quickly. It will also require fixture maintenance, which is dependent on the number of runs, but will handle more runs before requiring maintenance than 304.

Molybdenum is better than 600 since its expansion rate is very low. Thus, it will keep its shape for a long time. It is much more rugged than graphite.

Cost will be one consideration in making fixtures. Most companies use graphite since it holds up better than the metals, thus it has a lower overall cost.

The design of the fixture is all-important. If the graphite fixture is sizing the part, the fixture has not been designed properly. On occasion, we use differential expansion to round and size parts. I used a specially designed internal 304 fixture to size and put a 1-deg taper on a part during the brazing cycle. If the graphite fixture is being damaged in loading and unloading, this is a personnel problem, or a need for proper racks for storing the fixtures. I can only guess at the problem.

Fixturing is a science of its own and each different part will undoubtedly require a different type of fixture and design, except when the assembly is laid on a flat, graphite plate to retain the flatness of the assembly. The best fixture is NO fixture. If possible, the use of self-jigging, tack welding, etc., is best.

The question is, with the proper design, which material gives the longest life at the least cost with the least maintenance? For a metal fixture, Alloy 600 would be the best choice. The fixture design calculated for operation at the brazing temperature for a complex assembly is the most important consideration. ♦

R. L. PEASLEE is Vice President, Wall Colmonoy Corp., Madison Heights, Mich. This article is based on a column prepared for the AWS Detroit Brazing and Soldering Division's newsletter. Readers may send questions to Mr. Peaslee c/o Welding Journal, *550 NW LeJeune Rd., Miami, FL 33126 or via e-mail to* bobpeaslee@wallcolmonoy.com.

Gas Manifold Improves Plasma Cutting of Stainless Steel

The company's H35 gas manifold can be retrofitted to FineLine 200PC precision plasma cutting systems. The manifold regulates the amount of H35 plasma gas delivered to the torch. Coupled with nitrogen shielding gas, the process provides for quality cuts on stainless steel materials ⅜-in. thick and greater.

InnerLogic, Inc. 100
455 Fleming Rd., Charleston, SC 29412

Grinder Is Light and Quiet

The company's Depressed Center Wheel grinder features a 1-hp air motor with a one-piece governor that helps maintain 12,000 rpm under load. The unit includes a safety-lock throttle, a "Griptraction" side handle and a thermal insulated housing. Its rear inline muffler reduces sound to 78 dBA. The grinder uses type 27 reinforced depressed-center wheels.

Dynabrade, Inc. 101
8989 Sheridan Dr., Clarence, NY 14031

Portable Plasma Cutting Machine Weighs 57 Lb

The Spectrum® 625 portable air plasma arc cutting machine can sever ½-in. mild steel at a rate of 10 in./min using a hand-held torch. The lightweight unit can cut steel up to ⅞ in. It is designed to handle generator power fluctuations of 10%, and is engineered to handle rugged, dirty job site conditions.

Miller Electric Mfg. Co. 102
P.O. Box 1079, Appleton, WI. 54912-1079

Vacuum Lifters Customized for Awkward Loads

The company's full line of vacuum lifters can be customized for handling awkward or bulky loads up to 10 ft long without grabs or straps that can cause damage. Available with a variety of nonmarking vacuum pads mounted to spring

suspensions, the lifters gently attach and release their loads without using straps, grabs, or magnets that can damage and scratch products. Vacuum lifters are offered in air-, electric-, and battery-powered models with capacities up to 10,000 lb.

Anver Corp. **103**
36 Parmenter Rd., Hudson, MA 01749

Push-Pull Guns Offer Superior Feeding of Aluminum and Steel

The company's push-pull wire feeding guns, the Cobra MAX and the Python, virtually eliminate friction in the line for

smooth feeding and minimized damage to the wire. Each gun can handle both steel and aluminum wire from 0.030 to $\frac{1}{16}$ in. The Cobra Max fixed gooseneck is rated 150 A at 100% duty cycle. For more demanding applications, one of the five Python guns can be chosen.

The Lincoln Electric Co. **104**
22801 St. Clair Ave., Cleveland, OH 44117-1199

Recorder Stores Data on Thousands of Spot Welds

The WDR Multi-04 is a battery-powered data recorder for resistance spot welding machines. The portable unit displays and stores a dynamic electrode force trace on its LCD display, as well as the point of weld current initiation, weld current magnitude, and weld time. Data for 10,000 welds can be stored and may be

transferred to a computer for detailed production analysis.

Cellar Services, Inc. **105**
5580 Gatewood, Ste. 108, Sterling Heights, MI 48310

Sensor Tracks Weld Joints on Shiny Surfaces

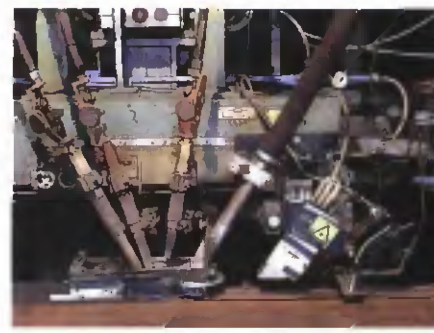

The A700 laser scanning sensor uses a linear camera to scan a high intensity laser spot across the joint, looking slightly ahead of the welding torch to capture a 3-D cross section of the joint that the system uses to determine its exact position. Along with automated welding machines, the system can be applied to postweld inspection and measurement in difficult applications, such as reflective metals, which thwart standard laser tracking techniques.

Meta Vision Systems Inc 106
1410 Begin, St-Laurent, Quebec, H4R 1X1, Canada

Thermal Camera Captures and Displays Temperature Data

The TVS-700 radiometric thermal imaging video system measures temperature differences as small as 0.08°C in the range of 8 to 14 μm. The compact unit uses a 320 × 240 microbolometer focal plane array to provide fine detail in less than 30 s. Real-time image analysis tools include 10 spot meters, isotherm and line profile tools, multiple color and grayscale palettes, and a status area that displays current object parameters for emissivity and background temperature.

Indigo Systems Corp. 107
50 Castilian Dr., Goleta, CA 93117

Fume Arms Are Easy to Adjust and Clean

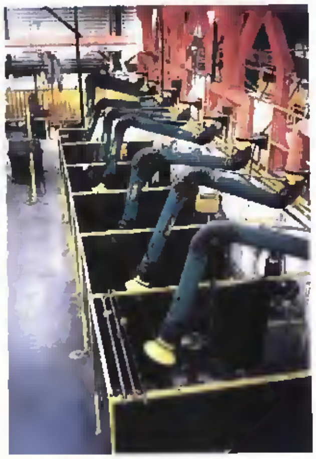

The company's heavy-duty fume arms have all their adjustments on the outside for easy access, with no encumbrances inside the arms, for clear and free air movement. They are available in 4, 6, and 8 in. diameters, in steel and stainless steel, with or without fans and filters.

OsKar Antipollution Inc. 108
8011 Jarry East, Montreal, Quebec H1J 1H6, Canada

Flap Discs Take Grind Out of Finishing

Z-Stainless flap discs feature a blend of high zirconia alumina and aluminum oxide, with a layer of lubricants that allow the zirconia to break down to reduce the heat on stainless steel and other heat-sensitive materials. Their polyester cloth backing is tougher than cotton backing, improving grain retention. Available sizes are 4, 4½, 5, and 7 in., in grits of 40, 60, and 80.

Camel Grinding Wheels 109
7530 N. Caldwell, Niles, IL 60714

Wire Brushes Put a New Twist on Cleaning

The company's Hurricane™ knot wire brushes for weld cleaning and other heavy-duty applications are made with an innovative wire twist in each knot, enabling long-lasting, aggressive cleaning with less operator fatigue.

Anderson Products, Inc. 110
1040 Southbridge St., Worcester, MA 01610

PlasmaSystem Cuts Deeper

The 110-A/16-kW Powermax1650® plasma cutting system has a maximum cut capacity of 1½ in. (38 mm) and can gouge at a rate of more than 22 lb/h. Auto-voltage™ input sensing allows operation from 200 to 600 V, three-phase with no rewiring. The system can be used as a portable unit or incorporated into mechanized cutting solutions.

Hypertherm, Inc. **111**
P.O. Box 5010, Hanover, NH 03755

Lightweight Metal Fabricator Goes Portable

The 155-lb Porta-Shear includes a $10,000\ lb/in.^2$ hydraulic power source for a rated capacity of 20 tons. Its standard attachment will shear flat bar stock up to ¼ in. by 6 in., as well as angle iron and round steel bar stock. Additional attachments will punch or bend mild steel up to ¼ in., notch pipe up to 2 in., and shear channel and square bar stock.

Cleveland Steel Tool Co. **112**
474 E. 105 St., Cleveland, OH 44108

Hydraulic Clamps Work Together as a System

The Stronghold line of hydraulic workholding clamps includes pneumatic swing/pull clamps with capacities up to 4500 lb, with a variety of mounting, plumbing, and body style options from a single source. Single-acting and double-acting versions are available.

DE-STA-CO Industries **113**
P.O. Box 2800, Troy, MI 48007-2800

Eyewear Protects from Industrial Laser Exposure

Uvex® laser safety eyewear conforms to ANSI Z136.1 guidelines for protection from laser light. Available in a variety of frame and over-glasses styles, the eyewear can be ordered with prescription vision correction. The company also offers acrylic safety windows that can be installed for protection from a variety of hazardous wavelengths.

Directed Light, Inc. **114**
633 River Oaks Pkwy., San Jose, CA 95134-1907

Portable Cooling System Saves Space

The Cool-Arc™ 40 water cooler is a self-contained cooling system for all Lincoln water-cooled systems, for use with guns and torches (including Cobramatic torches), and is suitable for gas tungsten and gas metal arc welding, as well as plasma arc welding and cutting. The unit weighs about 60 lb, and is easy to maneuver around the shop or job site. Inlet and outlet connections are color-coded, with standard CGA-style threads.

The Lincoln Electric Co. **115**
22801 St. Clair Ave., Cleveland, OH 44117

TiN-Coated Bits Perform End Prep Jobs on Boiler Tubes

The company's formed tool bits (cutting blades) are used for simultaneously beveling, facing, and boring clad boiler tube without cutting oils. Coated with titanium nitride (TiN), the bits are suit-

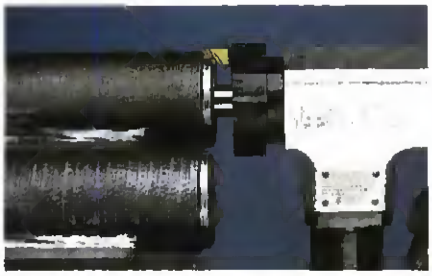

able for Millhog® end prep tools for tubes from ½-in. I.D. to 18-in. O.D.

ESCO Tool 116
P.O. Box 530, Medfield, MA 02052

Pneumatic Scaler Generates Less Vibration

The LV-1 Scaler generates less vibration without sacrificing metal-removing power. The tool delivers 4000 blows per min at 90 lb/in. Air inlet size is ¼-in. NPT, with ¼-in. BSPT available.

T. C. Service Co. 117
38285 Pelton Rd., Willoughby, OH 44094

Blowers Amplify Air to Move or Vacuum Scrap, Fumes, or Small Materials

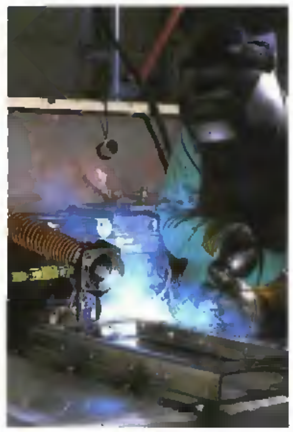

The company's Round Transvectors® use a small amount of filtered compressed air to deliver a large airflow for conveying, ventilation, drying, and cooling operations. With no moving parts, the air amplifiers deliver flow rates from 32 to 2300 ft/min as vacuum or blowoff devices.

ITW Vortec 118
10125 Carver Rd., Cincinnati, OH 45242-9976

Brazing Alloy Paste Joins Copper and Brass Parts

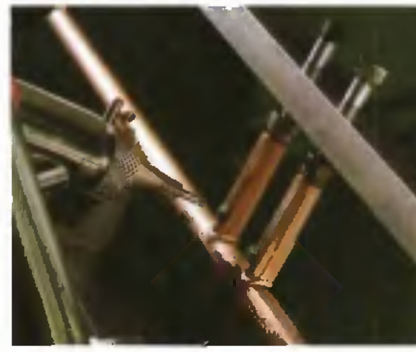

The company's #1311 brazing paste can join copper/copper, copper/brass, and brass/brass with visible silver-gray fillets to allow easy confirmation of sealed joints. With a liquidus of 1247°F (674°C), the paste can be automatically dispensed in measured amounts and heated with gas/air, gas/oxygen, or induction heat methods.

Fusion, Inc. 119
4658 E. 355 St., Willoughby, OH 44094

PLASMA ARC CUTTING MACHINE SELECTION AND TECHNIQUES

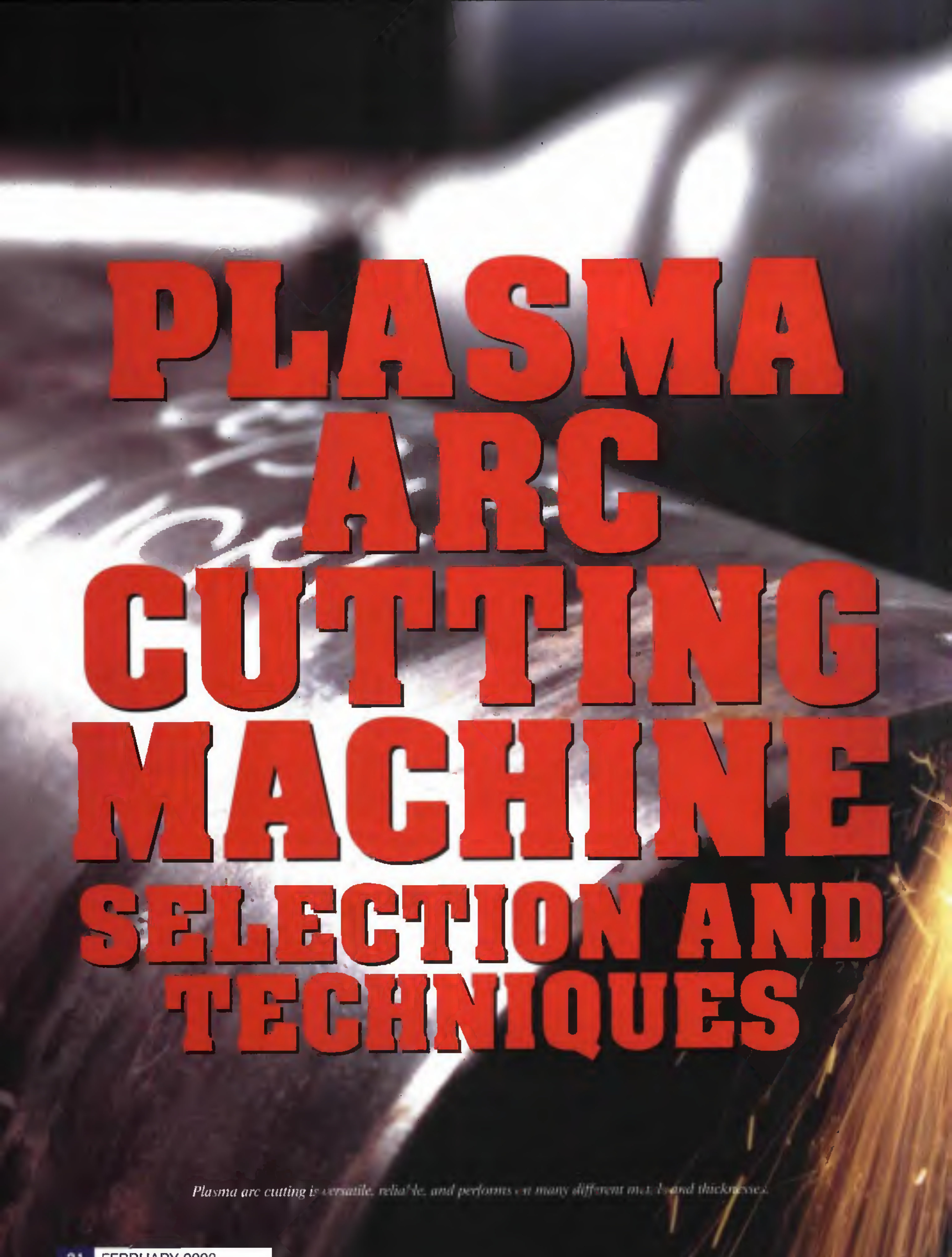

Plasma arc cutting is versatile, reliable, and performs on many different metals and thicknesses.

New machine designs have a smaller footprint, but they retain the same cutting abilities as the larger machines of old

BY BRIAN SCHMIDT

When selecting a plasma arc cutting machine, the criterion is simple: you need to know the thickness of your material. Plasma cutting has advanced to a point where 75-lb machines can perform jobs once restricted to 400-lb monsters. Adaptability is no longer an issue as some of today's plasma arc cutting machines can run without difficulty on any input power in the world — and almost flawlessly off of engine drives. Product design has made a machine once susceptible to the elements (heat, dirt, moisture, etc.) resistant to those problems and turned it into a workhorse that has sent traditional machines to the retirement home.

BRIAN SCHMIDT (bschmi@millerwelds.com) is product manager, Miller Electric Mfg. Co., Appleton, Wis.

Fig. 1 — Dave Robertson of Peterson Manufacturing cuts caps out of ¼-in. mild steel.

What You Need to Know

- Plasma arc cuts all electrically conductive metals (oxyfuel is usually limited to steel).
- Plasma arc cutting requires no preheating.
- Turnaround time is fast.
- The process produces a small heat-affected zone.
- The machines have great portability.

When selecting a plasma cutting machine, it's important to know what thickness ranges you'll be cutting on a regular basis. You'll be presented with a machine and its rated, quality, and sever cutting capabilities. Rated cut refers to the thickness of material that can be cut at the amperage and voltage the unit produces for a given duty cycle. Quality refers to the thickness of material that can be cut successfully and cleanly while exceeding that suggested duty cycle. Sever is the maximum thickness recommended for a specific machine.

For example, if you're in a shop that consistently cuts ½-in. stainless steel, shop around for a plasma arc cutting machine with a rated cut at ½-in. With such a machine, you're likely to find the capability to cut up to ⅞-in. material.

Plasma systems that cut up to 6-in. steel are available, but are rarely used. The majority of the market has shifted to inverter-sized plasma cutting machines that can cut up to 2-in. material and are commonly used in heavy manufacturing, fabrication, and construction. It's a simple decision whether you want a machine that weighs 80 lb or one at 400 lb. Today's contractor, plant maintenance worker, and fabricator need something that can be moved from place to place and in and out of service trucks and trailers. Inverter technology, such as that found in much of today's welding equipment, is responsible for the reduced size, replacing the conventional, transformer-based plasma cutting machines of old.

Features

When searching for a plasma arc cutting machine, a few things can greatly assist in most work environments.

- Power factor correction is a universal industry term that describes the ability to draw less amperage without sacrificing cutting abilities. This helps save on utility bills and minimizes the effect of voltage drops when plugged into shop outlets.
- Look for a cooling system that operates only when needed. This reduces the amount of airborne impurities that can hamper a machine's performance.
- Wind Tunnel Technology™ is a feature that prevents abrasive dust and particles from damaging internal components by blowing them through a tunnel that runs through the center of the machine. Sensitive electrical components are isolated on the other side of the tunnel wall.
- By using a contact start, plasma cutting machines no longer require high-frequency starts. Problems commonly arose when the machines were located near electronically sensitive equipment, and the high-frequency could interfere with its usage.
- Ask for a machine that will provide peak performance power under variable

Peterson Manufacturing: Plasma Arc Cutting in Action

Embarrass, Wis., is typical of most small towns in the north-central region of the state. Flanked on all sides by farmland, Peterson Manufacturing fabricates feeders, harrows, buckets, manure spreaders, and bale spears sold throughout the Midwest.

The company was using a 40-A plasma arc cutting machine to typically cut 18 gauge to ¼-in. materials. A problem with "dirty power," or line voltage fluctuations, resulted in the cutting arc extinguishing or not penetrating at all. Also, slag would build up on the backside of the cut material, which required removal. This type of problems can be eliminated with available plasma arc cutting technology.

The company purchased a 40-A Spectrum 625 cutting machine, which has line voltage compensation technology. This technology manages input power from 176 to 264 V and steadies the arc. With the help of a steady arc, a string of pipe support caps cut from ¼-in. mild steel (Fig. 1) previously took ten minutes for the operation. The operation is now reported to be completed in five minutes.

input voltage conditions. These features offer a steady arc even if your shop experiences voltage fluctuations, which are common in rural areas, in plants that start large loads on the same line, and when running off of welding generators.

Consumables

One of the most costly and time-consuming items with plasma arc cutting machines is consumables. New technology helps extend their life, reducing downtime and costs while increasing productivity. Drag shields are now available on plasma torches that protect the tip from the workpiece. Today's machines also provide better amperage control at the beginning and end of each cutting sequence, helping extend tip life. Machines with a pilot arc control extend tip life by boosting pilot current only when needed for a strong arc transfer. Considering tips can cost up to $15 and that these features extend tip life by as much as four hours, huge savings can be had.

Technique

Plasma arc cutting is not quite as involved as welding. The manner in which you cut the piece will vary depending on the output of your plasma arc cutting machine and the thickness of your material. When cutting metals at and below a machine's rated thickness, hold the gun at a 90-deg angle to the workpiece. Make sure to take note of a machine's inches per minute (ipm) capabilities on varying thicknesses, as that gives you an idea of how fast to move across the cutting surface. When cutting materials at the rated size and above, it's recommended to slightly tilt your gun into the workpiece. If you find yourself needing to make multiple passes on a piece to properly cut it (and you're not cutting it too quickly), you simply need a more powerful plasma cutting machine. Pay close attention to the machine's capabilities and your needs when purchasing a plasma arc cutting machine.

An Option to Gouge

A plasma arc cutting machine is not always the first product one thinks of when needing to gouge, but it can prove effective for this application. Using a special tip, the narrow cutting arc is transformed into a relatively wide and highly effective gouging arc. This can eliminate the need for a welding power source to perform carbon arc gouging. When gouging with a plasma arc cutting machine, hold the torch at a 40-deg angle to the workpiece. Plasma gouging requires only that you maintain the suggested distance between the arc and gouging surface to adjust for travel speed. With carbon arc gouging, the operator needs to continually adjust the distance of his hand to the cutting surface as the carbon rod is consumed.

Universal Technology

The challenges that face an industrial manufacturer are not much different than a contractor working out of the back of his or her truck. Anywhere you have numerous people running tools off the same power source, anywhere you have a rural setting far removed from primary power, and anytime you're running a plasma cutting machine off an engine drive, you're going to have to deal with power issues. Look for plasma cutting machines from any number of manufacturers that provide some kind of input power management technology. Ask about which machines have solid track records in even the dirtiest environments. Make sure you're getting technology that will extend the life of your consumables — the costs that can add up from an inadequate plasma arc cutting machine may eventually equal the quality product you should have bought in the first place. ◆

THERMAL DISTORTION in Aluminum Welded Structures

Strategies minimize nonuniform dimensional changes caused by heat stress

BY TONY ANDERSON

TONY ANDERSON (tanderson@alcotec.com) is Technical Services Manager for AlcoTec Wire Corp., Traverse City, Mich. He is Chairman of the AWS D10H Subcommittee on Aluminum Piping and D8G Subcommittee on Automotive Arc Welding — Aluminum, Vice Chairman of the AWS D1G Subcommittee 7 on Aluminum Structures, and Chairman of the Aluminum Association Advisory Committee for Welding and Joining.

Welding distortion can be defined as the nonuniform expansion and contraction of weld metal and adjacent base metal during the heating and cooling cycle of the welding process. Distortion is a consideration when arc welding all materials, and the principles behind this reaction are fundamentally the same. However, when welding aluminum, compared to carbon steels, the effects of some of the main contributing factors for distortion are increased. Aluminum has high thermal conductivity, a property that substantially affects weldability. The thermal conductivity of aluminum is about five times that of low-carbon steel. Aluminum also has high solidification shrinkage, around 6% by volume, and also a high coefficient of thermal expansion. When arc welding aluminum, high localized heating to the material in and around the weld area is applied. There is a direct relationship between the amount of temperature change and the change in dimension of a material when heated. This change is based on the coefficient of expansion — the measure of the linear increase per unit length based on the change in temperature of the material. Aluminum has one of the highest coefficient of expansion ratios, and it changes its dimension almost twice as much as steel for the same temperature change.

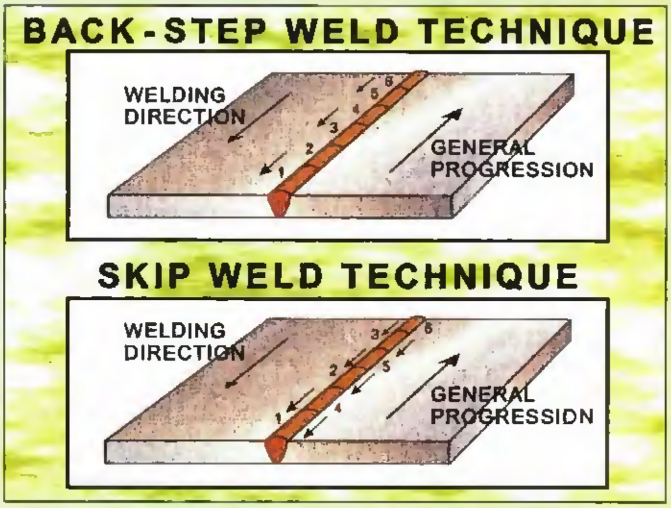

Fig. 1 — Welding sequences can help minimize thermal distortion. Prior welds on small sections create a locking effect.

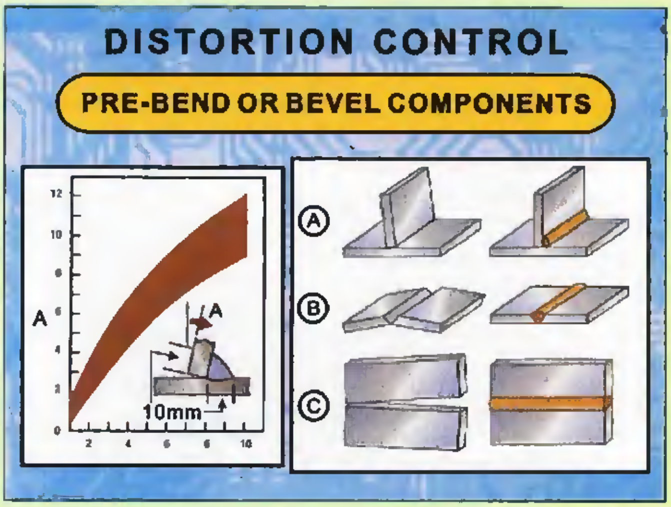

Fig. 2 — Presetting components by an offset angle to compensate for weld shrinkage.

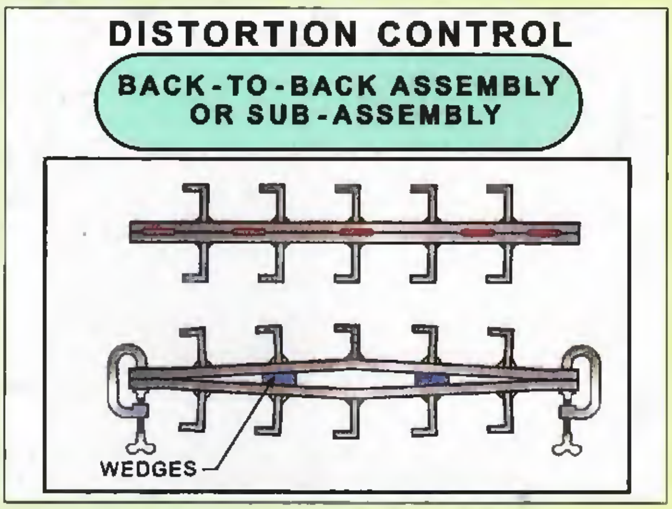

Fig. 3 — Restraints and back-to-back assembly can reduce distortion, and can be combined with prebending.

If a nonrestrained piece of metal in a furnace is evenly heated to a prescribed temperature and then allowed to cool to its original temperature, it will first expand (to a degree based on its coefficient of expansion), and then contract as cooled to its original size. If this kind of uniform heating and cooling is applied to an unrestrained structure, the heating and cooling process should promote no distortion of the structure. Unfortunately, when arc welding, nonuniform localized heating is usually applied to the structure being welded. This heating is limited to the area of the weld and its close vicinity. Also, the heating and cooling is conducted under varying amounts of restraint during the welding process. The part of the welded component outside of the weld area that is not heated, or heated to a much lower temperature, acts as a restraint on the portion that is heated to the higher temperatures and undergoes higher expansion. The nonuniform heating, resulting in nonuniform expansion and contraction, along with weld metal and base metal shrinkage and the partial restraint from the less affected parts of the structure, are the primary causes of thermal distortion problems in welding.

Ways to Reduce Distortion

■ Probably the most common cause of excessive distortion is from over welding. In order to reduce distortion, heating and shrinkage forces should be kept to a minimum. Design the weldment to contain only the amount of welding necessary to fulfill its service requirements. The correct sizing of fillet welds to match the service requirement of the joint can help to reduce distortion. Do not produce fillet welds that are larger than specified on engineering drawings.

Provide welders with fillet weld gauges so they are able to measure their welds to ensure they are not producing welds that are much larger than specified. With butt joints, always control edge preparation, fitup, and excessive weld buildup on the surface in order to minimize the amount of weld metal deposited, and thereby reduce heating and shrinkage.

■ When welding thicker material, a double-V-groove joint requires about half the weld metal of a single-V-groove joint and is an effective method of reducing distortion. Changing to a J-groove or a U-groove preparation can also assist by reducing weld metal requirements in the joint.

■ Try to use intermittent fillet welds where possible. Often adequate strength requirements can be maintained and the volume of welding reduced by 70%, if the design allows, by using intermittent fillet welds over continuous welding.

■ Balance welding around — and position welds near to — the neutral axis of the welded structure. The neutral axis is the center of gravity of the cross section of the part. Placing similarly-sized welds on either side of this natural centerline can balance one shrinkage force against another. Placing the weld close to the neutral axis of the structure may reduce distortion by providing less leverage for shrinkage stresses to move the structure out of alignment.

■ Reduce the number of weld beads if possible. Few passes with a large electrode are preferable to many passes with a small electrode. The additional applications of heat can cause more angular distortion in multipass single fillet welds and multipass single-V-groove welds.

■ Carefully select the welding process to be used. Use a process that can provide the highest welding speeds, and is able to make the weld in the least amount of weld passes. Make use of automated welding whenever possible as automated techniques are often capable of depositing accurate amounts of weld metal at extremely high speeds. Fortunately, with modern arc welding processes, it is often possible to use high welding speeds, which help fight distortion.

■ Use welding sequences or backstep welding to minimize distortion — Fig. 1. The backstep technique allows for the general welding progression to be in one direction, but enables us to deposit each smaller section of weld in the opposite direction. This provides the ability to use prior welds as a locking effect for successive weld deposits.

■ Whenever possible, weld from the center outward on a joint or structure. Wherever possible, alternate sides for successive passes on double-sided multipass welding. An even better method to control distortion is to weld both sides of a double-sided weld simultaneously.

■ Preset components so they will move during welding to the desired shape or position after weld shrinkage. This is a method of using the shrinkage stresses to work for you during the manufacturing process. Through experimentation, determine the correct amount of offset required to compensate for weld shrinkage. Then, only control of the size of the weld is needed to produce consistently aligned welded components — Fig. 2.

■ Consider the use of restraints such as clamps, jigs and fixtures, and back-to-back assembly. Locking the weldment in place, with clamps fixed to a solid base plate to hold the weldment in position and prevent movement during welding, is a common method of combating distortion. Another method is to place two weldments back-to-back and clamp them tightly together. The welding is completed on both assemblies and allowed to cool before the clamps are removed. Prebending can be combined with this technique by inserting spacers at suitable positions between the assemblies before clamping and welding — Fig. 3.

In Summary

Weld distortion is caused by localized expansion and contraction of metal as it is heated and cooled during the welding process. Constraint from the unheated surrounding metal produces permanent changes in the internal tension stresses generated. If these stresses are high enough and cannot be adequately resisted by the structure, distortion results. A large number of factors determine what stress levels are developed, their orientation, and whether they will cause unacceptable distortion. These factors include the size and the shape of the welds, where they are located in the structure being welded, the rate of heat input during the welding process, the size and material thickness of the components being welded, the assembly sequence, the welding sequence, and others. Ideally, to avoid distortion, there should be as little welding as possible in a structure, and especially where thin gauge metal is involved. With aluminum, there are some options available at the design stage that may help to eliminate excessive welding. The use of castings, extrusions, forgings, and bent or roll-formed shapes can often help to minimize welding and thereby reduce distortion. Many complex aluminum structures are welded every day without excessive distortion problems. This is often achieved through the combined effort of designers and manufacturers. The designers need to carefully consider options that are available to help reduce the amount of welding within the structure — and to position those welds that are necessary in areas that least promote distortion. The manufacturer needs to develop, employ, and control the necessary equipment (welding process, fixturing, etc.) and techniques (welding sequences and balancing methods) to reduce those effects of the welding process that promote distortion.♦

The ABCs of Steel Metallurgy

A basic knowledge of the metallurgy of carbon steels will help welders better understand the materials they join

BY DAVE McGOWAN

Carbon steel is the most commonly welded material. This article serves as a primer on the metallurgy of carbon steels, with the aim of helping welders better understand the material they work with so often. It is not intended to be a definitive article on the subject of carbon steel metallurgy.

All metals solidify as crystalline material, meaning their atomic arrangement is in an ordered fashion. There are approximately 14 types of atomic arrangements in crystalline structures. This article will concentrate on four of those: body-centered cubic (BCC), face-centered cubic (FCC), orthorhombic, and the highly distorted body-centered tetragonal. In addition to carbon steel, this article will examine the following pure metals: chromium, copper, and iron.

DAVE McGOWAN is with Industrial Welding Instruction and Consulting, Port Coquitlam, B.C., Canada, (604) 941-4724.

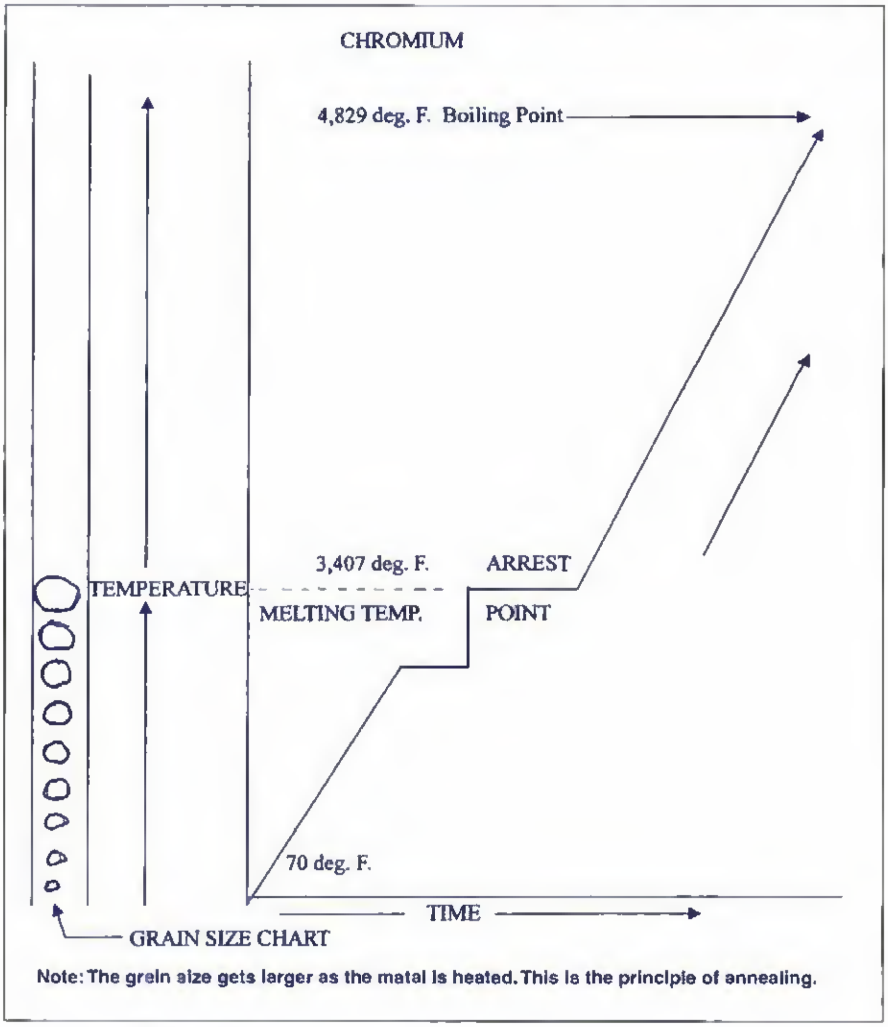

Fig. 1 — The effects of temperature changes on chromium.

Three Pure Metals

Chromium

Pure chromium contains only chromium atoms in its crystalline structure. If a piece of pure chromium is heated, the metal expands. On continued heating, chromium reaches its melting point at 3407°F — Fig. 1. The chromium will then melt at a constant temperature.

Metals like chromium have a definite atomic arrangement that conforms to a typical pattern. In chromium's case, the atoms are arranged in cube symmetry, meaning they look like a cube. With chromium, one atom is located at each corner of the cube and one atom is in the cube's center (Fig. 2), an arrangement known as body-centered cubic (BCC). Some other metals that have a BCC atomic arrangement are molybdenum, tungsten, vanadium, and columbium. All of these metals retain the BCC structure from room temperature to their melting temperature.

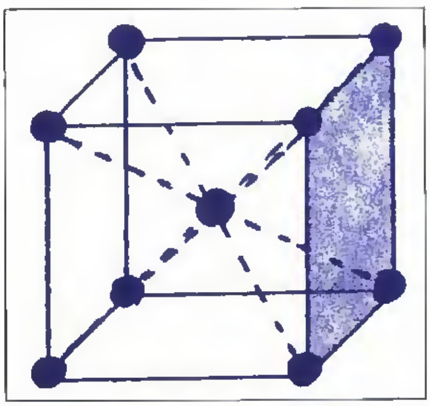

Fig. 2 — The body-centered cubic arrangement of chromium atoms.

An exception is iron, which is BCC from room temperature to 1670°F and from 2534°F to its melting temperature at 2790°F. Below room temperature, electroplated chromium is hexagonal. However, the phase is unstable and transforms to BCC slowly.

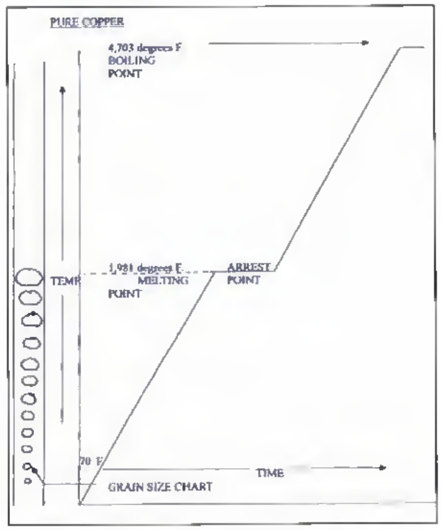

Fig. 3 — The effects of temperature changes on copper.

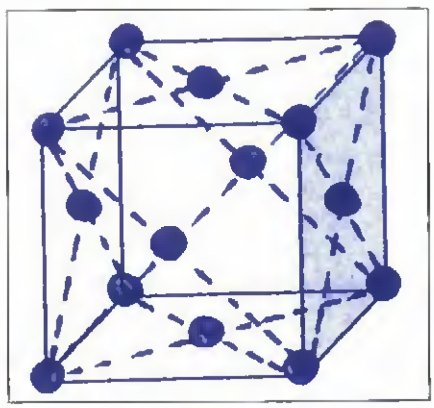

Fig. 4 — The face-centered cubic arrangement of copper atoms.

Copper

When heated, a piece of pure copper goes through the same series of events as does chromium. The only difference is copper has different melting and boiling temperatures — Fig. 3. Copper melts at 1981°F and boils at 4703°F. Although copper also has a cubic arrangement, the atoms are arranged somewhat differently. One atom is located at each corner of the cube and one atom is located at the center of each face of the cube, an arrangement called face-centered cubic (FCC) — Fig. 4. Other metals with a FCC atomic arrangement include aluminum, nickel, silver, gold, and lead, all of which retain their FCC structure to their melting temperature. Again, iron is an exception; iron is FCC from 1670 to 2534°F.

Keep in mind the atoms that make up the BCC and FCC structures are not actually joined by lines as shown in the figures. The lines are only there to assist in visualizing the arrangement. The atoms are tiny, hard balls about 10^{-8} cm in size. This means 254 million of them could be placed end to end to make one inch. It takes many of these cubes to form a crystal, which is also called a grain. These grains grow and interfere with other grains to form metal.

Iron

Pure iron is quite different from chromium or copper. When heated to the correct temperature, it has the ability to transform from one cubic arrangement to another, a phenomenon called allotropy. The temperature transformation stages of pure iron are as follows: It is body-centered cubic at room temperature. Once the metal is heated to 1670°F, it fully transforms to the face-centered cubic form. It stays FCC until it reaches 2534°F. At that temperature, it transforms back to the body-centered cubic form. Heating pure iron above 2534°F to its melting temperature of 2790°F has no effect on the BCC form. Once the metal reaches its melting temperature, the body-centered cubic form begins to break up and the atoms move freely about because the metal is now in the liquid state. Note that these allotropic transformations are only obtained under equilibrium conditions. If the metal is heated or cooled quickly, the allotropic transformation temperatures will change. These transformation points suffer arrests just like a melting point arrest. Another temperature worth mentioning is the Curie point, or magnetic change point. At 1414°F and above, iron is nonmagnetic. This Curie point is not a structural change point.

A grain size chart is located on the left-hand side of Fig. 5. The grains are smallest at 1670°F. This is the best state for the iron to be in because a small grain size has more desirable mechanical properties. If we recall that at 1670°F the iron is in the FCC state and on cooling below 1670°F it changes to the BCC state, we can see the change from FCC to BCC creates an additional grain refinement. In short, if a piece of pure iron is heated to 1670°F (FCC stage), it will have a small grain size. If it is cooled, the FCC transforms to BCC, causing an additional grain refinement due to the fact the atoms had to rearrange themselves. If the pure iron was substantially heated above 1670°F, for example, to 2000°F, it would result in a large grain size. Then, on cooling, the structural change would not be as beneficial as a grain refiner because of the large grain size.

Pure iron is very ductile and has low tensile strength. There is virtually no use for it in industry; however, when carbon is added to iron its strength increases and good ductility is retained.

Steel

Steel is an alloy composed of iron, carbon, manganese, silicon, phosphorus, and sulfur. The raw materials for steel are iron ore, limestone, and coke. These raw materials are charged in a blast furnace, pro-

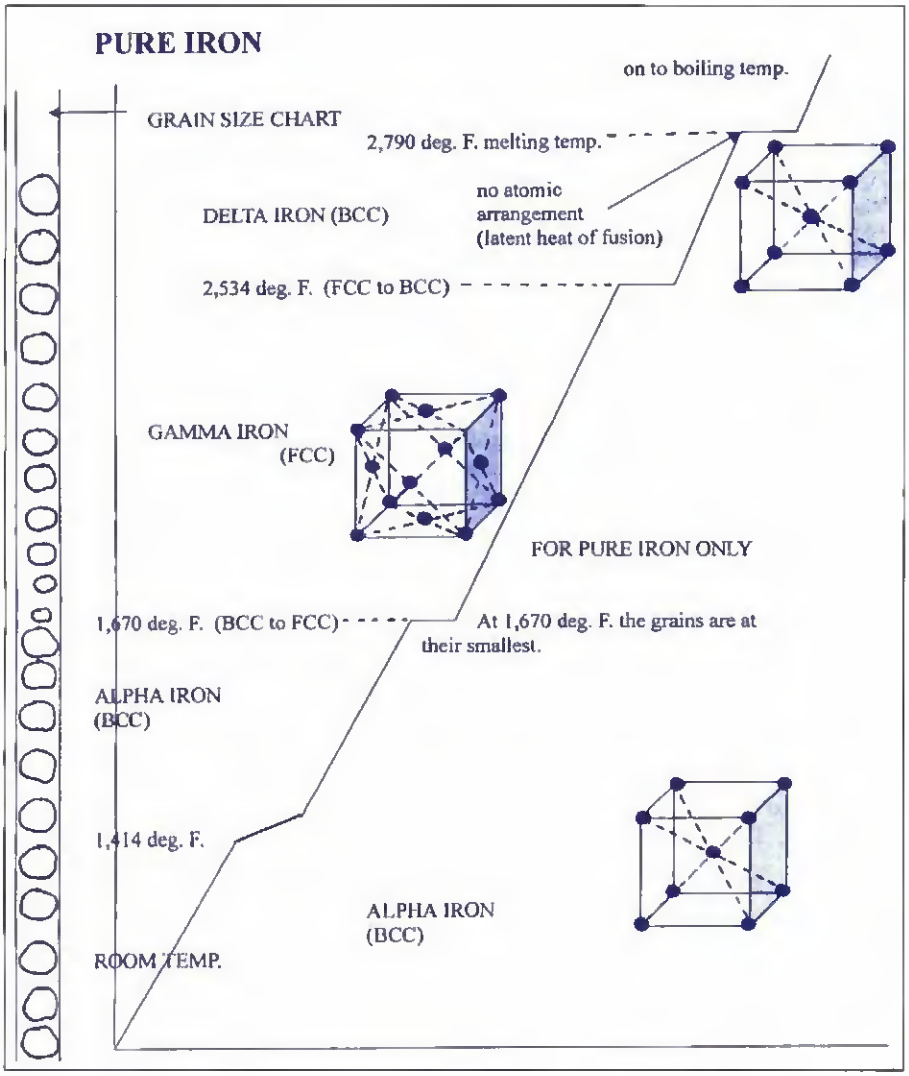

Fig. 5 — The effects of temperature changes on pure iron.

ducing pig iron. Pig iron is high in carbon, silicon, manganese, sulfur, and phosphorus and must be further refined before it can be used as an engineering material. The pig iron is transferred from the blast furnace to either an open hearth process, electric process, or the basic oxygen steelmaking process. These processes have the ability to refine the pig iron to the desired steel quality. Mild steel has a nominal composition of 0.17% carbon, 0.85% manganese, 0.15% silicon, 0.04% sulfur, and 0.02% phosphorus.

Following is a closer examination of the elements that combine to form steel. An element is the smallest unit particle of a substance. There are approximately 102 naturally occurring elements; three-quarters of them are classed as metals.

Carbon. This is the main element in the formulation of steel. Adding up to 0.8% carbon increases hardness and strength. The more carbon added, the more difficult the steel is to weld.

Manganese. At percentages of 0.25 to 1.0, manganese combines with the low sulfur content to form a compound called manganese sulfide. This reduces the chance of cracks occurring at elevated temperatures (termed hot shortness). Manganese is also a hardener and toughener.

Silicon. This element is primarily a deoxidizing and scavenging agent. The amount present in the steel is usually around 0.35%; however, it can be as low as 0.05%.

Sulfur. Sulfur is an impurity that adversely affects impact energy absorption. It is kept to a low of 0.05%. On its own, sulfur combines with iron to form iron sulfide, which has a melting temperature of 1814°F. This is why manganese is added to steel. It combines with the sulfur to form manganese sulfide. Some steels — called free machining steels — have a high sulfur content of around 0.35%. Manganese is added to these high-sulfur steels because it helps the steel to be free cutting. The high manganese combines with the high sulfur to form the manganese sulfide compound. This type of steel is then cold drawn through dies, making the manganese sulfide elongated or needle-like and easy to machine.

Phosphorus. This element is also an impurity. It does have the ability to strengthen steel but at the expense of ductility. Maximum percentage should be approximately 0.05%.

Heat Treatment of Steel

With a basic understanding of atomic arrangements, grain size, and the important elements of steel, we can proceed to the actual heat treatment of steel. It was stated earlier that carbon is the main element in the formulation of steel. Carbon is also an austenite stabilizer; so much so that above 0.5% the delta phase is completely eliminated. Following are definitions of the terms austenite, ferrite, cementite, martensite, and pearlite. Some of these constituents were given names related to their appearance when viewed through a microscope. For instance, cementite is an intermetallic compound of iron and carbon, and pearlite was so named because of its pearl-like appearance. Other structures were named after individuals. E. C. Bain discovered bainite. Martensite was named after Adolf Martens. Austenite was named after James Austen.

Austenite. This is the face-centered cubic structure of steel. It is also known as gamma iron. It is a solid-stage structure stable only at high temperatures. This structure can take on 1.8% C.

Ferrite. Also known as alpha iron, this is the body-centered cubic structure of steel. It is a solid-stage structure stable at room temperature. This structure can only take on 0.008% C at room temperature.

Cementite. This is a crystalline compound of iron and carbon (Fe_3C) with an orthorhombic crystal structure. Cementite joins with ferrite to produce pearlite. It contains 6.67% C by weight.

Pearlite. Cementite and ferrite join in a lamellar form to produce pearlite. It results from the transformation of austenite on slow cooling.

Martensite. This structure is obtained only when austenite is suppressed down to a temperature where it has to transform to a body-centered tetragonal. If there is sufficient carbon in the steel, it will not be able to precipitate out of this shear type of transformation and will be trapped in the body-centered tetragonal lattice.

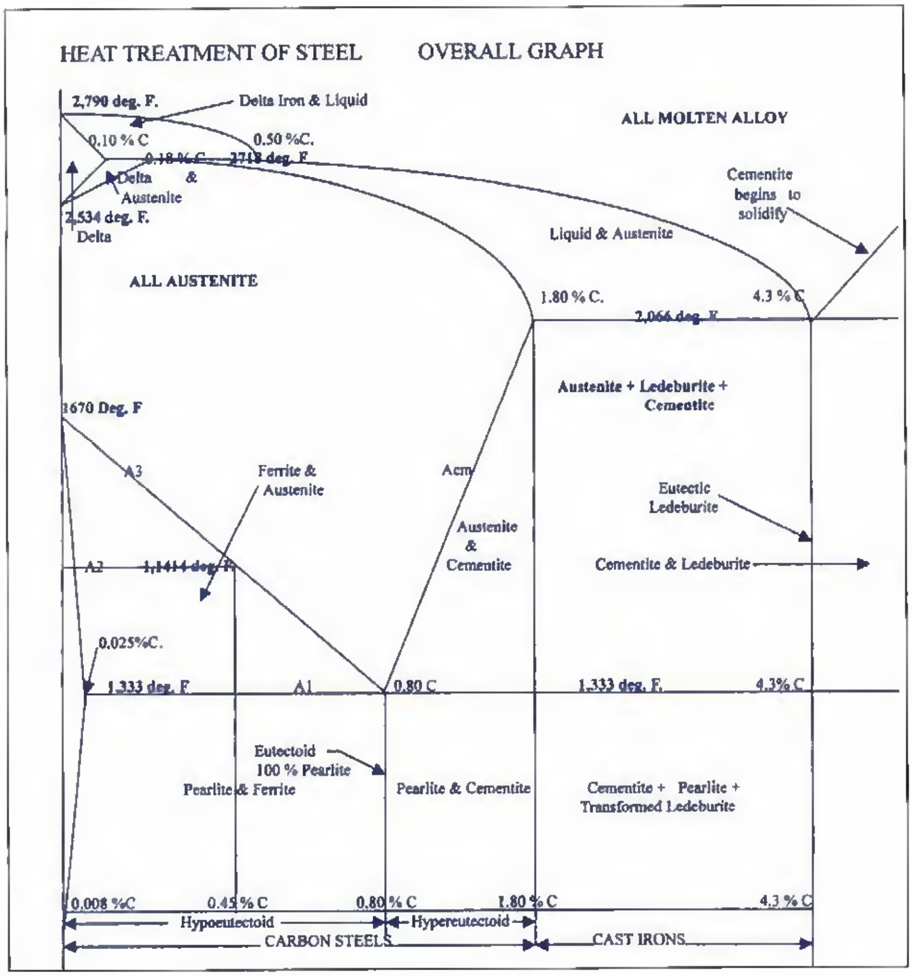

Fig. 6 — An overall graph of the iron-iron carbide equilibrium diagram.

Iron-Iron Carbide Equilibrium Diagram

The iron-iron carbide equilibrium diagram shown in Fig. 6 is helpful when discussing heat treatment. Note that carbon is plotted horizontally and is shown in terms of weight-percent. Temperature is plotted vertically up to the melting temperature of pure iron. While the diagram appears complicated at first glance, the areas of our discussion are quite simple.

Figure 7 shows the cubic lattice structure of ferrite and cementite, and the formation of pearlite. It must be remembered that the stages shown in Fig. 6 are obtained only under equilibrium conditions, meaning that if we heat or cool rapidly, the structures will not form at the temperatures shown or may not form at all.

As stated previously, the most important alloying element in steel is carbon. When carbon is added to iron, the iron is naturally no longer pure, hence the iron-iron carbide diagram shown in Fig. 6 is needed. The top line shows when carbon is added to iron, the melting temperature drops. As you follow the line down, notice it meets another line going up. This point, called the eutectic point, is at a temperature of 2066°F and has a carbon content of 4.3%. It is the lowest melting point of iron carbon alloys. It also solidifies at a constant temperature. At a carbon content above or below 4.3%, the metal will solidify over a range of temperatures. The arrows at the top left-hand side of Fig. 6 show first the amount of carbon that delta can absorb. The maximum amount is 0.1% C.

Next, examine the lower part marked delta and austenite. At 2718°F, a carbon content of 0.1% must reject surplus carbon if cooling is continued. This rejected carbon combines with the iron to produce the interstitial solid solution austenite. This will continue until 2534°F is reached, then it will all be austenite. In discussing heat treatment of steel, however, we are not concerned with this upper part of the graph. Our area of concern is the lower left-hand corner of the overall graph shown in Fig. 6 and on the condensed graph — Fig. 8. In examining Fig. 8, the left area labeled "ferrite with carbon in solid solution" is another area that is not relevant to heat treatment of steel. However, the A1 line — 1333°F — is very important. Steel of any carbon content can be heated to just below this 1333°F line and no structural change will take place; above 1333°F solid structural changes occur.

To understand these structural changes, we will discuss only the steels. Look at the 0.2% carbon steel labeled #1. In examining Fig. 8 just above the A3 line, we can see the steel is all austenite FCC. On cooling the steel very slowly down to the A3 line, the first crystals of ferrite start to form. On continued slow cooling, more ferrite crystals form. At this stage, there is ferrite (BCC) and austenite (FCC). If the steel is cooled to the A1 line (1333°F), there is more ferrite and some untransformed austenite.

At this temperature the remaining austenite transforms to a ferrite cementite lamella form. Hence, below 1333°F, the 0.2% C steel contains ferrite (BCC) and cementite. The two phases form a lamella configuration commonly called pearlite. On slow heating, the reverse occurs, and, on reaching 1333°F, the pearlite begins transforming back to austenite. As heating continues, more and more ferrite transforms to austenite and at the A3 line it is all austenite.

We should at this time discuss grain size and its formation relative to carbon steels. Pure iron transforms from BCC to FCC at 1670°F. The grain size is at its smallest at this temperature. Carbon steels, however, start to form austenite at 1333°F (A1 line) and are completely austenitic at the A3 line. This means the grain size starts to become smaller at the A1 line and is at its smallest at the A3 line. If heated way above the A3 line, the grain size increases. We will return to this subject later.

Look at the 0.45% C steel labeled #2. On slow cooling from the A3 line, crystals of ferrite begin forming as they did with the #1 steel. As the steel continues to slowly cool, more ferrite crystals are present. At the A1 1333°F line, ferrite and more untransformed austenite than in the #1 steel are present. Keep in mind this untransformed austenite must transform to the ferrite cementite lamella form called pearlite. Below 1333°F, there is a little less ferrite (BCC) and a little more pearlite than in the #1 steel.

Take a look at the #3 0.8% C steel, which is termed a eutectoid steel. The eutectoid transformation of austenite to the ferrite and cementite lamella called pearlite occurs isothermally. It is also the lowest temperature structural change point for carbon steels. At slightly above 1333°F, the steel is all austenite (FCC). On slow cooling to 1333°F, the ferrite cementite lamella formation takes place. In this case it is 100% pearlite. Pearlite contains 88%

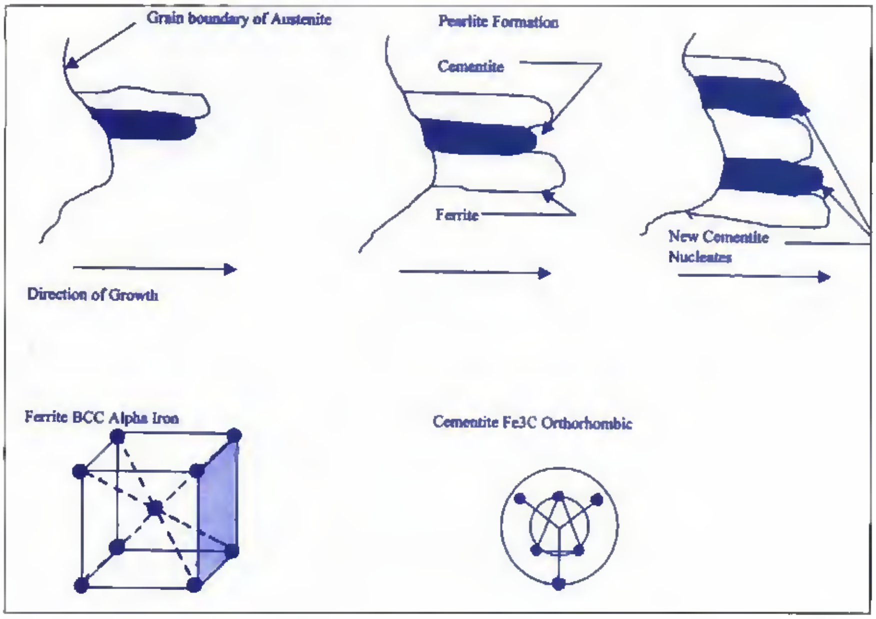

Fig. 7 — The cubic lattice structure of ferrite, cementite, and the formation of pearlite.

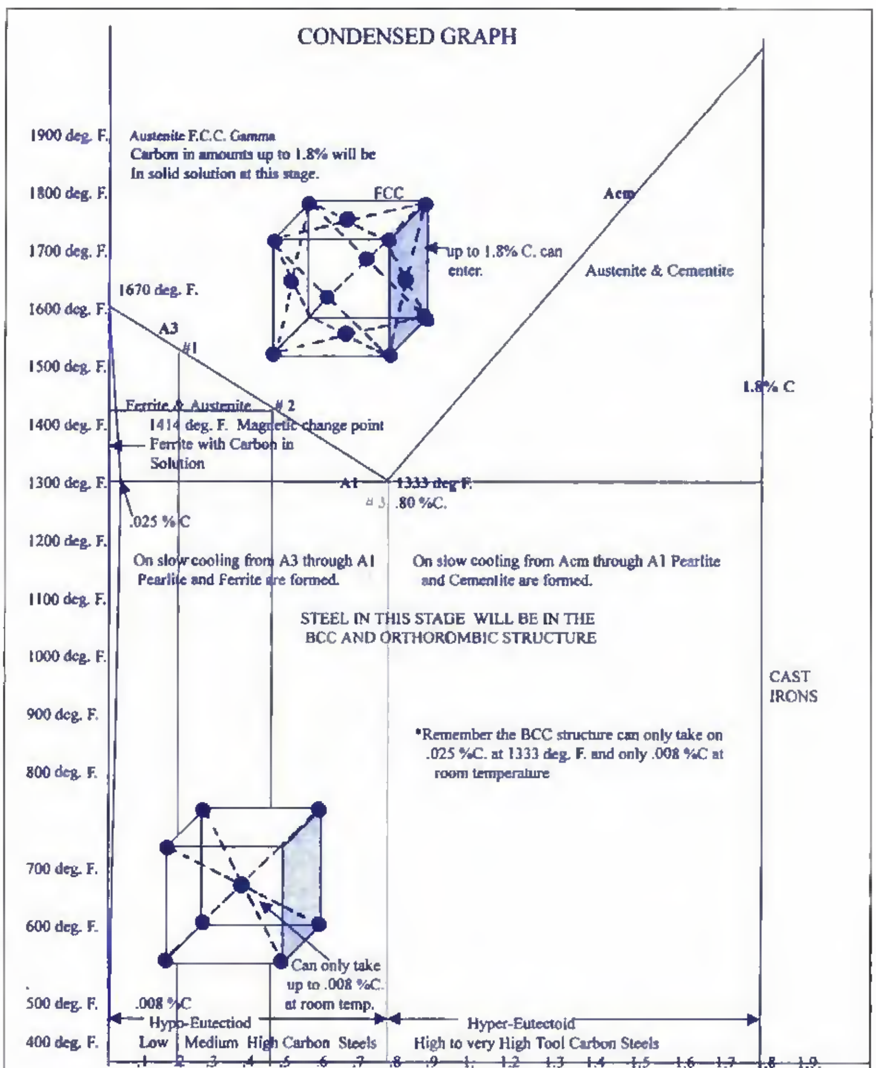

Fig. 8 — The cubic lattice structure of ferrite and austenite with carbon in solution.

ferrite and 12% cementite. On heating the reverse occurs and at 1333°F all the pearlite transforms to austenite. Keep in mind that at this temperature or just above, the grain size is at its smallest.

Thus far, we have discussed what happens when the steel is heated or cooled very slowly. Let's see what happens when we rapidly cool a piece of 0.8% carbon steel from the fully austenitic state. When this steel is rapidly cooled, the FCC state is actually suppressed down to around 200°F. By doing this, the austenite pearlite change has been completely passed and we have a FCC structure that has to change to a BCC structure. The transformation at this temperature is a shear-type transformation. Remember that the FCC structure can take on 1.8% C and the BCC structure can take on only 0.008% C at room temperature. If the 0.8% C steel is cooled in cold water, the FCC state is suppressed down to around 200°F, where it has to immediately transform to the BCC state. Due to this shear type of transformation, the carbon in the FCC state does not have sufficient time to precipitate, resulting in a BCC structure that has more carbon than normal. In fact, the BCC structure is highly distorted. This type of structure is called a highly distorted body-centered tetragonal, more commonly known as martensite. What we have done to this 0.8% C steel is fully harden it. A fully hardened steel has little use as an engineering material; therefore, we usually temper or draw the steel to a desired hardness. Tempering is a heat treating process in which a fully hardened piece of steel is reheated between 300 and 1000°F. Tempering releases some of the trapped carbon atoms. These released carbon atoms combine with iron atoms to produce iron carbide (Fe_3C) also known as cementite. The 0.8% C steel was chosen because it is one of the easiest to harden. Theoretically, a 0.1% C steel can be hardened if a fast enough cooling rate can be accomplished. A water quench, however, would not be fast enough; therefore, it is said a 0.1% C steel (mild steel) cannot be hardened. A 0.45% C steel is about the minimum carbon content steel that can be easily hardened using a water quench. It must be remembered that in order to harden steels in the 0.45–0.80% C range, they must be heated to just above the upper critical A3 line, then cooled in the desired cooling medium. Steels above 0.8% C can also be easily hardened. The only difference is they do not have to be heated to the Acm line and then cooled. The steel has to be heated to just above the A1 line then cooled, usually in oil. The reason is that steels above 0.8% C con-

Heat Treating Terms and Definitions

Hardening. Heating to just above the upper critical temperature A3 range and cooling in a desired cooling medium (cold water, brine, or oil).

Tempering. Reheating a hardened steel to a temperature between 300 and 1000°F, followed by cooling at any rate.

Annealing. Heating a piece of steel to 50°F above the A3 line, then holding at that temperature for one hour per inch of thickness, followed by cooling in a furnace.

Normalizing. Heating a piece of steel to 50°F above the A3 line, holding at that temperature for one hour per inch of thickness, followed by cooling in still air.

Stress Relieving. Heating to 50°F below the A1 line, holding long enough to relieve internal stresses, followed by cooling in still air. This process completely tempers a steel that has been hardened.

tain cementite as well as martensite on fast cooling. Cementite is a very hard constituent in steels.

Much has been said about grain size, and it is very important when hardening steels in the 0.45–0.8% C range. We know now that on heating to the A3 line, a small grain size is obtained and the steel is in the FCC structure. When this steel is cooled in water, martensite is formed and, most importantly, the small grain size is retained. When it is reheated to the desired temper, grain size is not affected but the carbon does precipitate a little and joins with existing iron atoms to form cementite. It produces a tempered, fine-grained steel.◆

Acknowledgments

Special thanks to the following people for their help in reviewing the article and for their comments: W. R. Irvine, department head, Department of Metallurgy, BCIT; Bruce Hawbolt, professor, UBC Dept. of Metallurgy; and Ernie Gill(deceased), western director, WIC.

Suggested Reading

The following are additional sources of information regarding metallurgy.

1. *Metals and their Weldability.* Miami, Fla.: American Welding Society.
2. *Metals And How To Weld Them.* Cleveland, Ohio: James F. Lincoln Arc Welding Foundation.
3. *Basic Metallurgy Programmed Instruction.* Materials Park, Ohio: The Metals Park Engineering Institute of the American Society for Materials.
4. Linnert, George. *Welding Metallurgy*, Vols. 1 and 2. Miami, Fla.: American Welding Society.
5. Krauss, George. *Principles of Heat Treatment of Steel.* Materials Park, Ohio: American Society for Materials.

REGISTER TO WIN A HARLEY SPORTSTER XL 1200 TODAY

And help advance the education of tomorrow's welders!

Visit our Silent Auction on-line at www.aws.org/foundation/auction. Bids are now being accepted!

The AWS Foundation Inc. will be raffling a Harley-Davidson Sportster during the AWS Annual Exposition to be held at Cobo Center, Detroit, Michigan, April 8-10, 2003.

For advance tickets fill out the enclosed coupon and mail back to the AWS Foundation. Coupons must be received no later than Wednesday, March 26. All monies received are used to benefit Welding Education Scholarships.

Name ______________________________

Address: ______________________________

City: ______________ State: ______________ Zip: ______________

Daytime Phone: ______________ Evening Phone: ______________

______ Tickets @ $5 each

______ Tickets @ 3 for $10

______ Tickets @ 7 for $20

Check Amount Enclosed: ______________

Credit Card Payment: (Circle One) Visa Master Card American Express

Card #: ______________ Expiration Date: ______________

Signature: ______________________________

Please Mail Response To:

AWS Foundation, Inc.
550 N.W. LeJeune Road
Miami, FL 33126
Phone: 305-443-9353 extensions 293

Rules:
Participant need not be present to win
Winner is responsible for shipping
Harley from Chicago

AWS Foundation, Inc.
Building Welding's Future through Education

NOTE: A DIAMOND (♦) DENOTES AN AWS-SPONSORED EVENT.

Conferences and Exhibitions

♦ **Seventh Robotic Arc Welding Conference and Exhibition.** February 10–11, Orlando, Fla. Sponsored by the American Welding Society. Contact: AWS Conferences, 550 NW LeJeune Rd., Miami, FL 33126, (800) 443-9353 ext. 449 or, outside the U.S., (305) 443-9353 ext. 449, FAX: (305) 443-1552; *www.aws.org*.

♦ **2nd International Brazing & Soldering Conference.** February 17–19, San Diego, Calif. Sponsored by the American Welding Society and ASM International. Contact: AWS Conferences, 550 NW LeJeune Rd., Miami, FL 33126, (800) 443-9353 ext. 449 or, outside the U.S., (305) 443-9353 ext. 449, FAX: (305) 443-1552; *www.aws.org*.

Essen Welding India 2003. The International Joining, Cutting, Surfacing Trade Fair and Conference. February 21–23, HITEX Hyderabad International Trade Exhibition Center. Hyderabad, India. Held in conjunction with Tube India International 2003 and Sheet Metal India. Organized by the Indian Welding Society. Contact: 49 (0) 201 7244-227 or -529; e-mail: *gedig@messe-essen.de*.

26th Annual Meeting of The Adhesion Society. Adhesion Fundamentals: From Molecules to Mechanisms and Modeling. February 23–26, Embassy Suites Kingston Plantation Resort, Myrtle Beach, S.C. The Adhesion Society Short course "Adhesion: Theory and Practice" will be held before the Annual Meeting February 21 and 22. For further information or to register, contact: *www.adhesionsociety.org*.

WESTEC Advanced Productivity Exposition. March 24–27, Los Angeles Convention Center, Los Angeles, Calif. Sponsored by the Society of Manufacturing Engineers (SME), American Machine Tool Distributors' Association, and the Association for Manufacturing Technology. Contact: SME Customer Service, (800) 733-4763 or, outside the United States, (313) 271-1500; *www.sme.org/westec*.

♦ **AWS Welding Show.** April 8–10, Cobo Conference/Exhibition Center, Detroit, Mich. Exhibition of the latest and best technology in the welding industry. Contact: AWS Convention and Exhibition Dept., 550 NW LeJeune Rd., Miami, FL 33126, (800) 443-9353 ext. 256 or, outside the U.S., (305) 443-9353 ext. 256, FAX: (305) 441-7451; *www.aws.org*.

Rapid Prototyping & Manufacturing Advanced Product Solutions Conference and Exposition. May 12–15, Hyatt Regency Chicago, Chicago, Ill. Contact: SME Customer Service (800) 733-4763 or, outside the United States, (313) 271-1500; *www.sme.org/rapid*.

♦ **Conference on Welding of Earthmoving and Construction Equipment.** May 20–21, Chicago, Ill. Sponsored by the American Welding Society. Contact: AWS Conferences, 550 NW LeJeune

Rd., Miami, FL 33126, (800) 443-9353 ext. 449 or, outside the U.S., (305) 443-9353 ext. 449, FAX: (305) 443-1552; *www.aws.org*.

JOM-11, Eleventh International Conference on the Joining of Materials. May 25–28, Helsingør-Denmark. Contact: JOM Institute, Gilleleje Strandvej 28, DK-3250 Gilleleje, Denmark, (45) 4835 5458, FAX: (45) 4835 5457, e-mail: *jom_aws@post10.tele.dk*.

ASME TURBO EXPO 2003: Power for Land, Sea, and Air and International Joint Power Generation Conference. June 16–19, Georgia World Congress Center, Atlanta, Ga. The two conferences will host a joint exposition. For more information, visit *www.asme.org*.

Welding Korea 2003. August 27–30, Indian Hall, COEX, Seoul, Korea. Organized by the Korea Welding Industry Cooperative and COEX. Contact: Welding Korea 2003 Secretariat, COEX World Trade Center, Samsung-dong, Gangnam-gu, Seoul, 135-731, Korea, (02) 6000-1055, 1056, FAX: (02) 6000-1309, e-mail: *kbc@coex.co.kr* or *donhan@coex.co.kr*; *www.weldingshow.co.kr*.

2003 International Construction and Utility Equipment Exposition (ICUEE). September 23–25, Kentucky Fair and Exposition Center, Louisville, Ky. Owned and produced by the Association of Equipment Manufacturers. Contact: ICUEE, (866) 236-0442, FAX: (414) 272-1170, e-mail: *info@icuee.com*; *www.icuee.com*.

Aluminum USA 2003, The North American Event for Production, Processing, and Applications. September 30–October 2, Navy Pier, Chicago, Ill. For registration and complimentary tickets, e-mail: *tickets@uk.dmgworldmedia.com*. For conference details, contact: Group Managing Editor Ken Stanford, 44 (0) 1737 855156, FAX: 44 (0) 1737 855469, e-mail: *kenstanford@uk.dmgworldmedia.com*; *www.dmgworldmedia.com*.

Educational Opportunities

ASME Continuing Education Institute Short Courses on Welding. ASME Section IX, Welding and Brazing Qualifications. March 10–12, Las Vegas, Nev.; May 5–7, Houston, Tex. Practical Welding Technology. March 10–12, Las Vegas, Nev.; June 2–4, Pittsburgh, Pa. Contact: (800) THE-ASME.

Victor 2003 Training Seminars. Victor Equipment Co. will be conducting training programs for gas apparatus and service repair technicians, end users, and sales personnel in 2003. For a complete schedule, contact: Aaron Flippen, (940) 381-1217; *www.victorequip.com*.

The Fabricators & Manufacturers Association, International (FMA), and the Tube and Pipe Association, International (TPA) Courses. A course schedule is available by calling (815) 399-8775; e-mail: *info@fmametalfab.org*; *www.fmametalfab.org*.

Malcom Plastic Welding School. A comprehensive two-day, hands-on course that leads to certification in accordance with the latest European DVS-approved plastic welding standards for hot gas and extrusion welding techniques. Contact: Sheila Carpenter, Administration, Malcom Hot Air Systems, 1676 E. Main Rd., Portsmouth, RI 02871, (888) 807-4030, FAX: (401) 682-1904, e-mail: *info@malcom.com*; *www.plasticweldingtools.com*.

Educational Opportunities

AWS Schedule — CWI/CWE Prep Courses and Exams

Exam application must be submitted six weeks before exam date. For exam information and an application, contact the AWS Certification Dept., (800) 443-9353 ext. 273. For exam prep course information, contact the AWS Education Dept., (800) 443-9353 ext. 229.

Cities	Exam Prep Courses	CWI/CWE Exams
Anchorage, Alaska	April 6–11 (API 1104 Clinic also offered)	April 12
Charlotte, N.C.	March 2–7 (API 1104 Clinic also offered)	March 8
Columbus, Ohio	February 3–7 (API 1104 Clinic also offered)	February 8
Corpus Christi, Tex.	February 9–14 (API 1104 Clinic also offered)	February 15
Detroit, Mich.	March 31–April 5 9-YEAR RECERTIFICATION COURSE	
Detroit, Mich.	April 6–11 (API 1104 Clinic also offered)	April 12
Houston, Tex.	March 30–April 4 (API 1104 Clinic also offered)	April 5
Las Vegas, Nev.	March 9–14 (API 1104 Clinic also offered)	March 15
Miami, Fla.	EXAM ONLY	February 13
Miami, Fla.	February 17–22 9-YEAR RECERTIFICATION COURSE	
Miami, Fla.	February 23–28 (API 1104 Clinic also offered)	March 1
Miami, Fla.	EXAM ONLY	March 20
Miami, Fla.	EXAM ONLY	April 24
Minneapolis, Minn.	March 30–April 4 (API 1104 Clinic also offered)	April 5
Mobile, Ala.	EXAM ONLY	March 29
Newark, N.J.	March 16–21 (API 1104 Clinic also offered)	March 22
Norfolk, Va.	February 2–7 (API 1104 Clinic also offered)	February 8
Oklahoma City, Okla.	April 6–11 (API 1104 Clinic also offered)	April 12
Perrysburg, Ohio	EXAM ONLY	March 15
Phoenix, Ariz.	March 23–28 (API 1104 Clinic also offered)	March 29
Rochester, N.Y.	EXAM ONLY	March 22
St. Louis, Mo.	EXAM ONLY	April 26
San Francisco, Calif.	March 2–7 (API 1104 Clinic also offered)	March 8
Seattle, Wash.	February 9–14 (API 1104 Clinic also offered)	February 15
Springfield, Ill.	March 9–14 (API 1104 Clinic also offered)	March 15
Tampa, Fla.	February 2–7 (API 1104 Clinic also offered)	February 8

AWS President Levert Attends Indiana Section's Student Night

AWS President Ernest Levert, center, with Indiana Section Chairman Bennie Flynn, right, and past Chairman Bob Richwine.

American Welding Society President Ernest Levert attended the AWS Indiana Section's Student Night open house hosted by Lawrence Township's McKenzie Career Center in Indianapolis, Ind., on November 18, 2002. Levert spoke to students about the welding of the International Space Station. Levert was honored to be invited to attend the event as he has stressed the importance of welding education throughout his term as the Society's president. Whenever his busy schedule allows, Levert can be found speaking to high school and junior high students, and even elementary school classes.

Education is always the focus of Student Night — learning about schools, what is needed to advance in the profession, and what career and job opportunities are available in the welding field. "(The students) should gain a knowledge that there's a lot more to welding than putting pieces together," said Indiana Section Chairman Bennie Flynn. He pointed out there are other jobs in the welding industry for kids to consider including sales, engineering, education, research and development, manufacturing, repair, and robotics.

The Indiana Section's Student Night was a huge success with more than 300 students and guests attending. Students had the opportunity to speak with welding educators from universities, representatives from the various unions that use welders, welders working in the field, researchers, distributors, and more. Workers and educators from throughout the state and nation gathered to demonstrate and teach students about welding and let them learn first hand about the other jobs available in the field. In addition to Levert, Steve Houston, director of the Training Materials Department at Hobart Institute of Welding, and Bob Richwine, past AWS Indiana Section chairman, also spoke to students and guests.

AWS President Ernest Levert, far left, addressing students at the AWS Indiana Section's Student Night at the McKenzie Career Center.

During the evening, students were able to watch demonstrations of the various welding processes and view computer welding simulators. They also got the chance to learn about orbital welding and weld alongside welding robots.

The Bernard K. McKenzie Career Center in Indianapolis was invited to host the Indiana Student Night by Flynn. The center is a high school offering both academic and vocational classes. The school's welding program currently has 125 students. Instructor Ed Wyatt said the goal of the welding program is to prepare students for employment at the entry level so they can advance to more technical skills through either on-the-job training or higher education.

The McKenzie Career Center is the only high school in the nation with a blacksmithing program. The program was brought to the school last year by Wyatt with the help of retired Indianapolis lawyer Robert Dalrymple, who donated more than $15,000 worth of blacksmithing supplies to the school.

As an added attraction Wyatt's students from the blacksmithing program gave demonstrations and assisted those visitors who wanted to try their hand at it. ♦

AWS Foundation Announces Its Third Annual Silent Auction

The AWS Foundation is proud to announce the present donors to its Third Annual Silent Auction, April 8–10, at Cobo Hall in Detroit, Mich.

The auction benefits the AWS Foundation's scholarship programs. Companies wishing to donate items for the auction ($250 minimum value), please call Neida Herrera at (800) 443-9353 ext. 461 or e-mail to: *neida@aws.org.*

To bid in advance, visit the American Welding Society's Web site at *www.aws.org/foundation/auction/* or contact the AWS Foundation at (800) 443-9353 ext. 461 with the item name and your bid, complete name, address, and telephone number. To bid on an item while attending the AWS Welding Show, please go to the AWS Foundation booth.

Malcolm Gilliland
Model MTG-600 CV Power Source
Minimum Bid: $1500

Select Arc
1 Pallet - 1200 lb Welding Wire
Minimum Bid: $900

BMS/BTU
Three Spools (28 lb) of Kobelco Wire
Minimum Bid: $500

Calco Controls, Inc.
Mellath Automatic Electric Heater
Minimum Bid: $350

Vic Matthews
AWS District 10 Director
Two Joe Gibbs Autographed Footballs
Minimum Bid: $225 Per Item

Jackson Products, Inc.
NexGen EQC
Minimum Bid: $190

Inweld Corp.
Welding and Cutting Kit
Minimum Bid: $170

Earl Lipphardt, AWS Treasurer
One Set of Proteactic Stainless Steel Flex Shaft Firm Golf Clubs
Minimum Bid: $160

The Lincoln Electric Co.
Joe Gibbs Simpson Racing Helmet
Minimum Bid: $150

Flexovit Abrasives
Metal Hog Basket
Minimum Bid: $130

AWS St. Louis Section
Sony DSC-P51 Digital Camera
Minimum Bid: $130

Welding Engineering Supply Co.
TRUMPF TKF 700-0 Beveller
Minimum Bid: $1300

Quality 1 Welding & Consulting, Inc.
Welder Training Fixture
Minimum Bid: $650

Jerry Uttrachi, AWS Vice President-Elect
L-TEC ST-21 Water-Cooled GMA Torch
Minimum Bid: $300

AWS New Orleans Section and New Orleans Mardi Gras Club
Two Tickets for a Ride on a Mardi Gras Float
Minimum Bid: $300

Wyndham Miami Beach Resort
Two-Night/Three-Day Stay for Two
Minimum Bid: $225

Hornell, Inc.
Speedglas Flexview with 900XF Lens
Minimum Bid: $175

IWDC (WeldMark)
Weldmark Welding & Cutting Outfit
Minimum Bid: $170

Metabo Corporation
W14-125 Ergo
Minimum Bid: $160

Revco Industries, Inc.
12 Pairs Alpha TIG™ Welding Gloves and 12 pairs Tool Handz Plus Ergonomic Gloves
Minimum Bid: $140

PFERD, Inc.
PFERD New Thin Cut-Off Wheels
Minimum Bid: $130

AWS York-Central Pa. Section
Patriotic Cylinder Bell with Stand
Minimum Bid: $125

Chart Industries
Dura-Cyl Cryogenic Container
Minimum Bid: $1100

The Victoria Group, Inc.
Five-Day Lead Auditor Class
Minimum Bid: $650

Sonesta Beach Resort
Two-Night/Three-Day Stay for Two
Minimum Bid: $375

Saf-T-Cart
Two 1324 HE
Minimum Bid: $275 Per Item

John Brown Limited, Inc.
Two-Night Stay at the Harvard Club
Minimum Bid: $225

Hyatt Regency McCormick Place
Two-Night Weekend for Two
Minimum Bid: $175

Mathey Dearman
Model DS-50 lb Fixed Temperature Electrode Oven
Minimum Bid: $160

ArcOne Welding & Safety Products
80-Amp Welding Machine
Minimum Bid: $160

The Lincoln Electric Co.
Gear Leather Bomber Jacket
Minimum Bid: $130

Welding & Joining Management Group
Longaberger Basket
Minimum Bid: $130

Susquehanna Pfaltzgraff Co.
Twenty-Piece Set of Pfaltzgraff Stoneware
Minimum Bid: $120

AWS Foundation Silent Auction

— Continued from previous page

Steiner Industries
Weldon's Safety Package
Minimum Bid: $100

Laser Quest of Austin, Texas
Two Birthday Parties for Ten People
Minimum Bid: $75 Each Party

Sellstrom Manufacturing Co.
Titan Welding Helmet with X554 Autodarkening Filter
Minimum Bid: $75

Sellstrom Manufacturing Co.
Titan Welding Helmet with X554 Autodarkening Filter
Minimum Bid: $75♦

Deadline Nears for AWS District Scholarships

Don't forget to contact your AWS Section representatives for an application for an AWS District Scholarship. The deadline for AWS District Scholarships is March 15 for the 2003–2004 school term.

For further information on the AWS Foundation scholarship and student loan programs, visit the AWS Foundation on the Web at *www.aws.org/foundation/* or contact Neida Herrera at AWS Foundation, 550 NW LeJeune Rd., Miami, FL 33126, (800) 443-9353 ext. 461, e-mail *neida@aws.org*.♦

Ordering AWS Publications

AWS publications are distributed by Global Engineering Documents. To order publications, call Global Engineering at (800) 854-7179 or, outside the United States, (303) 397-7956. Publications can also be ordered from the e-store on the AWS Web site at *www.aws.org/cgi-bin/shop/*.♦

Nominations for AWS District Directors

The term of office for District Directors in the following AWS Districts will terminate on May 31, 2004. As District Nominating Committees will be appointed this spring, it is time to be thinking of position nominations. For further information, use your current District Director's contact information below.

District 2
***Al F. Fleury**, President
A. Fleury & Associates
10 Glen Rd.
Bound Brook, NJ 08805
(732) 868-0768
FAX: (732) 868-0768
e-mail: *alnpat@cnjnet.com*

District 5
Wayne J. Engeron
Engineered Alloys/Systems
4175 Oaknoll Circle
Duluth, GA 30096
(404) 501-9185
FAX: (404) 501-0956
e-mail: *eas1corp@aol.com*

District 8
Wallace E. Honey
Anchor Research Corp.
8775 Old Water Plant Rd.
Russellville, AL 35654
(256) 332-3366
e-mail: *Cehoney75@aol.com*

District 11
***Scott C. Chapple**, Corp. Welding Eng.
Midway
21693 Harding
Rockwood, MI 48173
(586) 772-1514
FAX: (586) 772-1230
e-mail: *schapple@flexngate-mi.com*

District 14
Tully C. Parker, District Manager
Miller Electric Mfg. Co.
123 Olde Farm Rd
Troy, IL 62294
(618) 667-7744
FAX: (618) 667-7744
e-mail: *tparke@millerwelds.com*

District 17
Oren P. Reich, Instructor
Texas State Technical College at Waco
208 Gerald Lane
Elm Mott, TX 76640
(254) 867-2203
FAX: (254) 867-3570
e-mail: *oren.reich@tstc.edu*

District 20
Jesse A. Grantham, Owner
Welding and Joining Management Group
7100 N. Broadway, Ste. 1C
Denver, CO 80221
(303) 451-6759
FAX: (303) 280-4747
e-mail: *jesse@wjmg.com*

*Denotes current District Director is not eligible for reelection to another three-year term.

Third International Conference on Welding

The JOM Institute sponsored the Third International Conference on Education in Welding on October 13–16, 2002, in Helsingnør, Denmark. American Welding Society Director-at-Large Osama Al-Erhayem, shown at right during his opening remarks at the conference, is general secretary of the JOM Institute as well as chairman of the AWS Scandinavian Section.

Also at the conference were AWS Vice President Jim Greer and AWS Education Committee members Phil Pratt and Chris Pollock, AWS educational development director.♦

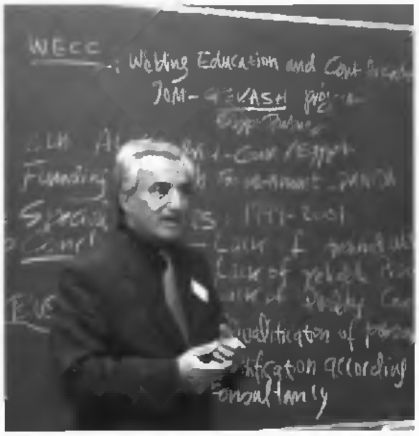

AWS Publications

Specification for the Qualification of Welding Sales Representatives Published

Specification for the Qualification of Welding Sales Representatives (AWS B5.14:2002) has been released by the American Welding Society (AWS). This ANSI-approved specification outlines the minimum requirements to fulfill on-the-job responsibilities in a welding sales representative position. The welding sales representative is required to demonstrate the use of welding equipment and supplies, direct sales of welding merchandise, determine customer needs, and make appropriate recommendations. Basic qualifying factors, such as education, prior work experience, and examination requirements are identified in this standard. The AWS B5.14:2002, *Specification for the Qualification of Welding Sales Representatives*, is four pages long and costs $18 for AWS members and $24 for nonmembers.

Guide for Thermal-Spray Operator Qualification Released

In order to ensure the safe and successful execution of job duties, thermal-spray operators must possess a comprehensive set of skills and knowledge. To provide recommendations and documentation for thermal-spray operator qualification based on knowledge and skill testing, the American Welding Society, with the approval of the American National Standards Institute, has published AWS C2.16/C2.16M:2002, *Guide for Thermal-Spray Operator Qualification*.

Guide for Thermal-Spray Operator Qualification contains 12 separate qualification tests for engineering and corrosion control applications. These include qualification tests for high-velocity oxygen fuel (HVOF) spraying, flame spray-fusing, arc spraying, plasma spraying, and flame spraying.

The cost of AWS C2.16/C2.16M:2002, *Guide for Thermal-Spray Operator Qualification*, is $24 for AWS members and $32 for nonmembers.

New Operator's Manual for Oxyfuel Gas Cutting Now Available

The American Welding Society has issued AWS C4.2:2002, *Operator's Manual for Oxyfuel Gas Cutting*. This ANSI-approved standard describes the oxyfuel gas cutting process and includes information on recommended equipment as well as safety and operating procedures. Safety is stressed throughout this manual, but it is recommended operators also consult ANSI Z49.1, *Safety in Welding, Cutting, and Allied Processes*, which is also available from the American Welding Society.

This edition of *Operator's Manual for Oxyfuel Gas Cutting* supersedes the previously published AWS C4.2-90 standard by the same name. New additions to AWS C4.2:2002 include the latest procedures and safety requirements to be used when working with oxyfuel gas cutting equipment.

AWS C4.2:2002, *Operator's Manual for Oxyfuel Gas Cutting*, is 25 pages long. The price is $24 for AWS members and $32 for nonmembers.

Ordering Information

To order AWS specifications and standards, call Global Engineering Documents at (800) 854-7179 or, outside the United States, (303) 397-7956 or visit the AWS Web store at *www.aws.org/cgi-in/shop*.♦

Nominations Sought for National Offices

American Welding Society members who wish to nominate candidates for president, vice president, and director-at-large on the AWS Board of Directors for the term starting June 1, 2004, may either:

1) Send their nominations before March 15, 2003, to Richard L. Arn, National Nominating Committee Chairman, American Welding Society, 550 NW LeJeune Rd., Miami, FL 33126;

or

2) Present the nomination in person at the open session of the National Nominating Committee Meeting scheduled for 10:00 to 11:00 a.m., Tuesday, April 8, 2003, at the COBO Conference/Exhibition Center, Detroit, Mich., during the AWS 2003 Welding Show.

Nominations must be accompanied by biographical material on each candidate, including a written statement by the candidate as to willingness and ability to serve if nominated and elected, and a 5 x 7 in. black-and-white or color photograph.♦

Submit Your Technical Committee Reports

Committee Chairmen — We want to recognize the efforts of your committee and inform our readers of its accomplishments. Send a brief profile of its activities and recent accomplishments, along with a member roster and contact numbers, and we will publish it in the Welding Journal's Society News section.

Send your submissions to

Susan Campbell, Associate Editor
American Welding Society
550 NW LeJeune Rd.
Miami, FL 33126
Telephone, (305) 443-9353 ext. 244
FAX: (305) 443-7404
e-mail: *campbell@aws.org*.♦

AWS Membership

Member Grades	As of January 1, 2003
Sustaining Companies	419
Supporting Companies	261
Educational Institutions	306
Affiliate Companies	57
Total Corporate Members	**1043**
Individual Members	43,162
Student Members	4,451
Total Members	**47,613**

Standards Notices

Standards for Public Review

AWS was approved as an accredited standards-preparing organization by the American National Standards Institute (ANSI) in 1979. AWS rules, as approved by ANSI, require all standards be open to public review for comment during the approval process. This column also advises of ANSI approval of documents. The following standards are submitted for public review. A draft copy may be obtained by contacting Rosalinda O'Neill at AWS, Technical Services Business Unit, 550 NW LeJeune Rd., Miami, FL 33126; telephone: (800) 443-9353 ext. 451 or, outside the United States, (305) 443-9353 ext. 451; e-mail: roneill@aws.org.

A5.25/A5.25M-97, *Specification for Carbon and Low-Alloy Steel Electrodes and Fluxes for Electroslag Welding.* Reaffirmed standard. $9.00. [ANSI Public Review expires February 25, 2003.]

A5.26/A5.26M-97, *Specification for Carbon and Low-Alloy Steel Electrodes for Electroslag Welding.* Reaffirmed standard. $9.00. [ANSI Public Review expires February 25, 2003.]

C2.21M/C2.21:200X, *Specification for Thermal Spray Equipment Acceptance Inspection.* New standard. $6.50. [ANSI Public Review expires March 12, 2003.]

D1.2:200X, *Structural Welding Code — Aluminum.* Revised standard. $58.00. [Second ANSI Public Review expires February 10, 2003.]

F1.6:200X, *Guide for Estimating Welding Emissions for EPS and Ventilation Permit Reporting.* New standard. $3.00. [ANSI Public Review expires February 25, 2003.] ♦

Technical Committee Meetings

All AWS technical committee meetings are open to the public. Persons wishing to attend a meeting should contact the staff secretary of the committee as listed below at AWS, 550 NW LeJeune Rd., Miami, FL 33126; telephone: (800) 443-9353 or, outside the United States, (305) 443-9353.

February 12, Committee on Robotic and Automatic Welding. Orlando, Fla. Standards preparation and general meeting. Staff contact: Peter Howe, ext. 309.

February 13–14, Technical Activities Committee. Miami, Fla. General meeting. Staff contact: Leonard P. Connor, ext. 302.

February 20, Committee on Brazing and Soldering. San Diego, Calif. Standards preparation and general meeting. Staff contact: Cynthia L. Jenney, ext. 304.

February 20, Subcommittee on Brazing Handbook. San Diego, Calif. Standards preparation and general meeting. Staff contact: Cynthia L. Jenney, ext. 304.

February 20, Subcommittee on Soldering. San Diego, Calif. Standards preparation and general meeting. Staff contact: Cynthia L. Jenney, ext. 304.

February 20, Subcommittee on Education and Safety. San Diego, Calif. Standards preparation and general meeting. Staff contact: Cynthia L. Jenney, ext. 304.

February 20, Subcommittee on Brazing Specifications. San Diego, Calif. Standards preparation and general meeting. Staff contact: Cynthia L. Jenney, ext. 304.

February 20, Subcommittee on Brazing Conferences. San Diego, Calif. Standards preparation and general meeting. Staff contact: Cynthia L. Jenney, ext. 304.

February 21, Subcommittee on Filler Metals and Fluxes for Brazing. San Diego, Calif. Standards preparation and general meeting. Staff contact: Cynthia L. Jenney, ext. 304.

March 17, SSPC/NACE/AWS Tri-Society Thermal Spray Committee on the Corrosion Protection of Steel. San Diego, Calif. Standards preparation and general meeting. Staff contact: Edward F. Mitchell, ext. 254.

March 17, Subcommittee on Stainless Steel Alloys. San Diego, Calif. Standards preparation and general meeting. Staff contact: Edward F. Mitchell, ext. 254.

March 18, Subcommittee on Titanium and Zirconium Filler Metals. San Diego, Calif. Standards preparation and general meeting. Staff contact: Edward F. Mitchell, ext. 254.

March 18, Subcommittee on Reactive Alloys. San Diego, Calif. Standards preparation and general meeting. Staff contact: Edward F. Mitchell, ext. 254.

March 19, Subcommittee on Hot Gas Welding and Extrusion Welding. San Diego, Calif. Standards preparation and general meeting. Staff contact: Edward F. Mitchell, ext. 254

March 24–28, Committee on Structural Welding. Atlantic City, N.J. Standards preparation and general meeting. Staff contact: John L. Gayler, ext. 472. ♦

Notice of Annual Meeting, American Welding Society

The Annual Meeting of the members of the American Welding Society will be held on Monday, April 7, 2003, beginning at 9:00 a.m. at COBO Conference/Exhibition Center, Detroit, Michigan.

The regular business of the Society will be conducted, including election of officers and nine members of the Board of Directors. Any business properly brought before the membership will be considered. ♦

Sustaining Member Company

ZJ Industries, Inc.
25 W. Laura Dr.
Addison, IL 60101
(630) 543-6655
FAX (630) 543-6644

ZJ Industries is a full-service resistance welding product manufacturer specializing in electrodes, tips, adapters, holders, welding machine arms, seam welding wheels, and more.

The company is dedicated to providing quality products, on-time delivery, and low prices. ♦

American Welder Gear Available on the AWS Web Site

The American Welding Society proudly introduces a new line of American Welder™ Gear. The line carries more than 60 products ranging from pens to apparel to watches. AWS members receive a 10% discount on purchases. To check out the full line of Gear, visit *www.aws.org/gear/* or call (800) 443-9353 to request a catalog. ♦

AWS Welcomes New Supporting Companies

New Educational Institutions

Henderson County High School
2424 Zion Rd.
Henderson, KY 42420

Morrison R. Waite High School
301 Morrison Dr.
Toledo, OH 43605

New Supporting Companies

Carolina Steel Services, Inc.
1235 Sandwood Ave.
Florence, SC 29506

Quality Control & Inspection
134 Peak Station Rd.
Clinton, TN 37716

AWS Welcomes New Affiliate Member Companies

Varsity Welding
1673 Austin
Troy, MI 48083

South Texas Welding
Inspection Services
841 N. Hustin St.
San Benito, TX 78586

Commerce Construction Corp.
603 Heron Dr., Unit 1
P.O. Box 662
Bridgeport, NJ 08014-0662

Advance Welding
47 Allston Ave.
West Springfield, MA 01089

Mike Knowlton Welding
2568 Holmes Rd.
New Concord, OH 43762

Springfield Metal Products
8 Commerce St.
Springfield, NJ 07081-2983

Slob and Son's Pipe & Casing, Inc.
207 N. State St.
Marion, OH 43302

Welding/Exhaust
381 Huku Lii Pl.
Kihei, HI 96753

Spiers Welding
1277 Long Ridge Rd.
Stamford, CT 06903

Best Welding & Metal Repair
245 Landing Rd.
Blackwood, NJ 08012

RJay's Mobile Welding &
Custom Fabrication
185 Fort Hall Ave.
American Falls, ID 83211

Premier Industries
P.O. Box 70
Harvey, LA 70059

Announce Your Section's Activities

Stimulate attendance at your Section's meetings and training programs with free listings in the Section Meeting Calendar column of Society News.

Useful information includes your Section name; activity date, time, and location; speaker's name, title, affiliation and subject; and notices of golf outings, seminars, contests, and other special Section activities.

If some of your meeting plans are sketchy, send the name and phone number of a person to contact for more information.

Send your new calendar to Susan Campbell, Associate Editor, Welding Journal Dept., AWS, 550 NW LeJeune Rd., Miami, FL 33126 or e-mail: *campbell@aws.org*. ♦

SECTION NEWS

DISTRICT 1

Director: Geoffrey H. Putnam
Phone: (802) 439-5916

Central Massachusetts Section Chairman Michael Wunschel, right, presenting a Plaque of Appreciation to his son Robert Wunschel for hosting a tour of the Baystate Piping facility.

CENTRAL MASSACHUSETTS/ RHODE ISLAND

October 17, 2002
Speaker: **Michael Wunschel,** foreman.
Affiliation: Baystate Piping, Middleboro, Mass.
Activity: Section members toured the Baystate Piping facility. The tour was hosted by Section Chairman **Robert Wunschel**'s son **Michael.**

DISTRICT 2

Director: Alfred F. Fleury
Phone: (732) 868-0768

NEW JERSEY

September 17, 2002
Speaker: **Robert Wallach**, development engineer.
Affiliation: Permabond, a division of National Starck and Chemical Co.
Topic: The four types of commercial adhesives for joining and their properties, applications, and limits.
Activity: **August Manz** was presented with the Section Meritorious Award. **James Dolan** and **Fred Wensor** each received the District Meritorious Award.

DISTRICT 3

Director: Alan J. Badeaux, Sr.
Phone: (301) 449-4800, ext. 286

Ann Marie Arcure, left, and Ray Stout, right, of Sandvik Steel, with Lehigh Valley Section Program Chairman Dan Marino.

Mike Galler, host of the November Lehigh Valley Section meeting, demonstrating metal spraying.

LEHIGH VALLEY

October 1, 2002
Speaker: **Ray Stout**, sales manager-welding products.
Affiliation: Sandvik Steel, Clarks Summit, Pa.
Activity: Members received a plant tour of Sandvik Steel's welding and wire division.

Lehigh Valley Section Student Affairs Chairman Rich Gallagher, left, with Bethlehem Area Vocational-Technical School instructor Mike Galler.

Master Bladesmith Bill Moran during his presentation at Maryland's Cumberland Valley Satellite Section's December meeting.

November 5, 2002
Activity: Bethlehem Area Vocational-Technical School instructor **Mike Galler** hosted an evening of hands-on metal spraying and discussions on thermal arc spray coatings.

MARYLAND

December 12, 2002
Speaker: **Bill Moran**, master bladesmith.
Topic: The art of custom knifemaking, including the history and techniques of forging Damascus steel blades.
Note: This meeting was held by the Cumberland Valley Satellite Section.

DISTRICT 4

Director: Roy C. Lanier
Phone: (252) 321-4285

DISTRICT 5

Director: Wayne J. Engeron
Phone: (404) 501-9185

William C. Thompson, recipient of an AWS scholarship, poses with the Certificate of Recognition presented to him by the South Carolina Section.

Kelly Morrow, left, and Ken Fisher, center, of Miller Electric Mfg. Co., with Florida West Coast Chairman Lee Clemens.

SOUTH CAROLINA

NOVEMBER 21, 2002
Activities: The Section held its Annual Frogmore Stew Social. **William C. Thompson**, a welding technology student at Trident Technical College, was awarded a Certificate of Recognition as a recipient of an AWS Scholarship.

FLORIDA WEST COAST

NOVEMBER 13, 2002
Speaker: **Ken Fisher**, high-deposition process manager.
Affiliation: Miller Electric Mfg. Co., Appleton, Wis.
Topic: Advancements in submerged arc technology.

NORTH CENTRAL FLORIDA

NOVEMBER 19, 2002
Speaker: **Steve Weaver**, district manager.
Affiliation: Thermal Dynamics, West Lebanon, N.H.
Topic: GMAW/FCAW and plasma cutting machines for the homeowner, hobbiest, and automotive enthusiast.
Activities: Past Chairman **Mark Hynzy** was presented with a Certificate of Appreciation. Holox of Ocala provided an oxyfuel welding/cutting set as a door prize. Hands-on demonstrations followed the evening's technical presentation.

DISTRICT 6

Director: Neal A. Chapman
Phone: (315) 349-6960

SYRACUSE

OCTOBER 2, 2002
Speaker: **E. Burrell Fisher**, P.E.
Affiliation: Consulting engineer.
Topic: Certified Mill Test Reports.

NOVEMBER 13, 2002
Speaker: **Ken Phy**, senior project manager.
Affiliation: Entergy Nuclear Northeast, Inc.
Topic: Spent nuclear fuel storage and welding.
Activity: District 6 Director **Neil Chapman** attended the meeting.

NORTHERN NEW YORK

DECEMBER 3, 2002
Speaker: **Bob Sinuc**, vice president of engineering.
Affiliation: Plug Power.
Topic Fuel cells, current and future.
Activities: Members toured the Plug Power plant. **David Parker** was recognized for having reached 35 years as an AWS member.

DISTRICT 7

Director: Robert J. Tabernik
Phone: (614) 488-7913

CINCINNATI

NOVEMBER 19, 2002
Speakers: **Jeff Minter**, senior project manager, and **Van Campbell**, welder, ironworker, Local 44 foreman.
Affiliations: Ben Hur Construction Company.
Topic: Stadium construction — the Paul Brown stadium and the Cincinnati Reds.
Activity: **Michael Kreiner** and **Uwe Aschemeier** were presented with the Dalton E. Hamilton Memorial CWI of the Year Award.

Guest speakers Van Campbell, left, and Jeff Minter, right, with Cincinnati Section member Uwe Aschemeier.

Cincinnati Section member Uwe Aschemeier, left, accepting the Dalton E. Hamilton Memorial CWI of the Year Award from District 7 Director Robert Tabernik.

Members of the Pittsburgh Section during their tour of the American Bridge Co. facility viewing a massive piece of steel slated to be used for the guard rail on the side of a bridge.

PITTSBURGH

NOVEMBER 19, 2002
Activity: The Section toured the American Bridge Co. plant. **Jon Young** hosted the tour. Students from Beaver Valley Vo-Tech attended the tour.

SPECIAL OFFER (See reverse) – IT'S EASIER THAN EVER TO RECRUIT NEW AWS INDIVIDUAL MEMBERS

AWS is nearly 50,000 members strong. Imagine how much stronger we would be if each of our members took just a few minutes to encourage one of their colleagues to join AWS. We could potentially boast a membership of nearly 100,000 – making us one of the largest associations in the world...and giving us the resources necessary to expand your benefits as an AWS Member. Referrals are our most successful member recruitment tool. Our Members know first-hand how useful AWS Membership is. Who better than you to encourage someone to join us?

In appreciation for your instrumental role in helping us grow our membership base, you will receive a variety of awards and prizes for your involvement. The more members you sponsor, the more rewards you'll receive.

We've worked out a "Top Ten" list of reasons our members think AWS is THE resource for staying on top of today's materials joining industry. You already know what AWS does for you. Why not take a moment or two to point out some of these reasons to one of your co-workers?

Top Ten Reasons to be an AWS Member:

10. To encourage the next generation with AWS Scholarships awarded through the AWS Foundation and discounted student memberships.
9. To have a voice in a global community that promotes and takes pride in the materials joining industry.
8. For Members'-only discounts on car rentals, insurance, and more!
7. To obtain valuable technical knowledge with 300+ publications available.
6. To experience the wave of the future through the world's largest materials joining show by attending the AWS Welding Show.
5. For on-going training through AWS seminars and conferences.
4. To save hundreds of dollars with Members'-only discounts on all AWS publications, conferences, seminars and certification programs.
3. Because your FREE annual subscription to the *Welding Journal* will provide you with valuable information to keep you at the forefront of the materials joining industry.
2. For career advancement through networking opportunities at local Section Meetings and by utilizing the AWS Website which includes AWS JobFind.

And the #1 reason to become an AWS Member...

...**Because of the savings, knowledge and prestige you'll receive from the premier Society for materials joining professionals.**

PRIZE CATEGORIES

President's Honor Roll:

Recruit 1-5 new Individual Members and receive an American Welder™ T-shirt.

President's Club:

Recruit 6-10 new Individual Members and receive an American Welder™ polo shirt.

President's Roundtable:

Recruit 11-19 new Individual Members and receive an American Welder™ watch.

President's Guild:

Recruit 20 or more new Individual Members and receive an American Welder™ watch, a one-year free AWS Membership, the "Shelton Ritter Member Proposer Award" Certificate and membership in the Winner's Circle.

Winner's Circle:

All Members who recruit 20 or more new Individual Members will receive annual recognition in the *Welding Journal* and will be honored at the AWS Welding Show.

SPECIAL PRIZES

Participants will also be eligible to win prizes in specialized categories. Prizes will be awarded at the close of the campaign (June 2003).

Sponsor of the Year:

The individual who sponsors the greatest number of new Individual Members during the campaign will receive a plaque, a trip to the 2004 AWS Welding Show, and recognition at the AWS Awards Luncheon at the AWS Welding Show.

Student Sponsor Prize:

AWS Members who sponsor two or more Student Members will receive an American Welder™ T-shirt.

The AWS Member who sponsors the most Student Members will receive a free, one-year AWS Membership and an American Welder™ polo shirt.

International Sponsor Prize:

Any member residing outside the United States, Canada and Mexico who sponsors the most new Individual Members, will receive a complimentary AWS Membership renewal.

LUCK OF THE DRAW

For every new member you sponsor, your name is entered into a quarterly drawing. The more new members you sponsor, the greater your chances of winning. Prizes will be awarded in November 2002, as well as in February and June 2003.

Prizes Include:

- American Welder™ T-shirt
- Complimentary AWS Membership renewal
- American Welder™ polo shirt
- American Welder™ baseball cap

SUPER SECTION CHALLENGE

The AWS Section in each District that achieves the highest net percentage increase in new Individual Members before the June 2003 deadline will receive special recognition in the *Welding Journal* and a District Membership Award.

The AWS Sections with the highest numerical increase and greatest net percentage increase in new Individual Members will each receive the Neitzel Membership Award.

American Welding Society

550 N.W. LeJeune Rd. • Miami, FL 33126
Visit our website http://www.aws.org

DISTRICT 8

Director: Wallace E. Honey
Phone: (256) 332-3366

NORTHEASTERN MISSISSIPPI

NOVEMBER 21, 2002
Activity: The Section held the two-day seminar "Innovations in Modern Manufacturing" at the Center for Manufacturing Technology Excellence.

NOVEMBER 21, 2002
Activity: A representative of Harris spoke at the East Mississippi Community College for the Section's Student Night.

DECEMBER 6, 2002
Activity: A holiday party and Ladies' Night was held at the Golden Horn Restaurant.

GREATER HUNTSVILLE

NOVEMBER 21, 2002
Activity: The Section held a Welding Contest at the Blount County Area Vocational School.

NASHVILLE

DECEMBER 3, 2002
Activity: The Section toured the Bobby Hamilton racing shop in Juliet, Tenn.

DECEMBER 7, 2002.
Activity: Members celebrated the holiday season with a dinner at Rawlings County Club.

COLUMBUS

DECEMBER 12, 2002
Activity: The Section held its Annual Holiday Dinner at The Athletic Club of Columbus. The Hilliard Davidson High School Choir performed songs of the season.

DISTRICT 9

Director: John Bruskotter
Phone: (504) 367-0603

NEW ORLEANS

NOVEMBER 19, 2002
Speaker: **Dan E. Civello**, vice president.
Affiliation: Gas Technology Consultants, Metarire, La.
Topic: 911 emergency response and post-traumatic stress — keeping you, your family, and workplace safe.

New Orleans First Vice Chairman David Foster, left, and Joe Golemi, right, presenting a speaker's award to Dan E. Civello, center.

Steven A. Mondrowski during his presentation to Pascagoula Section members and guests on Student Night.

PASCAGOULA

NOVEMBER 21, 2002
Speaker: **Steven A. Mondrowski**, vice president.
Affiliation: PCI Energy Services.
Topic: Welding today and in the future.
Activity: Student Night.

DISTRICT 10

Director: Victor Y. Matthews
Phone: (216) 383-2638

DISTRICT 11

Director: Scott C. Chapple
Phone: (586) 772-1514

NORTHERN MICHIGAN

SEPTEMBER 30, 2002
Speaker: **Charles Hunt**, director of welding.
Affiliation: Career Technical Center.
Activity: **Rick Mathis** was awarded a $400 scholarship toward his teaching degree for welding.

NOVEMBER 4, 2002
Speakers: **Joe Jones**, owner, and **Mike Stuwe**.
Affiliation: Great Lakes Motor Works.
Activity: Members toured the classic car collection of the previous owner of Industrial Magnetics. **Peter Freidrich**, product manager, hosted the tour.

DISTRICT 12

Director: Michael D. Kersey
Phone: (262) 650-9364

District 12 Director Michael D. Kersey, right, with Milwaukee Section Vice Chairman John A. Kozeniecki at the Section's November meeting.

The Milwaukee Section Board members pose for a photograph during the Section's holiday party at Miller Brewing Co.

LAKESHORE FOX VALLEY MILWAUKEE

NOVEMBER 12, 2002
Speaker: **Ernest Levert**, AWS president and senior staff engineer.
Affiliation: Lockheed Martin Fire and Missiles Control.
Topic: Manufacturing of the heat exchanger for the space station.

Posing with AWS President Ernest Levert, second from right, at the Lakeshore, Fox Valley, and Milwaukee Section's combined November meeting are, from left, John Kozeniecki, District 12 Director Mike Kersey, Tom Tueiber, and James Hennessey.

MILWAUKEE

DECEMBER 5, 2002
Speaker: **John A. Kozeniecki**, AWS Milwaukee Section vice chairman.
Affiliation: Longview Inspection.
Activity: Section members enjoyed a plant tour and their annual holiday party at the Miller Brewing Co.

DISTRICT 13

Director: J. L. Hunter
Phone: (309) 888-8956

AWS Vice President Damian Kotecki, left, accepting a Plaque of Appreciation from Chicago Section Chairman Bob Zimny.

CHICAGO

NOVEMBER 13, 2002
Speaker: **Damian Kotecki**, AWS vice president and technical director for stainless and high-alloy product development.
Affiliation: The Lincoln Electric Co., Cleveland, Ohio.
Topic: Fundamentals of welding austenitic stainless steel.
Activity: National Officers' Night. AWS Vice President Jim Greer was also in attendance.

DISTRICT 14

Director: Tully C. Parker
Phone: (618) 667-7744

Indianapolis Section October guest speakers Josh Hyde, left, and Jeff Barrow.

Gene Beghtel, standing, of PFERD Abrasives during his November presentation to the Lexington Section.

INDIANAPOLIS

NOVEMBER 13, 2002
Speakers: **Josh Hyde** and **Jeff Barun.**
Affiliation: Tregaskiss.
Topic: Gas metal arc welding guns.

LEXINGTON

NOVEMBER 21, 2002
Speakers: **Gene Beghtel**, technical support, and **David Squibb**, sales representative.
Affiliation: PFERD Abrasives.
Topic: Abrasives and brushes.

ST. LOUIS

NOVEMBER 21, 2002
Activity: The Section held Student Technical Night at Cee Kay Supply in St. Louis. Live demonstrations of the latest welding equipment technology were given. More than 100 students participated in the event.

DECEMBER 14, 2002
Activity: The Section had its Annual Holiday Party at the Royal Orleans Banquet Center.

St. Louis Section board members, from left, Jerry Simpson, Gay Cornell, and Jerry Ingram, presenting door prizes at the Section's Annual Holiday Party.

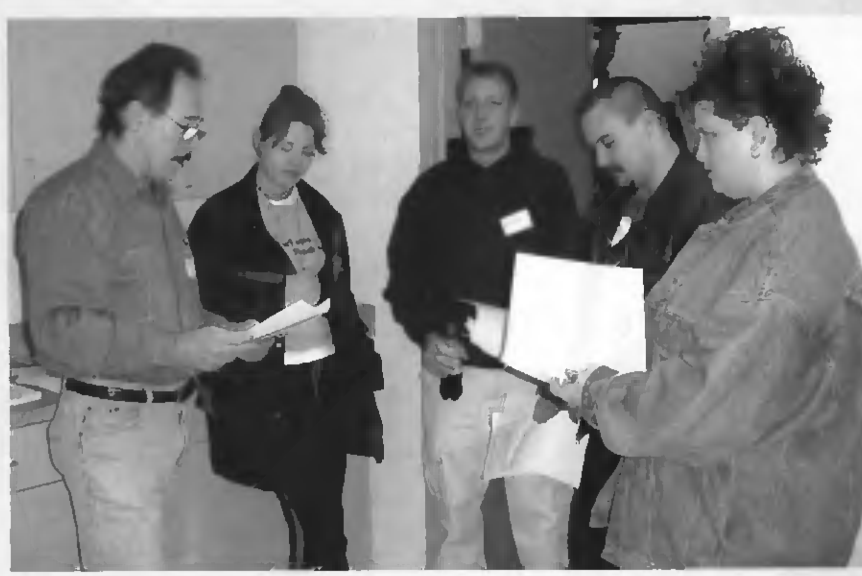

St. Louis Section Past Chairman Don Kimbrell, left, assisting students with AWS St. Louis Section and District 14 scholarship forms.

DISTRICT 15

Director: J. D. Heikkinen
Phone: (218) 741-9693

Looking on as guest speaker David Rands, center, explains weld X-ray at the Arrowhead November meeting are District 15 Director Jack Heikkinen, left, and past District 15 Director Ron Leonzal.

ARROWHEAD

NOVEMBER 21, 2002
Speaker: **David Rands**, NDT lab manager.
Affiliation: Twin Ports Testing, Superior, Wis.
Topic: Nondestructive weld testing, including X-ray, ultrasound, radiology, chemistry, heat treating and stress relief, and construction material testing.

DISTRICT 16

Director: C. F. Burg
Phone: (515) 294-5428

NEBRASKA

SEPTEMBER 12, 2002
Speakers: **Dennis Laforge** and **Kevin Rinn**.
Affiliations: Fuch's and Simonds Industries, respectively.
Topic: Band saw blade welding technology.

Members of the Nebraska Section stop for a photograph during welding demonstration at the Section's September meeting.

IOWA

NOVEMBER 12, 2002
Speakers: **Michael** and **Debbie Jackson**.
Affiliation: AWS Iowa Section.
Topic: Demonstration of equipment used in small shops and by hobby welders.

DISTRICT 17

Director: Oren P. Reich
Phone: (254) 867-2203

Tulsa Section member Jerry Knapp, right, with guest speaker Paul Wittenbach.

TULSA

NOVEMBER 12, 2002
Speaker: **Paul Wittenback**, welding engineer.
Affiliation: CONOCO/Phillips, Ponca City, Okla.
Topic: Weld failure history and analysis.

OCTOBER 22, 2002
Speaker: **Shannon Fanning**.
Affiliation: Executive Committee Chair.
Activity: Appreciation Awards were presented to Sherry Laboratories and The Lincoln Electric Co. for their support of and service to the Tulsa Section.

Sherry Laboratories employees, from left, Cecil Burnett, Dan Lawson, and Bill Vesely with the Appreciation Award presented to the company by the Tulsa Section for its long-time support.

NOVEMBER 5, 2002
Speaker: **Jerry Knapp**, AWS Tulsa section chairman.
Affiliation: Alloy Welding, Sapula, Okla.
Topic: An Executive Committee meeting was held.

North Texas Section Chairman J. Jones presenting guest speaker Sylvia Farris with a Section shirt in appreciation of her September presentation.

NORTH TEXAS

SEPTEMBER
Speaker: **Sylvia Farris**, personnel placement specialist.
Affiliation: RESOURCE.
Topic: Methods of marketing yourself to employers.
Activity: **Mark Knappenberger**, **Jason Pack**, and **Nicholas Rawlings** each received a $500 Section scholarship. A TurboTorch ProLine kit was given away as the evening's door prize.

North Texas Section Chairman J. Jones, right, presenting a Section scholarship.

East Texas Section Chairman Yoni Adonyi, second from left, with guest speakers Ming De Song, left, Chang Ming Chen, right, and Dragana Jandic.

EAST TEXAS

NOVEMBER 21, 2002
Speakers: **Ming De Song**, research associate; **Chang Ming Chen**, research associate; and **Dragana Jandic**, Ph.D. candidate.
Affiliation: Southern Methodist University, Dallas, Tex.
Topic: Friction stir welding research and development at Southern Methodist University.

DISTRICT 18

Director: John Mendoza
Phone: (210) 860-2592

LAKE CHARLES

OCTOBER 2002
Speakers: **Mike Adams** and **Tim Sonnier.**
Affiliations: Hedley Purvis and Triple S Hydrostatic, respectively.
Topic: Bolt torquing.

Lake Charles Section Chairman Tac Edwards, left, presenting a speaker's plaque to guest speaker Mike Adams.

Sabine Section Treasurer Ruel Riggs, left, presenting a sponsorship check to Lamar University engineering students Craig Schroerlucke, center, and Shawn Olsen, right, for the Mini-Baja Racing Car Design/Construction Competition.

HOUSTON

NOVEMBER 20, 2002
Speaker: **Ed Malmgren.**
Affiliation: AWS Houston Section member.
Topic: An overview of the Third Annual Construction Career Days event held at the Humble, Tex., Civic Center in late October. Welding, blacksmithing, and nondestructive examination were all part of this successful program for local students.
Activity: The Section's new Web site, *AWSHOUSTON.org*, was introduced. The site contains AWS national links as well as scholarship, sponsorship, events, and contact information specific to the Houston AWS Section.

NOVEMBER 22, 2002
Activity: The Section held its Fall Social at the Sam Houston Race Park in Houston, Tex.

Sabine Section guest speaker Bob Chenoweth, left, accepting a speaker's gift from Section Chairman Carey Wesley.

SABINE

NOVEMBER 19, 2002
Speaker: **Bob Chenoweth,** president.
Affiliation: Water Scythe, Inc., Beaumont, Tex.
Topic: Abrasive water jet cutting.
Activity: Chairman **Carey Wesley** presented a sponsorship check to a group of engineering students from Lamar University for the Mini-Baja Racing Car Design/Construction Competition. Students must design and build a mini-Baja racing car for this national competition against other universities. The competition will be held May 8–12 at Brigham Young University in Provo, Utah.

DISTRICT 19

Director: Phil Zammit
Phone: (509) 468-2310 ext. 120

Puget Sound Section Chairman Ken Johnson, left, presenting Chuck Daily with the District 19 Director's Certificate Award.

PUGET SOUND

NOVEMBER 7, 2002
Activity: The Section's executive officers met to discuss upcoming meetings and events.

Puget Sound Section Officers during their November meeting. Pictured, clockwise from left, are Sid Capouilliez, Gordy Robertson, Mike Hyes, Steve Nielsen, Hank Drumm, Shawn McDaniel, Gary Diseth, Ken Johnson, and Jerry Hope

Southern Colorado Section guest speaker John Cantlin demonstrating a cutting technology using an Arcair SLICE System.

Puget Sound Section Chairman Ken Johnson, left, presenting speaker's plaques to Fitz Acheson, center, and Jim Remfert.

Eastern Idaho/Montana Treasurer Art Watkins with guest speaker McIntyre Louthan.

NOVEMBER 7, 2002
Speakers: **Fitz Acheson**, engineering and technical support manager, and **Jim Remfert.**
Affiliation: Bortech Corporation.
Topic: The applications of Bortech automated gas metal arc welding machines with Cilmax tools.
Activity: Chairman **Ken Johnson** presented **Chuck Daily** with the District 19 Director's Certificate Award.

DISTRICT 20

Director: Jesse A. Grantham
Phone: (303) 451-6759

EASTERN IDAHO/ MONTANA

SEPTEMBER 4, 2002
Speaker: **McIntyre Louthan.**
Affiliation: Savannah River Site, Department of Energy.
Topic: Closure welding of the 3013 canisters.

OCTOBER 30, 2002
Speakers: AMET technical representatives including **Craig Dees** and **Jason Williams.**
Affiliation: AMET, Rexburg, Idaho.
Topic: Welding automation and control systems.
Activity: Members toured the AMET facility. Dees discussed control strategy and Williams demonstrated Space Shuttle fuel tank system welding.

DECEMBER 12, 2002
Speakers: **Mark Miskin**, president, and **Devun Park.**
Affiliation: Miskin Sraper Works, Idaho Falls, Idaho.
Activity: A tour was given of the Miskin Scraper Works manufacturing facility. The group saw the largest scraper in the world; it measures 27 yards.

SOUTHERN COLORADO

SEPTEMBER 24, 2002
Speaker: **John Cantlin**, treasurer.
Affiliation: AWS Southern Colorado Section.

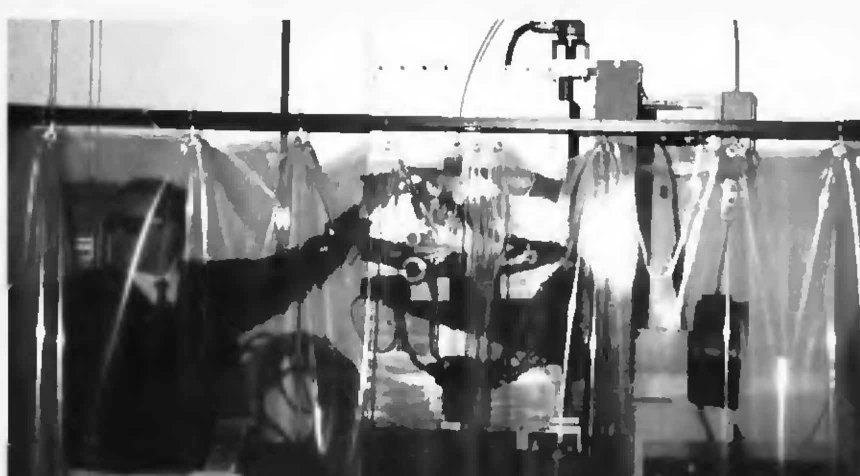

Jason Williams demonstrating Space Shuttle fuel tank system welding for members of the Eastern Idaho/Montana Section.

Southern Colorado Section members during their tour of the Ellicott High School Welding Lab and Building.

Activity: Cantlin presented and demonstrated a cutting technology using an Arcair SLICE System, which, combined with a torch that feeds oxygen and electrical power to the SLICE exothermic cutting rod, can save time, work, and money.

OCTOBER 30, 2002
Activity: Members toured the new Ellicott High School Welding Lab and Building in Ellicott, Colo. Most of the school, including the welding lab, was destroyed in a tornado on Memorial Day 2001. Members were joined by the Advisory Committee of Pikes Peak Community College. Representatives of the college discussed the school's welding program and the possibility of coordinating curriculum with the other community colleges throughout Colorado.

DISTRICT 21

Director: Les Bennett
Phone: (805) 929-2356

HAWAII

NOVEMBER 23, 2002
Activity: AWS members and ASME members joined together to tour the new double-hull fuel barge, *NOA*, purchased and operated by Smith Maritime. The barge is used by Smith Maritime for interisland service under contract with Hawaiian Electric. Representatives of the company conducted the tour.

DISTRICT 22

Director: Mark Bell
Phone: (209) 367-1398

FRESNO

OCTOBER 30, 2002
Activity: Annual Social/Trap Shoot.

Fresno Section Chairman Fred Mattern, left, with Henry Hickinbotham, winner of the Section Trap Shoot.

Sacramento Valley Section guest speaker Jon Gibson, left, with members Wilber Newsom, center, and Rodney Bechler during the Section's December meeting.

The top five shooters in trap round competed in a shoot off in 5-stand. **Henry Hickinbotbam** was the first-place winner and **Kenny Kimura** came in second.

SACRAMENTO VALLEY

DECEMBER 11, 2002
Speaker: **Jon Gibson**.
Topic: Morals, ethics, and integrity in the welding industry, with examples based on the September 11 tragedy.
Activity: The evening was also the Section's Ladies' Night Out celebration.♦

Section Events Calendar

ALASKA

FEBRUARY 14, 2003
Activity: Welding equipment show.
Location: UAA Welding Lab, Anchorage, Alaska.

LANCASTER

MARCH 1, 2003
Activity: Ladies' Night Dance (a '50s/'60s Sock Hop held with the York-Central Pennsylvania Section).
Location: Lancaster Tennis & Yacht Club.

MARCH 5, 2003
Speaker: AWS President **Ernest Levert**.
Topic: Keeping cool in space.

SACRAMENTO VALLEY

FEBRUARY 19, 2003
Speaker: **Jack Compton**, welding instructor.
Affiliation: College of the Canyons.
Topic: The future of AWS.

MARCH 19, 2003
Speaker: **David Diaz**, owner.
Affiliation: ETMS.
Topic: Weld inspection.

APRIL 16, 2003
Speaker: **Ron Rabo**, general manager.
Affiliation: Design Concepts
Topic: Aluminum GMA and GTA welding power systems.

TIDEWATER

FEBRUARY 3–7, 2003
Activity: CWI seminar.

FEBRUARY 8, 2003
Activity: CWI exam.

MARCH 13, 2003
Activity: To be announced.

YORK-CENTRAL PENNSYLVANIA

FEBRUARY 6, 2003
Topic: Fox Hot Tapping

MARCH 1, 2003
Activity: Ladies' Night Dance (a '50s/'60s Sock Hop held with the Lancaster Section).
Location: Lancaster Tennis & Yacht Club.

MARCH 6, 2003
Speaker: AWS President **Ernest Levert**.

APRIL 3, 2003
Activity: Joint meeting with ASNT.

AWS Life Members Offered Free Registration for the Welding Show and Professional Program

As long-time supporters of the American Welding Society, AWS Life Members are being offered complimentary registration to the 2003 Welding Show and the Professional Program (a $325 value).

The Professional Program will take place April 7–10 in Detroit, Mich. The 2003 Welding Show will run from April 8–10.

Registration to the Professional Program entitles AWS Life Members to attend any of the seminars or sessions occurring over the four-day period. Please be sure to include any applicable fees for special events or spouse attendance when you register. A registration form is available in this issue of the *Welding Journal*. The Advanced Program, which will be mailed to members, also contains a registration form and information.

When registering, please mark "AWS Life Member: Free Registration" at the top of the form and fax both sides to Cassie Burrell, Associate Executive Director, Membership, at (305) 443-5647 or mail the form to AWS, 550 N.W. LeJeune Road, Miami, FL 33126.♦

District 9 2002 District and Section Awards

Rickye D. Messer
Baton Rouge
Section Private Sector Instructor

C. Lavon Mills
Mobile
Section Private Sector Instructor

Joseph Golemi, Jr.
New Orleans
Section Private Sector Instructor

Bobby Duhon
New Orleans
Section Private Sector Instructor

Byron L. Darcey, Jr.
New Orleans
Section Private Sector Instructor

2002–2003 Member-Get-A-Member Campaign

Listed below are the people participating in the 2002–2003 Member-Get-A-Member Campaign. For campaign rules and a prize list, please see page 49 of this Welding Journal.

If you have any questions regarding your member proposer points, please call the Membership Department at (800) 443-9353 ext. 480.

Winner's Circle

(AWS Members sponsoring 20 or more new Individual Members, per year, since June 1, 1999.)

J. Compton, *San Fernando Valley****
E. H. Ezell, *Mobile***
J. Merzthal, *Peru***
B. A. Mikeska, *Houston**
R. L. Peaslee, *Detroit**
W. L. Shreve, *Fox Valley**
G. Taylor, *Pascagoula***
T. Weaver, *Johnstown/Altoona**
G. Woomer, *Johnstown/Altoona**
R. Wray, *Nebraska**

**Denotes the number of times an Individual Member has achieved Winner's Circle status. Status will be awarded at the close of each membership campaign year.*

President's Guild

(AWS Members sponsoring 20 or more new Individual Members between June 1, 2002, and May 31, 2003.)

S. McGill, *Northeast Tennessee* — 20

President's Round Table

(AWS Members sponsoring 11–19 new Individual Members between June 1, 2002, and May 31, 2003.)

G. Fairbanks, Jr., *Baton Rouge* — 13
J. Grantham, *Colorado* — 11

President's Club

(AWS members sponsoring 6–10 new Individual Members between June 1, 2002, and May 31, 2003.)

G. W. Taylor, *Pascagoula* — 8
M. Kincheloe, *Holston Valley* — 7
J. Scott, *Houston* — 7

President's Honor Roll

(AWS members sponsoring 1–5 new Individual Members between June 1, 2002, and May 31, 2003. Only those sponsoring 2 or more AWS Individual Members are listed.)

C. Dynes, *Kern* — 5
F. Luening, *Houston* — 5
T. Skaff, *LA/Inland Empire* — 5
J. Carney, *Western Michigan* — 4
W. Galvery, Jr., *Long Bch./Orange Cnty.* — 4
G. Baum, *Detroit* — 3
R. Corsaro, *Niagara Frontier* — 3
F. Juckem, *Madison-Beloit* — 3
G. Mulee, *Rochester* — 3
G. O'Connor, *New Jersey* — 3
R. Robles, *Corpus Christi* — 3
K. Tebeau, *Detroit* — 3
P. Zammit, *Spokane* — 3
A. M. Mechanical, *Holston Valley* — 2
J. Biegas, *Rochester* — 2
F. Bonifatti, *International* — 2
A. Duschere, *Long Island* — 2
T. Erichsen, *Santa Clara Valley* — 2
E. Ezell, *Mobile* — 2
R. Howard, *Louisville* — 2
S. Hunt, *Shreveport* — 2
E. Levert, *North Texas* — 2
D. Moulton, *Saginaw Valley* — 2
J. Norrish, *International* — 2
M. Perry, *Tulsa* — 2
M. Powell, *Lehigh Valley* — 2
C. Wesley, *NW Pennsylvania* — 2

Student Sponsors

(AWS members sponsoring 3 or more new AWS Student Members between June 1, 2002, and May 31, 2003.)

D. Scott, *Peoria* — 68
C. Wesley, *Northwestern Pa.* — 49
W. Galvery, Jr., *Long Bch./Orange Cnty.* — 31
B. Huff, *Sangamon Valley* — 26
J. Sullivan, *Mobile* — 26
S. Siviski, *Maine* — 24
W. Harris, *Pascagoula* — 20
J. Cox, *Northern Plains* — 19
K. Langdon, *Johnny Appleseed* — 19
G. Woomer, *Johnstown/Altoona* — 18
F. Juckem, *Madison-Beloit* — 16
M. Anderson, *Indiana* — 15
J. Hayes, *Oklahoma City* — 15
S. Zwilling, *Louisville* — 15
D. Combs, *Santa Clara Valley* — 14
R. Fulmer, *Twin Tiers* — 14
E. Soto Ruiz, *Puerto Rico* — 14
S. Caldera, *Portland* — 13
R. Grays, *Kern* — 13
F. Madrid, *Arizona* — 10
C. Jones, *Houston* — 9
D. Ketler, *Williamete Valley* — 9
M. Pointer, *Sierra Nevada* — 8
P. Walker, *Ozark* — 8
D. Hatfield, *Tulsa* — 7
C. Kipp, *Lehigh Valley* — 7
T. Strickland, *Arizona* — 7
J. Boyer, *Lancaster* — 6
R. Robles, *Corpus Christi* — 6
W. Kielhorn, *East Texas* — 5
J. Livesay, *Nashville* — 5
D. Zabel, *Southeast Nebraska* — 5
P. Baldwin, *Peoria* — 4
T. Buchanan, *Mid-Ohio Valley* —4
T. Kienbaum, *Colorado* — 4
D. Kowalski, *Pittsburgh* — 4
E. Norman, *Ozark* — 4
S. Strader, *Portland* — 4
J. Ciaramitaro, *North Central Fla* — 3
J. Goodson, *New Orleans* — 3
R. Huston, *Olympic* — 3
A. Mattox, *Lexington* — 3
W. Miller, Jr., *New Jersey* — 3
F. Ramos, *Sacramento* — 3
T. Shirk, *Tidewater* — 3
J. Yochum, *South Florida* — 3♦

GUIDE TO AWS SERVICES

550 NW LeJeune Rd., Miami, FL 33126
Phone (800) 443-9353; (888) WELDING
FAX (305) 443-7559; *Internet: www.aws.org*
Phone extensions appear in parentheses.
E-Mail addresses available on the AWS Web site.

AWS PRESIDENT
Ernest D. Levert, Senior Staff Engineer
Lockheed Martin Missiles and Fire Control
P.O. Box 650003, Mail Stop WT-48
Dallas, TX 75265-0003

ADMINISTRATION
Executive Director
Ray W. Shook. ....(210)

Deputy Executive Directors
Jeffrey R. Hufsey ....(264)
John J. McLaughlin ....(235)

Corporate Director Volunteer Services
Debbie A. Cadavid ....(222)

Corporate Director of Quality Management Systems and Human Resources Administration
Linda K. Henderson ....(298)

Chief Financial Officer
Frank R. Tarafa ....(252)

INFORMATION SERVICES
Corporate Director
Joe Cilli ....(258)

HUMAN RESOURCES
Director
Luisa Hernandez...(266)

DATABASE ADMINISTRATION
Corporate Director of Database Administration
Jim Lankford ....(214)

INTERNATIONAL INSTITUTE OF WELDING
Information ....(294)

Provides liaison activities involving other professional societies and standards organizations, nationally and internationally.

GOVERNMENT LIAISON SERVICES
Hugh K. Webster
Webster, Chamberlain & Bean
Washington, D.C.
(202) 466-2976
FAX (202) 835-0243

Identifies sources of funding for welding education and research & development. Monitors legislative and regulatory issues important to the industry.

WELDING EQUIPMENT MANUFACTURERS COMMITTEE
Associate Executive Director
Richard L. Alley ....(217)

WELDING INDUSTRY NETWORK (WIN)
Associate Executive Director
Richard L. Alley ....(217)

CONVENTION & EXPOSITIONS
Exhibiting Information .... (242, 295)

Associate Executive Director of Convention Sales
Richard L. Alley ....(217)

Director of Convention & Expositions
John Ospina...(462)

Organizes the week-long annual AWS International Welding and Fabricating Exposition and Convention. Regulates space assignments, registration materials, and other Expo activities.

PUBLICATION SERVICES
Department Information ....(275)

Director
Andrew Cullison ....(249)

WELDING JOURNAL
Publisher
Jeff Weber ....(246)

Editor/Editorial Director
Andrew Cullison ....(249)

National Sales Director
Rob Saltzstein ....(243)

WELDING HANDBOOK
Welding Handbook Editor
Annette O'Brien ....(303)

Publishes AWS's monthly magazine, the *Welding Journal*, which provides information on the state of the welding industry, its technology, and Society activities. Publishes *Inspection Trends*, the *Welding Handbook* and books on general welding subjects.

MARKETING AND DESIGN
Corporate Director
Jeff Weber ....(246)

Plans and coordinates marketing of AWS products and services. Responsible for print advertising, as well as design and print production of the *Welding Journal, Inspection Trends*, the annual Welding Show Program, and other AWS promotional publications.

COMMUNICATIONS/PUBLIC RELATIONS
Manager
Amy Townsend...(308)

MARKET RESEARCH AND DEVELOPMENT
Corporate Director
Debrah C. Weir ....(482)

Investigates and/or proposes new products and services. Researches effectiveness of existing programs.

MEMBER SERVICES
Department Information ....(480)

Associate Executive Director
Cassie R. Burrell...(253)

Director
Rhenda A. Mayo...(260)

Serves as a liaison between Section members and AWS headquarters. Informs members about AWS benefits and other activities of interest.

EDUCATIONAL PRODUCT DEVELOPMENT
Director
Christopher B. Pollock ....(219)

Information on education products, projects, and programs. Responsible for the S.E.N.S.E. program for welding education, and dissemination of training and education information on the Web.

CONFERENCES & SEMINARS
Director
Giselle I. Hufsey ....(278)

Responsible for national and local conferences/exhibitions and seminars on industry topics ranging from the basics to the leading edge of technology. Organizes CWI, SCWI, and other seminars designed for preparation for certification.

CERTIFICATION OPERATIONS
Managing Director
Wendy S. Reeve..(215)

Director
Terry Perez...(470)

Information and application materials on certifying welders, welding inspectors, and educators. ....(273)

INTERNATIONAL BUSINESS DEVELOPMENT
Director
Walter Herrera ....(475)

AWS AWARDS, FELLOWS, AND COUNSELORS
Managing Director
Wendy S. Reeve..(215)

Coordinates AWS awards and AWS Fellow and Counselor nominees.

TECHNICAL SERVICES

Department Information ....(340)

Managing Director
Leonard P. Connor ....(302)
Welding Qualification, Computerization, Technical Activities Committee

Andrew R. Davis...(466)
International Standards Program Manager, Welding in Marine Construction, Inspection, Mechanical Testing of Welds

Stephen P. Hedrick ....(305)
Safety and Health Manager, Metric Practices, Friction Welding

Engineers
John L. Gayler ....(472)
Structural Welding, Personnel and Facilities Qualification

Rakesh Gupta ....(301)
Filler Metals and Allied Products, Instrumentation for Welding, Sheet Metal Welding,

Ed F. Mitchell...(254)
Thermal Spray, Iron Castings, Joining Plastics & Composites, Joining of Metals and Alloys, Railroad Welding

Harold P. Ellison ....(299)
Resistance Welding, High-Energy Beam Welding and Cutting, Oxyfuel Gas Welding & Cutting, Automotive Welding, Aircraft and Aerospace

Peter Howe ....(309)
Arc Welding & Cutting, Piping & Tubing, Machinery and Equipment, Robotics and Automatic Welding, Food Processing Equipment

Technical Editor
Cynthia Jenney ....(304)
Definitions & Symbols, Brazing & Soldering

Senior Manager of Publications, Technical
Rosalinda O'Neill ....(451)

AWS publishes more than 160 volumes of material, including standards that are used throughout the industry.

With regard to technical inquiries, oral opinions on AWS standards may be rendered. However, such opinions represent only the personal opinions of the particular individuals giving them. These individuals do not speak on behalf of AWS, nor do these oral opinions constitute official or unofficial opinions or interpretations of AWS. In addition, oral opinions are informal and should not be used as a substitute for an official interpretation.

WEB SITE ADMINISTRATION
Manager
Keith Thompson ....(414)

Nominees for National Office

Only Sustaining Members, Members, Honorary Members, Life Members, or Retired Members who have been members for a period of at least three years shall be eligible for election as a Director or National Officer.

It is the duty of the National Nominating Committee to nominate candidates for national office. The committee shall hold an open meeting, preferably at the Annual Meeting, at which members may appear to present and discuss the eligibility of all candidates.

To be considered a candidate for positions of President, Vice President, Treasurer, or Director-at-Large, the following qualifications and conditions apply:

President: To be eligible to hold the office of President, an individual must have served as a Vice President for at least one year.

Vice President: To be eligible to hold the office of Vice President, an individual must have served at least one year as a Director, other than Executive Director and Secretary.

Treasurer: To be eligible to hold the office of Treasurer, an individual must be a member of the Society, other than a Student Member, must be frequently available to the National Office, and should be of executive status in business or industry with experience in financial affairs.

Director-at-Large: To be eligible for election as a Director-at-Large, an individual shall previously have held office as Chairman of a Section; as Chairman or Vice Chairman of a standing, technical or special committee of the Society; or as District Director.

Interested parties are to send a letter stating which particular office they are seeking, including a statement of qualifications, their willingness and ability to serve if nominated and elected, and 20 copies of their biographical sketch.

This material should be sent to Richard L. Arn, Chairman, National Nominating Committee, American Welding Society, 550 NW LeJeune Rd., Miami, FL 33126.

The next meeting of the National Nominating Committee is currently scheduled for 10 to 11 a.m., Tuesday, April 8, 2003, at COBO Conference/Exhibition Center, Detroit, Mich. The terms of office for candidates nominated at this meeting will commence June 1, 2004. ♦

Honorary-Meritorious Awards

The Honorary-Meritorious Awards Committee has the duty to make recommendations regarding nominees presented for Honorary Membership, National Meritorious Certificate, William Irrgang Memorial, and the George E. Willis Awards. These awards are presented in conjunction with the AWS Exposition and Convention held each spring. The descriptions of these awards follow, and the submission deadline for consideration is July 1 prior to the year of presentation. All candidate material should be sent to the attention of John J. McLaughlin, Secretary, Honorary-Meritorious Awards Committee, 550 NW LeJeune Rd., Miami, FL 33126.

National Meritorious Certificate Award: This award is given in recognition of the candidate's counsel, loyalty, and devotion to the affairs of the Society, assistance in promoting cordial relations with industry and other organizations, and for the contribution of time and effort on behalf of the Society.

William Irrgang Memorial Award: This award is administered by the American Welding Society and sponsored by The Lincoln Electric Co. to honor the late William Irrgang. It is awarded each year to the individual who has done the most to enhance the American Welding Society's goal of advancing the science and technology of welding over the past five-year period.

George E. Willis Award: This award is administered by the American Welding Society and sponsored by The Lincoln Electric Co. to honor George E. Willis. It is awarded each year to an individual for promoting the advancement of welding internationally by fostering cooperative participation in areas such as technology transfer, standards rationalization, and promotion of industrial goodwill.

International Meritorious Certificate Award: This award is given in recognition of the candidate's significant contributions to the worldwide welding industry. This award should reflect "Service to the International Welding Community" in the broadest terms. The awardee is not required to be a member of the American Welding Society. Multiple awards can be given per year as the situation dictates. The award consists of a certificate to be presented at the award's luncheon or at another time as appropriate in conjunction with the AWS President's travel itinerary, and, if appropriate, a one-year membership to AWS.

Honorary Membership Award: An Honorary Member shall be a person of acknowledged eminence in the welding profession, or who is accredited with exceptional accomplishments in the development of the welding art, upon whom the American Welding Society sees fit to confer an honorary distinction. An Honorary Member shall have full rights of membership. ♦

TELEWELD
FAX: (305) 443-5951

PUBLICATION SALES & ORDERS
Global Engineering Documents
(800) 854-7179 or (303) 397-7956

REPRINTS
To order custom reprints of articles in the *Welding Journal*, contact Denis Mulligan at (800) 259-0470

It is the intent of the American Welding Society to build the Society to the highest quality standards possible. We welcome any suggestions you may have.

Please contact any of the staff listed on the previous page or AWS President Ernest D. Levert, Senior Staff Engineer, Lockheed Martin Missiles and Fire Control, P.O. Box 650003, Mail Stop WT-48, Dallas, TX 75265-0003.

AWS MISSION STATEMENT

The mission of the American Welding Society is to provide quality products and services to our members and the industry which will advance the science, technology and application of materials-joining throughout the world.

AWS FOUNDATION, INC.
550 NW LeJeune Rd.
Miami, FL 33126
(305) 445-6628
(800) 443-9353, ext. 293
Or e-mail: *bobw@aws.org*
General Information
(800) 443-9353, ext. 689

Chairman, Board of Trustees
Ronald C. Pierce

Executive Director
Ray W. Shook

Director of Development
Robert B. Witherell

The AWS Foundation is a not-for-profit corporation established to provide support for educational and scientific endeavors of the American Welding Society. Information on gift-giving programs is available upon request.

ISO9001
Registered Organization

Navy Joining Center Presents Projects at DMC 2002

The Defense Manufacturing Conference (DMC), hosted by the U.S. Navy in conjunction with the Joint Defense Manufacturing Technology Panel (JDMTP), was held in Dallas, Tex., December 2–5, 2002. Based on the theme "ManTech: Strategic Edge for Transformation," the conference provided an overview of government and industry programs as well as a vision for the future of defense manufacturing and sustainment needs. The Navy Joining Center (NJC) and more than 70 organizations exhibited to more than 800 attendees at the conference. NJC personnel gave several presentations during the Technical Sessions.

NJC Program Manager Tim Trapp presented "Friction Stir Welding of Titanium for Aircraft Engine Applications" and a poster titled "Translational Friction Welding of Titanium Engine Blisks." Friction stir weld development is being done to join titanium alloys for gas turbine engine hardware. The project is part of the Metals Affordability Initiative (MAI) aimed at friction stir welding "hard metals." Trapp's presentation highlighted successful development in friction stir welding (FSW) processing upon several titanium alloys for producing hybrid material structures. The initial project activities have shown excellent mechanical properties at room and elevated temperature using tensile, low cycle fatigue, and fatigue crack growth tests. An implementation plan has been developed for a primary application. As a result of this effort, several patent disclosures for turbine engine applications and FSW process techniques have been filed.

The Navy Joining Center booth at the Defense Manufacturing Conference in Dallas, Tex.

Trapp's poster for translational friction welding (TFW) highlighted a process for fabrication of a titanium bladed disk (a blisk). This method of fabrication produces a blisk component by frictional heating and local forging of turbine engine blades directly and permanently to a rotor disk. TFW permits the use of smaller disk and individual blade forgings, which could be made of the same or dissimilar materials and processed to produce optimum mechanical properties for enhanced design. The goal of this project is to provide the necessary design data and fabrication experience to implement TFW in production for new manufacture and repair of turbine engine blisks.

Larry Brown, project manager, presented "Aircraft Primary Structure Adhesive Bonding Development," an overview of project development activities. The project is part of the Composite Affordability Initiative (CAI), which is addressing the need to improve the reproducibility and reliability of adhesive-bonded primary aircraft structures by defining process capability and controls to develop an enhanced understanding of the manufacturing variabilities that can affect the adhesive-bonded joint. The targeted application is for skin-to-ribbed box composite structures that are currently riveted (i.e., fuselage and wing structures). Development activities are directed at characterization of adhesive bond joints by examining the effect of defects. The results of this project are to support Navy and Air Force requirements for future adhesive bonded aircraft structures. The CAI will be provided with data to support design specifications and manufacturing processes to aid in maturing the technology.

For more information, contact Larry Brown at (614) 688-5080 or *larry_brown@ewi.org*. ♦

EWI's Government Programs Office and the NJC Announces the Addition of John D. Coffey

John D. Coffey

As a project manager for the NJC, John D. Coffey's duties include planning and control of NJC technology development projects. Coffey has more than seven years of experience in the materials joining industry and holds a B.S. in welding engineering from The Ohio State University. Throughout his years of experience, he has obtained a working knowledge of welding automation and various welding and manufacturing processes.

Prior to joining EWI, Coffey worked for John Deere as a senior welding engineer. At several U.S. and Canadian facilities, he led the welding operations team responsible for the specification, procurement, and implementation of robotic and manual arc welding equipment and tooling. He also supported the manufacturing engineering group on a number of new plant start-ups implementing Demand Flow Technology principles as a project manager.♦

NJC
Operated by
EWI

The Navy Joining Center
1250 Arthur E. Adams Dr.
Columbus, OH 43221
Phone: (614) 688-5010
FAX: (614) 688-5001
e-mail: *NJC@ewi.org*
www: *http://www.ewi.org*
Contact: Larry Brown


Comerica

FOR MORE INFORMATION, CIRCLE NUMBER ON READER INFORMATION CARD.

Blast Cleaning Equipment Featured in Catalog

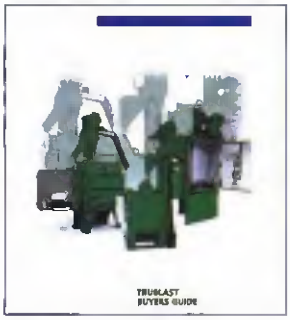

The company's *Trublast Buyers Guide* outlines the entire product line of surface preparation products. The blast cleaning equipment featured in the catalog is designed for light to medium users who do not require more costly high-volume or heavy-duty machines. Tumbler, spinner hanger, and swing table machines are highlighted, as well as the line's dust collector series.

USF Surface Preparation Group 120
215 Union Blvd., Ste. 315, Lakewood, CO 80228

Video Features Orbital Welding System

The company's product video features its orbital welding system with a welding torch designed for thick-walled pipe and vessel applications. The torch oscillates across the entire width of the groove with less total heat input, creating a smaller heat-affected zone.

Arc Machines, Inc. 121
10500 Orbital Way, Pacoima, CA 91331

Guide Details Plasma Arc Cutting

The company's *Quick Reference Product Guide* details its manual plasma arc cutting systems, torches, and accessories. The fully illustrated, 16-page guide is divided into five sections, each featuring a particular product. The guide's introduction provides information on how to choose the proper plasma arc cutting system.

Thermal Dynamics Corp. 122
101 S. Hanley Rd., Ste. 600, St. Louis, MO 63105

Guide Features Machine and Process Safeguarding

The company's 650-plus-page *Machine and Process Safeguarding Guide* provides comprehensive machine and process safety product information and technical reference. It features nearly 30 new products including safety light curtains, safety contact strips and bumpers, safety mats, safety interlock switches, safety monitoring relays, two-hand controls, enabling switches, and process safeguards. Each product category details product features, options, application examples, specifications, schematic/system drawings, dimensions, and ordering information. Additionally, more than 100 pages of the guide are dedicated to educational resource material. The reference guide also comes in a CD-ROM version that contains the catalog, product certificates, declarations of conformity, and downloadable CAD drawings.

Scientific Technologies Inc. 123
6550 Dumbarton Circle, Fremont, CA 94555-3611

Brochure Highlights Dust Collectors

The Dalamatic dust collector brochure highlights product line features, operational advantages, and technical specifications. The collectors provide continuous collection, compact design, reduced bag changes, ultra-efficient and durable filter media, and a five-year warranty.

Donaldson Co., Inc. 124
Industrial Air Filtration
P.O. Box 1299, Minneapolis, MN 55440-1299

Directory Profiles Leading Automation Suppliers

The *Robotics Industry Directory* profiles nearly 200 top supplier companies and is available free from the Robotic Industries Association (RIA). The directory provides complete company information with industries served, application types, principal contact information, and Web sites. In addition to company listings, the directory also includes two articles providing helpful tips to individuals searching for automation solutions, titled "The Robotics Industry: Key Components to Productivity and Growth" and "Your First Robot." Directories may be requested from RIA through its Web site, *www.roboticsonline.com*, or by calling RIA headquarters at (734) 994-6088.

Robotic Industries Association
900 Victors Way, Ann Arbor, MI 48106

Catalog Showcases Welding Lenses and Helmets

The company's 52-page, full-color *Complete Catalog* features the Speedglas® autodarkening welding lenses and helmets, including the 9000 series of breathable, CO_2-reducing helmets and SideWindows™ peripheral-vision helmets. Also included is information about the Adflo®-powered air-purifying respirator, and the individual supplied-air purification and regulation system.

Hornell, Inc. 125
2374 Edison Blvd., Twinsburg, OH 44087

Brochure Describes Clean Air Booth

The company's full-color brochure shows how correctly configured booths can protect workers from airborne hazards and noise associated with welding, cutting, and finishing. Pre-packaged and custom booths feature power modules, integrated air ducts, self-cleaning filtration, lighting fixtures, and galvanized wall and ceiling panels.

Micrn Air Clean Air Systems 126
P.O. Box 1138, Wichita, KS 67201

Brochure Highlights Thermal Spray Systems

The company's 12-page, full-color *Arc Spray Equipment Solutions* brochure details features and benefits of wire arc spray equipment configurations, options, and wires used for thermal spray coatings.

Praxair Surface Technologies 127
1555 Main St., Indianapolis, IN 46224

CD-ROM Demos Cutting Machines

The company's NavCat CD-ROM includes video demonstrations of dry cutting abrasive cut-off machines, wet cutting, special machines, options, specifications, and prices. The program enables users to order products electronically.

Everett Industries, Inc. 128
P.O. Box 2068, Warren, OH 44484

Catalog Features Gouging Torches

The company's eight-page, full-color *Extreme Gouging Torch Catalog* details the features and benefits of its torches, with a "family tree" matching gouging torch models to their applications. Models include Angle-Arc® manual gouging torches, Straight Handle manual gouging torches, and the Tri-Arc® foundry torch.

Tween Arcair 129
101 S. Hanley Rd., Ste. 600, St. Louis, MO 63105

Catalog Features Specialty Gases and Equipment

The company's catalog features more than 460 pages of information on its complete line of specialty gases and equipment, including ordering information. Specifications, gas handling equipment recommendations, gas mixtures, cylinders, gas generators, purification systems, gas detectors, monitors, analyzers, flow measurement and control, filters, purifiers, reference tables, and compatibility charts are included.

Matheson Tri-Gas, Inc. 130
166 Keystone Dr., Montgomeryville, PA 18936

CSA Appoints Vice President

Randall W. Luecke

CSA International, Toronto, Ontario, Canada, has appointed **Randall W. Luecke** vice president, certification. Previously vice president, finance, CSA Group, Luecke joined the company in 1994 as a member of the executive team at International Approval Services (IAS), the certification and testing arm of the American and Canadian Gas Associations. He holds a B.A. in business administration from McMaster University, a M.B.A. from Lehigh University, Bethlehem, Pa., is a Certified Public Accountant, a Certified Management Accountant, and possesses a Certification in Financial Management.

Sherry Laboratories Names Director

Jennifer Marek

Sherry Laboratories, Muncie, Ind., has named **Jennifer Marek** director-metallurgical for its Madison Street facility. She was promoted to the position after serving as the facility's assistant lab director for the past ten months. Previously employed by the company as a metallurgical engineer, Marek left to join American Axle and Mfg. as a metallurgical engineer in 1998, where she was employed until her return ten months ago. Marek graduated from Michigan State University with a B.S. in materials science and engineering and earned a master's in engineering and manufacturing systems from Lawrence Technological University.

PCI Appoints Chief Engineer

PCI Energy Services, LLC, Lake Bluff, Ill., and Ashland, Va., has appointed **Paul Kreitman** [AWS] as chief engineer. He is a licensed engineer in the state of Illinois and holds a B.S. in mechanical engineering from Northwestern University and a M.B.A. from Keller Graduate School. Kreitman has more than 25 years of experience with PCI, which is a subsidiary of Westinghouse Electric Company.

Scott Semiconductor Gases Announces New Vice President/General Manager

Scott Specialty Gases, Plumsteadville, Pa., has appointed **Harald Mynster** as group vice president and general manager of its Semiconductor Group. Before joining the company, Mynster was vice president of sales and marketing of Exsil, Inc. He holds a bachelor's degree in industrial technology from California State University at Fresno.

CONCOA Appoints Manager

Richard Green

CONCOA, Virginia Beach, Va., has promoted **Richard Green** [AWS] to product manager. Prior to his promotion, Green served as territory manager. A graduate of Purdue University with a degree in material science engineering, Green also holds a M.B.A. from Saint Ambrose University.

EWI Appoints Director

Wangen Lin

Edison Welding Institute (EWI), Columbus, Ohio, has appointed **Wangen Lin** [AWS] director of research and technology. While at EWI, Lin has also served as an adjunct assistant professor for The Ohio State University's Industrial Welding and Systems Engineering Dept. He was previously with Pratt & Whitney, where he led the Pratt & Whitney Materials Joining Community and UTC's Materials Joining Team. Lin received his Ph.D. in welding engineering from The Ohio State University in 1991 and holds a M.B.A. from Rensselaer Polytechnic Institute, Troy, N.Y.

Sulzer Metco Names Head of Thermal Spray Unit

Daniel Moraschetti

Sulzer Metco (U.S.) Inc., Westbury, N.Y., has named **Daniel Moraschetti** to head the company's Thermal Spray Operational Unit. Moraschetti has worked in management positions in Europe and the United States. He joined the company in 1994, coming from the Corporate Finance and Controlling Department of the parent company, Sulzer Ltd., which he joined in 1991. Prior to that, he was with Leica plc. as head of finance of the Special Products Division and director of finance for Leica Aarau Ltd. Moraschetti holds a degree in economics.

HI TecMetal Announces Appointments

HI TecMetal Group (HTG), Cleveland, Ohio, has appointed **John Sparenga** corporate quality engineer. Sparenga has more than 16 years of experience in various quality-related positions in the metals industry. He is a certified Quality Engineer and holds a B.S. degree in physics from the University of Akron.

Celeste Pauley was named customer service representative for HTG Duncan in Duncan, S.C. Pauley studied business for two years at a technical college and has seven years of experience in data entry and inventory control in the thermal treatment industry.

Look for the AWS Welding Show Preview in next month's *Welding Journal*

The New Handi-Grinder™

Circle No. 1050

ABICOR Binzel Corp. introduces the new Handi-Grinder™, the portable solution to grind tungsten electrodes on the job site from 15° to 180°. Light weight and easily manageable, the Handi-Grinder longitudinally fine grinds electrodes for a precise and repeatable concentrated welding arc. Handi-Grinder's integrated filter housing captures dust while protecting the operator. The Hand-Grinder has variable speeds and multiple grinding positions, extending the wheel life. By using a dedicated tungsten grinder, such as ABICOR's Handi-Grinder, electrodes are less susceptible to contaminates from residual materials found on a standard grinder wheel.

ABICOR BINZEL Corp.
650 Research Dr., Ste 110
Fredrick, MD 21703-8619
(800) 542-4867
FAX: (301) 846-4497

Atlas Model 500 Welding Positioner

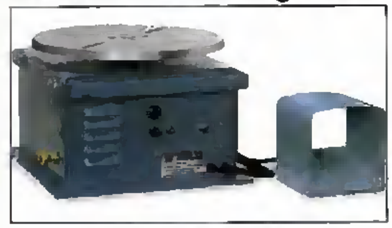

Circle No. 1054

The Atlas Welding Positioner is designed for strength and stability in handling and welding loads of up to 500 pounds when properly balanced in the horizontal position. • 1/4 hp DC motor • 400 amp welding ground circuit • Dynamic Braking rapidly stops table rotation • Full speed advanced for stitch welding • 14" x 5/8" thick rotary table • On/off foot switch • Front panel speed and rotation controls

Atlas Welding Accessories
Troy, MI 48099
(800) 962-9353
FAX: (248) 588-3720
Email: atlaswelding@ameritech.net • www.atlasweld.com

Capacitor Discharge Welders

Circle No. 1051

Aelectronic Bonding Inc. Celebrating 20 years, makes capacitor discharge welders utilizing resistance, pulse arc and fusion technologies. These inexpensive welders are used in the jewelry, dental, medical, auto and electronics industries. Applications from butt-welding wires, thermocouple leads, stud, optical frames, jewelry repairs, cathode de-burring of similar and dissimilar metals, tack weld positioning amongst many. ABI 888-494-2663. Visit our website at www.abiusa.net.

Aelectronic Bonding Inc.
1655 Elmwood Ave., Bldg #7
Cranston, RI 02910
(401) 461-4140
FAX: (401) 461-5250

Bohler Stainless Steel Flux-Cored Wires Save You Welding Time and Money!

Circle No. 1055

Bohler makes welding easier, more cost effective and saves time with 50% faster travel speeds in VUP welding, 20-50% in flat or horizontal passes and 70-80% in FCAW wire versus solid or stick electrodes.

Bohler Thyssen Welding
P.O. Box 721678
Houston, TX 77272-1678
(800) 527-0791
FAX: (281) 499-4347
Website: www.btwusa.com

If It Can Be Welded We Know How

New Airgas GOLD GAS

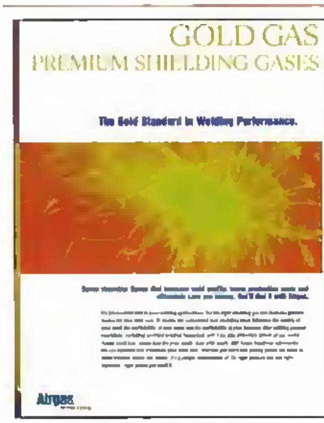

Circle No. 1052

It's the smallest cost in your welding applications. Yet the right shielding gas can have the greatest impact on your total cost, because shielding gases influence the quality of your weld, the productivity of your labor and the profitability of your business. Ask for information on new Airgas GOLD GAS, premium shielding gases for MIG, TIG, flux-cored and robotic applications.

Airgas Inc.
259 Radnor Chester Road
Suite 100
Radnor, PA 19087
(610) 902-6270
FAX: (610) 687-6932
Email: doug.sherman@airgas.com

Cored Welding Wire Guide

Circle No. 1056

This brochure shows Cor-Met's wide offerings of sizes and alloys in Cored Welding Wires, Stick Electrodes and TIG wires (both spools and cut lengths). It includes descriptive, classification and physical data on low alloy steels, cobalt-base and nickel-base alloys, tool and stainless steels, and hard-facing alloys. Alloys are available for resistance to high temperatures, erosion and corrosion; cored wires, electrodes and TIG and MIG solid alloy steels; cast iron and stainless steel.

Cor-Met Inc.
12500 E. Grand River
Brighton, MI 48116
(800) 848-2719
FAX: (810) 227-9266
Website: www.cor-met.com

New Decaled Helmets

Circle No. 1053

ArcOne's new decaled helmets not only look good but are functional and dependable. Optimally balanced and lightweight to reduce welder's fatigue and tough enough for virtually any welding application. Four families of auto darkening filters to choose from. All filters are water and dust resistant with the highest level of Ultra-violet/Infra-red protection up to shade 16.

ArcOne
85 Independence Dr.
Taunton, MA 02780
(800) 223-4685
Website: www.aceintl.com

WeldOffice™ Software

Circle No. 1057

Automatic creation and management of
WPS, PQR, WPQ
Welding Procedures
Welder Qualifications & Welder Maintenance
Expiration Reports
NDE Reports
Base Metals & Filler Metals
Joint Details
QA/QC Activities
Production Welding
Electronic Signatures
Multi Codes/Standards
Code Checking & Custom Reporting
Complete solutions for QA/QC management of plants, fabrication shops and construction projects. Free Demo at www.weldoffice.com.

C-spec
P.O. Box 27604
Concord, CA 94527
(888) 673-9777 toll free
FAX: (925) 930-8223

Circle No. 1058

End Tungsten Electrode Inconsistencies

DGP's brochure shows how to properly diamond grind GTAW and PAW electrodes easily and economically on one machine designed to maximize the consistency and repeatability of your tungsten electrodes. DGP Models allow users to correctly grind, blunt and cut to length on one machine that is quicker and easier to use than u any of the competition. Benefits include extended electrode life, better arc starting, and reduced arc wander. Free Sample electrodes ground on this machine available upon request.

Diamond Ground Products, Inc.
2550 Azurite Circle
Newbury Park, CA 91320
(805) 498-3837
FAX: (805) 498-9347

Circle No. 1062

EZ ARC Welding Systems

GENTEC offers affordable solutions to work station design. The EZ ARC product line includes complete welding workstations that accommodate a wide variety of part configurations. Components are attached to base rail system fixture parts for optimum results on a repetitive basis. Automation may be achieved using optional Sequencer. The product line also includes Welding Positioners and Turning Rolls.

Genstar Technologies Co.
4525 Edison Ave.
Chino, CA 91710
(909) 606-2726
E-Mail: sales@genstartech.com
Website: www.genstartech.com

Circle No. 1059

Divers Academy International Offers A Career That Will Take You Places.

Take your topside welding skills underwater and go places. Outstanding career opportunities await graduates of Divers Academy International, known world wide for training commercial divers and underwater welders to work on some of the worlds largest bridges, nuclear power plants and oilrigs. Our state of the art commercial diving program includes, underwater welding, non-destructive testing, HAZWOPER and remotely operated vehicle training. Divers Academy International is federally accredited and offers financial assistance if qualified, a student housing program and a career placement program. Our admissions coordinators are available to personally assist you.

Divers Academy International
2500 Broadway
Camden, NJ 08104
(800) 238-DIVE
FAX: (856) 541-4355
E-mail: diver@diversacademy.com

NEW! CLEARVISOR WITH ADFLO® WORKER PROTECTION SYSTEM

Circle No. 1063

ClearVisor with Adflo® system combines full eye and face protection with a slim, lightweight, powered air-purifying respirator. Polycarbonate ClearVisor Face Shield has exceptional clarity and wide viewing area, providing workers protection from high impact hazards. Can be used in metal grinding, sanding and refinishing, foundries, spray painting, woodworking, plastics, chemical and petrochemical processing, mining, aggregate processing, and other dusty environments.

Hornell, Inc.
2374 Edison Blvd.
Twinsburg, OH 44087, USA.
(800) 628-9218 or (330) 425-8880
FAX: (330) 425-4576
info.us@hornell.com • www.hornell.com

Circle No. 1060

ESAB PowerCut™ Plasmarc Cutting Packages

ESAB offers a new brochure on its PowerCut™ plasma cutting packages. PowerCut™ machines combine superior cutting performance with a new durable, weatherproof casing designed to handle the toughest work enviornments. Portable, easy to use, and incorporating ESAB's exceptional plasma cutting technology, PowerCut™ provides outstanding value in a "go anywhere" machine.

ESAB Welding & Cutting Products
411 S. Ebenezer Road
Florence, SC 29501-0545
(800) ESAB-123
Website: www.esabna.com

Circle No. 1064

Hypertherm's Powermax1650 — The Most Powerful G3 Plasma Cutting System Ever

The Powermax1650 promises greater speed, longer parts life and lower overall operating costs in heavy metal applications.Maximum cut capacity is 1-1/2 inches (38 mm). Gouging capabilities are in excess of 22 lbs. per hour. Increased cut quality and efficiency are assured through 100-amp/16-kilowatt output.

Hypertherm, Inc.
Etna Road
Hanover, NH 03755
(603) 643-3441
Website: www.hypertherm.com

ON-SITE FERRITE CONTENT MEASURMENT

Circle No. 1061

The rugged Feritscope® MP30 from Fischer Technology is a fast and accurate hand-held solution for measuring ferrite content in constructional steels, welded claddings, austenitic stainless steel and duplex steels. The Feritscope MP30 provides quick and precise non-destructive, on-site measurement in the range of 0–80% Fe or 0–120 WRC number.

Fischer Technology, Inc.
750 Marshall Phelps Rd.
Windsor, CT 06095
(800) 243-8417
FAX: (860)688-8496
E-mail: info@Fischer-Technology.com
Website: www.Fischer-Technology.com

Circle No. 1065

The Efficient, Ergonomic LX-31

LECO now offers the new LX-31 Inverted Metallurgical Microscope. Accommodating users with varying expertise, the LX-31 uses brightfield observation, and features ergonomically placed focusing and light intensity adjustment dials. Objectives ranging from 5X to 50X come standard on a 4-position revolving nosepiece. The 10X eyepiece (F.N. 20) offers greater inspection efficiency and clear observation. For more information contact LECO Corporation.

LECO Corporation
3000 Lakeview Ave.
St. Joseph, MI 49085-2396
(800) 292-6141
FAX: (269) 982-8977
Website: www.leco.com • Email: info@leco.com

Power MIG™ 300

Circle No. 1066

The Power MIG 300–a single phase, multi-process, synergic wire feeder welding package for the professional welder. This ready-to-weld package is unbeatable when it comes to superior multi-process welding. The synergic design, traditionally only available in more expensive welders, gives you ultimate control over the arc by automatically aligning wire feed speed and voltage. It also offers top quality aluminum welds with push-pull wire feed capability, not usually available in competitive models. True MIG pulsing and Pulse-on-Pulse™ capabilities ensure that superior feeding is matched by high quality arc performance.

Lincoln Electric Company
22801 St. Clair Ave.
Cleveland, OH 44117
(216) 481-8100
Website: www.lincolnelectric.com

Trailing Shield Kit

Circle No. 1070

The Weld Hugger Trailing Shield kit is an inert cover gas system designed to uniformly flow cover gas over and behind the weld pool to reduce part oxidation and discolorization. The kit's all stainless steel nozzles and manifold tube can be bent to conform to the geometry of many parts. The complete kit price is $249.95. To order, call toll-free or visit our website.

Weld Hugger LLC
7201 West Oakland St.
Chandler, AZ 85226-2434
(877) 935-3447
FAX: (480) 940-9366
Website: www.weldhugger.com

Sakura's "Solid Marker"

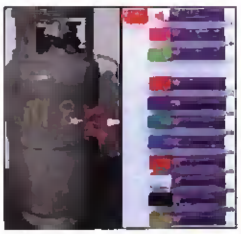

Circle No. 1067

Sakura's "Solid Marker" comes in 11 colors: white, black, blue, red, green, purple, orange, yellow, fluorescent lemon, fluorescent orange, fluorescent pink. Its twist-advance allows easy application and it can be recapped to avoid unwanted marks.Solid Marker is considered "waterproof" and permanently marks on all surfaces, including wet and greasy surfaces. It marks and won't smear on steel, sheet metal, iron, aluminum, plastic, rubber, vinyl, glass, concrete, and wood, along with other hard to mark surfaces. Solid Marker's original eight colors meets BS Class 5 and the fluorescent colors meet BS Class 2 weather resistance standards. Solid marker has a temperature range of 14°F to 212°F and has a 13mm tip and mark width.

Sakura of America
30780 San Clemente St.
Hayward, CA 94544
(800) 776-6257 x178
Website: www.sakuraofamerica.com

Literature Introduces Flux Recovery Vacuums Which Offers Low Maintenance and Safe Clean Work Environment

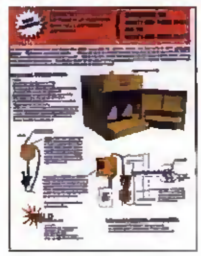

Circle No. 1071

The companyis new MIGHTY-MAC-3000X and MIGHTY-MAC-5000X heavy duty flux recovery vacuums are used with Weld Engineering Co., Inc.is optional flux separators and pressure feed systems to totally automate flux delivery, recovery and dust removal. Designed to be extremely low maintenance with automatic dust filter cleaning, while welding. A large hinged side door is opened for easy filter replacement and service. These units are eXtremely rugged for heavy, continuous recovery and eXtremely healthy because they filter dust below one micron to provide a clean, safe breathing environment.

Weld Engineering Company Inc.
34 Fruit Street
Shrewsbury, MA 01545
(508) 842-2224
FAX: (508) 842-3893 • Website: www.weldengineering.com

Metal-Cored Electrode For Harsh Conditions

Circle No. 1068

Select-Arc introduces a carbon steel, composite metal-cored electrode that features higher manganese and silicon contents to provide more deoxidation and a flatter bead geometry. The extra deoxidizers make Select 70C-6 the ideal choice to handle demanding applications such as heavier sheet metal fabrication, structural work, pipe welding and the welding of hot water heaters as well as general purpose welding.

Select-Arc, Inc.
P.O. Box 259
Fort Loramie, OH 45845-0259
(800) 341-5215
FAX: (937) 295-5217

New Line Of Heads Welds Pipe "IN PLACE"

Circle No. 1072

Two new models of weld Heads are specifically designed for multipass pipe welds. Configured for fast and simple operation, the Head is simply slipped over the pipe and clamped with a toggle lever. The Quickclamp weld Head models are designed for GTAW circumferential butt welding of pipes and tubes. The models cover the size range from 1" OD tube to 6" (6.625" OD) pipe. The new models incorporate all necessary functions required for multipass welding including electronic Arc Gap Control (AGC), filler wire feed capability, torch rotation, and torch oscillation with adjustable stroke width, speed, and end point "dwell". The Heads mount using an adjustable clamp - no Guide Rings or other separate components are required to use on specific pipe sizes. For more information contact Magnatech.

Magnatech Limited Partnership
P.O. Box 260
East Granby, CT 06026
(860) 653-2573
FAX: (860) 653-0486

New 1Torch™ Fits All Plasma Cutting Systems

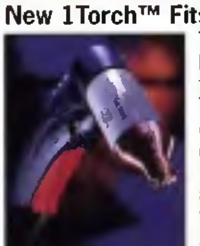

Circle No. 1069

The new 1Torch™ plasma torch from Thermal Dynamics, introduces a revolutionary technology that works with almost any plasma cutting system. The patent-pending 1Torch allows users to standardize torches and consumable parts on a variety of manufacturers' systems, thus reducing inventory requirements and corresponding expenses associated with operating multiple systems. The 1Torch features a new ergonomic torch handle and is rated superior for beveling, with greater pierce capability and easier straight-line cutting. The 1Torch's patent-pending ATC' (Advanced Torch Connector) makes it simple and quick to connect or disconnect the torch with less than one thread turn.

Thermal Dynamics
A Thermadyne Company
82 Benning Street
West Lebanon, NH 03784
(800) 752-7621or (603) 298-5711 (Intl.)
FAX: (800) 221-4401or (608) 298-0558 (Intl.)

Line Up Objects In Seconds,Instead of Minutes

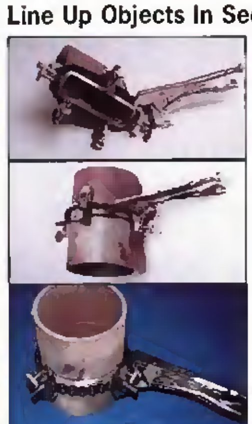

Circle No. 1073

The Piddler line up clamp, has an 18" chain, and (4) 3" long moveable, and removable nickel plated dogs. Weighing under 3 1/2 lbs. it works great in confined spaces. It will line up round, square, rectangle, triangle, hexagon, octagon, as well as other shapes, and different diameters. The capacity of the standard clamp is 1/8" standard pipe. 1 1/2" square, to 4", and up to 2" x 6" rectangle. By adding 18" more chain, it will line up 10" standard pipe, and still weigh less than 5lbs. It can be made even larger, by adding more chain and dogs. Stainless steel, and larger dogs will be available soon.

Piddler Tool Company
34 Volunteer Lane, PO Box 295
Decaturville, TN 38329
(866) 852-4818 Toll-free

EMPLOYMENT

TOP SALES JOB

Selectrode Industries, a 20 year old manufacturer of specialty flux coated welding electrodes is seeking the right person to be groomed for the eventual takeover of our sales manager's office in Huntington Station, New York, a suburb in Long Island.

The person we desire should have at least 5 years sales experience in the welding consumable field with an emphasis on stick electrodes. Computer literacy and the ability to occasionally travel both domestically and internationally are additional requirements.

The salary for this position is open, health and pension benefits are also included. Interested parties should fax their resume with full salary details to Paul at Selectrode Industries, Inc. Fax # 631-547-5475 or email them to { HYPERLINK "mailto:paulp@selectrode.com" }.

SELECTRODE INDUSTRIES

WELDING ENGINEERS

Positions available nationwide with major corporations. Recruitment demand in GMAW, GTAW, SMAW, RW, LBW including manual, semi-automated, & robotic welding. All costs paid by companies. Reply & resume to:

David Smith, CPC – Capital Source, Box 20987, Roanoke VA 24018, Fx 540-989-6557, Ph 540-989-6551, capitalsource@yahoo.com

Senior Level Executive

Nine years, experience in the welding industry. Can make a positive impact on your company's bottom line. As a leader, I possess strong problem solving and troubleshooting skills. I am extremely cost conscious and a strong team builder and mentor. I am particularly strong in sales and marketing as well as negotiation. I enjoy playing an active role in helping a company increase both profits and efficiencies. My name is Phil Pratt, former President of the Hobart Institute of Welding Technology. Phone: 937-498-0405; email: PPratt@woh.rr.com

CERTIFICATION/TRAINING

Training for 2003
REAL EDUCATIONAL SERVICES, INC.

CWI PREPARATORY
Guarantee - Pass or Repeat FREE!

SPECIAL WEEKEND COURSE
Houston, TX Mar. 21–23 & 28–30
Pascagoula, MS Mar. 14–16 & 21–23

SAT–FRI COURSE (7 DAYS)
Pascagoula, MS Mar. 15–21 • Jun. 14–20
Houma, LA Apr. 12–18 • Sep. 13–19

MON–FRI COURSE (5 DAYS)
Pascagoula, MS Mar. 17–21 • June 16–20
Houston, TX Feb. 10–14 • July 14–18
Houma, LA Apr. 14–18 • Sept. 15–19
Test follows on Saturday at same facility

APPLICATIONS OF VISUAL INSPECTION
Pascagoula, MS Mar. 10–14 • June 9–13
Houma, LA Apr. 7–11 • Sept. 8–12

RT FILM INTERPRETATION
Corpus Christi, TX Feb. 7–9 (Weekend)
Houston, TX Mar. 28–30 (Weekend)

MT/PT LEVEL I & II
Pascagoula, MS Feb 17–20
Houma, LA Mar. 3–6

For our entire class schedule, call
1-800-489-2890
GET REAL TRAINING!

ATTENTION
Welding Engineering Professional Engineers (PE)

If you possess a current PE license in welding engineering, you may be eligible to receive the IIW International Welding Engineer diploma.

For more information, contact Jeff Hufsey at *hufsey@aws.org.*

SERVICES

BUSINESS FOR SALE

BUSINESS FOR SALE

Twenty–year–old manufacturer of bench-top proprietary welders. Pulse arc, stored energy, resistance, fusion, stud projection. International markets, crafts, dental, jewelry, medical, appliance, auto, electronics assembly industries. Distributors, Reps and Direct Sales. Very Strong G.P. @ 85%, 22% B.T.E., and 11% after tax.

Business 4 Sale
P.O. Box 893
East Greenwich, RI 02818

EQUIPMENT TO BUY OR SALE

EQUIPMENT RENTAL

ADVERTISER INDEX

Advertiser	Website	Page
Abicor Binzel	www.binzel-abicor.com	IBC
Aelectronic Bonding, Inc.	www.abiusa.net	21
Airgas	www.airgas.com	19
American Torch Tip Co.	www.americantorchtip.com	17
Arc One	www.arc1weldsafe.com	21
Atlas Welding Accessories, Inc.	www.atlasweld.com	22
AWS Conference Dept.	www.aws.org	13
AWS Convention Services	www.aws.org	7
AWS Foundation Dept.	www.aws.org	37
AWS Membership Services	www.aws.org	10, 36, 40
Bohler Welding	www.btwusa.com	5
C&G Systems/Thermadyne	www.cgsystems.com	11
Centerline	www.cntrline.com	73, 74
Cor-Met	www.cor-met.com	23, 62
C-Spec	www.weldoffice.com	39
Detroit Convention Center	www.visitdetroit.com	61
Diamond Ground Products	www.diamondground.com	38
Divers Academy International	www.diversacademy.com	38
ESAB Welding and Cutting Prod.	www.esab.com	OBC
Fischer Technology	www.Fischer-Technology.com	16
Genstar Technologies	www.genstartech.com	18
Hi-Comm	www.saldat.it/www.weld.it	1
Hornell, Inc.	www.hornell.com	20
Hypertherm	www.hypertherm.com	27
LECO Corp.	www.leco.com	14
Lincoln Electric Company	www.lincolnelectric.com	2
Sakura of America	www.sakuraofamerica.com	39
Select Arc, Inc.	www.select-arc.com	IFC
Thermal Dynamics/Thermadyne	www.thermal-dynamics.com	9
Weld Academy	www.weldacademy.com	65
Weld Hugger, L.L.C.	www.weldhugger.com	15

IFC = Inside Front Cover
IBC = Inside Back Cover
OBC = Outside Back Cover

AWS Peer Review Panel

All papers published in the Welding Journal's Welding Research Supplement undergo Peer Review before publication for: 1) originality of the contribution; 2) technical value to the welding community; 3) prior publication of the material being reviewed; 4) proper credit to others working in the same area; and 5) justification of the conclusions, based on the work performed. The following individuals serve on the AWS Peer Review Panel and are experts in specific technical areas. All are volunteers in the program.

WELDING RESEARCH

SUPPLEMENT TO THE *WELDING JOURNAL*, FEBRUARY 2003
Sponsored by the American Welding Society and the Welding Research Council

The Mechanism of Stress-Relief Cracking in a Ferritic Alloy Steel

A novel stress-relaxation technique and extensive microstructural characterization of the carbide precipitation, elemental segregation, and fracture modes were used to investigate stress-relief cracking in a ferritic alloy steel

BY J. G. NAWROCKI, J. N. DuPONT, C. V. ROBINO, J. D. PUSKAR, AND A. R. MARDER

ABSTRACT. Stress-relief cracking is a major cause of weld failures in creep-resistant, precipitation-strengthened materials such as ferritic alloy steels, stainless steels, and Ni-based superalloys. Stress-relief cracking occurs primarily in the coarse-grained heat-affected zone of weldments. Although the general causes of stress-relief cracking are known, the underlying mechanisms are very much a topic of debate. The mechanism of stress-relief cracking in the coarse-grained heat-affected zone (CGHAZ) of a new ferritic alloy steel (HCM2S) was investigated through stress-relaxation testing and detailed microstructural characterization. The CGHAZ simulation and stress-relaxation testing was performed using Gleeble techniques. The time to failure exhibited C-curve behavior as a function of temperature. A balance of intergranular and intragranular carbide precipitation controlled the stress-relief cracking susceptibility. Cracking initiated at prior austenite grain boundaries by cavity nucleation on incoherent, Fe-rich M_3C carbides. The grain interiors were resistant to plastic deformation due to precipitation strengthening by small (5–40 nm) alloy carbides. Elemental segregation played no detectable role in the stress-relief cracking failures. Much of the microstructural characterization was performed using a VG603 FEG STEM having a probe size of about 1.5 nm. The small probe size allowed nano-sized precipitates to be individually analyzed by using EDS and elemental EDS traces taken across prior austenite grain boundaries. In addition, SE STEM imaging with the VG603 FEG STEM was able to resolve small precipitates that were previously unobservable using conventional TEM and STEM techniques. The results of this study form a basis for heat treatment and welding process variables for HCM2S to avoid stress-relief cracking. In addition, these procedures and analytical results can be applied to other materials to avoid microstructures that are susceptible to stress-relief cracking.

J. G. NAWROCKI, A. R. MARDER, and J. N. DuPONT are with Department of Materials Science and Engineering, Lehigh University, Bethlehem, Pa. C. V. ROBINO and J. D. PUSKAR are with Joining and Coating Department, Sandia National Laboratories, Albuquerque, N.Mex.

KEY WORDS

Stress-Relief Cracking
Carbide Precipitation
Coarse-Grained HAZ
Heat-Affected Zone
Ferritic Alloy Steel
High Temperature

Introduction

Ferritic alloy steels such as 2.25Cr-1Mo steel are commonly used for high-temperature applications in steam generators and pressure vessels for chemical and fossil power plants. Many components in these power plants operate at temperatures of approximately 300–700°C. New components fabricated from 2.25Cr-1Mo steel may require welding at both the installation and fabrication stages, and in-service material may be welded during repairs. In such applications, preheat and/or postweld heat treatments (PWHT) are often required to improve heat-affected zone (HAZ) mechanical properties and reduce susceptibility to hydrogen cracking. These preheat and PWHT steps represent a significant fraction of the overall fabrication/repair costs.

Recently, a new ferritic steel, denoted as HCM2S, was developed. HCM2S has been reported to exhibit improved mechanical properties and resistance to hydrogen cracking compared to 2.25Cr-1Mo steel (Refs. 1, 2). Table 1 compares the allowable composition ranges of both 2.25Cr-1Mo steel and HCM2S. Although the carbon content of HCM2S and 2.25Cr-1Mo can be identical, HCM2S is typically produced with a carbon content of ~0.06 wt-%, which is much lower than the typical carbon content of 2.25Cr-1Mo steel (Refs. 1–5). In addition, the maximum allowable C content is 0.1 and 0.15 wt-% for HCM2S and 2.25Cr-1Mo steel, respectively. The lowered carbon content of HCM2S relative to 2.25Cr-1Mo steel improves weldability by reducing hardenability and, therefore, the as-welded hardness of the HAZ. The creep rupture strength is improved by the substitution of Mo with W as a solid solution strengthener. Vanadium and niobium are added to improve creep strength by way of carbide precipitation strengthening. Boron is also added to improve creep strength. It has recently been suggested that the improved weldability from these composition modifications may permit elimination of costly preheat and/or PWHT requirements (Ref. 1). However, even if no PWHT is necessary, HCM2S will be exposed to comparable temperatures in service

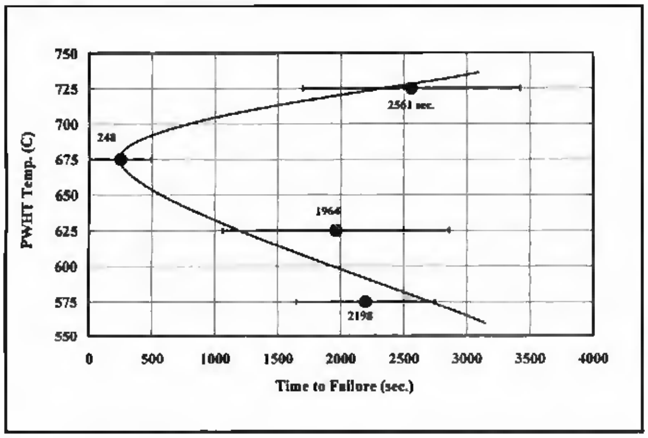

Fig. 1 — Time to failure during stress-relaxation testing for various test temperatures. The numbers within the graph represent the average of four to six tests at temperature.

Table 1 — Allowable Composition Ranges of HCM2S (wt-%)

Element	HCM2S (Ref. 1)	2.25Cr-1Mo (Ref. 3)
C	0.04–0.10	≤0.15
Cr	1.90–2.60	2.00–2.50
Mo	≤0.30	0.90–1.10
W	1.45–1.75	—
V	0.20–0.30	—
Nb	0.02–0.08	—
B	≤0.006	—
Al	≤0.03	—
Si	≤0.50	0.20–0.50
Mn	0.30–0.60	0.30–0.60
P	≤0.030	≤0.035
S	≤0.010	≤0.035

Table 2 — Chemical Composition of HCM2S Used in this Research

Element	Wt-%
C	0.061
Cr	2.52
Mo	0.11
W	1.50
V	0.24
Nb	0.05
B	0.0036
Al	0.013
Si	0.30
Mn	0.33
Ni	0.07
N	0.007
P	0.0013
S	0.006
Ar	0.0029
Sb	0.0001
Sn	0.007
Cu	0.022

where stress-relief cracking can occur during operation (Refs. 1, 2). In addition, HCM2S may be welded to existing 2.25Cr-1Mo steel that requires a PWHT. Previous work has shown HCM2S to be susceptible to stress-relief cracking, but the underlying mechanisms are largely undetermined (Ref. 6).

Stress-relief cracking is a common cause of weld failures in many creep-resistant, precipitation-strengthened alloys such as ferritic alloy steels (Refs. 7–9), stainless steels (Refs. 10, 11), and Ni-based superalloys (Refs. 12, 13). The general definition of stress-relief cracking is intergranular cracking in a welded assembly that occurs during exposure to elevated temperatures produced by post-weld heat treatments (PWHT) or high-temperature service (Ref. 14). Residual stresses are typically relieved during a PWHT through plastic deformation of the material. Therefore, a susceptible microstructure is one with strong grain interiors that resist plastic deformation and weak grain boundaries. Failure can occur in the heat-affected zone or fusion zone, but the coarse-grained heat-affected zone (CGHAZ) is the most susceptible region of a steel weldment.

Although the details of stress-relief cracking mechanisms are not totally understood, general knowledge of the causes of stress-relief cracking for ferritic alloy steels has been well developed (Refs. 8, 14–17). During a typical arc welding process, the unmelted base metal directly adjacent to the fusion zone reaches temperatures close to the melting point of the material, high in the austenite phase field of the Fe-C phase diagram. During the time spent in the austenite phase field, pre existing carbides, nitrides, carbonitrides, and even some inclusions dissolve into the austenite matrix. Since dissolution of the precipitates is diffusion-controlled, the degree of dissolution is dependent on the welding parameters that influence the thermal profile (time and temperature). However, if sufficient dissolution occurs, austenite grains grow essentially unimpeded, resulting in a large austenite grain size. Due to the fast cooling rates associated with arc welding, dissolved alloying elements remain trapped in solution and the austenite transforms to low-ductility martensite or bainite depending on the hardenability and thermal cycle. Another possibility is that the newly formed martensite may auto-temper during cooling, which is favored in systems with high martensite start and finish temperatures.

Carbides begin to precipitate when the CGHAZ is exposed to elevated temperatures during postweld heat treatment for stress-relief and/or during service. Eventually, stable carbides such as those based on V, Mo, Nb, and W nucleate on the many dislocations present in the grain interiors. The result is a fine, uniform dispersion, producing significant precipitation strengthening and even secondary hardening. These alloy carbides are mainly coherent or semicoherent with the ferrite matrix and stable at relatively high temperatures for long times (Refs. 7, 8, 14). The precipitates retard dislocation movement and restrict relaxation of residual stresses during postweld heat treatment. Carbides will also form on the energetically favorable prior austenite grain boundaries. These carbides are typically Fe_3C, $M_{23}C_6$, and M_6C and, at later stages of coarsening, are mainly incoherent with the matrix. They coarsen easily due to the incoherency and the fact they are located along high diffusivity paths. The matrix adjacent to the boundaries can then become devoid of alloying elements, and a precipitate-free or denuded zone is thereby formed along the prior austenite grain boundary (Refs. 9, 11). This region is soft and ductile relative to the remaining precipitation-strengthened grain interior.

Elemental segregation is also known to cause stress-relief cracking (Refs. 14, 15). Tramp elements (S, P, Sn, Sb, As) and intentionally added elements (Al, B, Mn) can segregate to prior austenite grain boundaries causing decohesion and weakening of the boundaries. In addition, sulfides are thought to precipitate at prior austenite grain boundaries, act as cavity nucleation sites, and promote crack propagation through stress-driven diffusion (Ref. 18).

The result of the above microstructural features is a precipitation-strengthened matrix with comparatively weak grain boundary areas caused by one or more of the following: coarse, incoherent precipitates; a soft denuded zone; and/or elemental segregation. Therefore, stress (residual or applied) will not be relieved through the intended macroscopic plastic deformation of the grains, but rather by cracking along prior austenite grain boundaries culminating in catastrophic, stress-relief cracking failure.

As described above, numerous theories exist on the causes of stress-relief cracking and these theories may all be valid under certain circumstances. The general reasons for stress-relief cracking are known, but the underlying mechanisms are still a source of debate. Many studies explore only one mechanism and disregard others. In addition, various

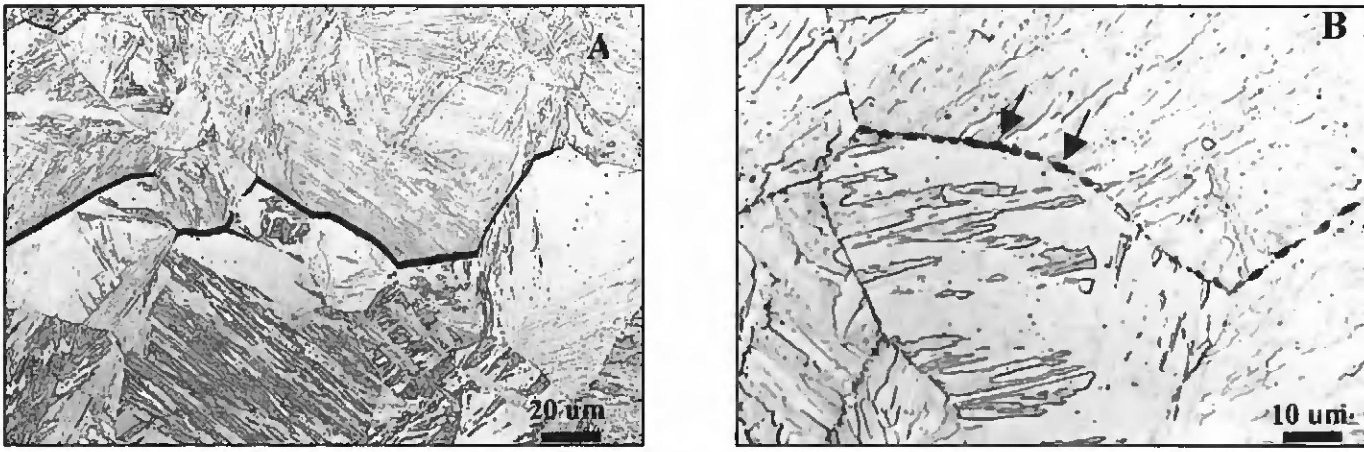

Fig. 2 — Representative LOM photomicrographs of failed samples viewed in cross section. Arrows indicate areas of void formation.

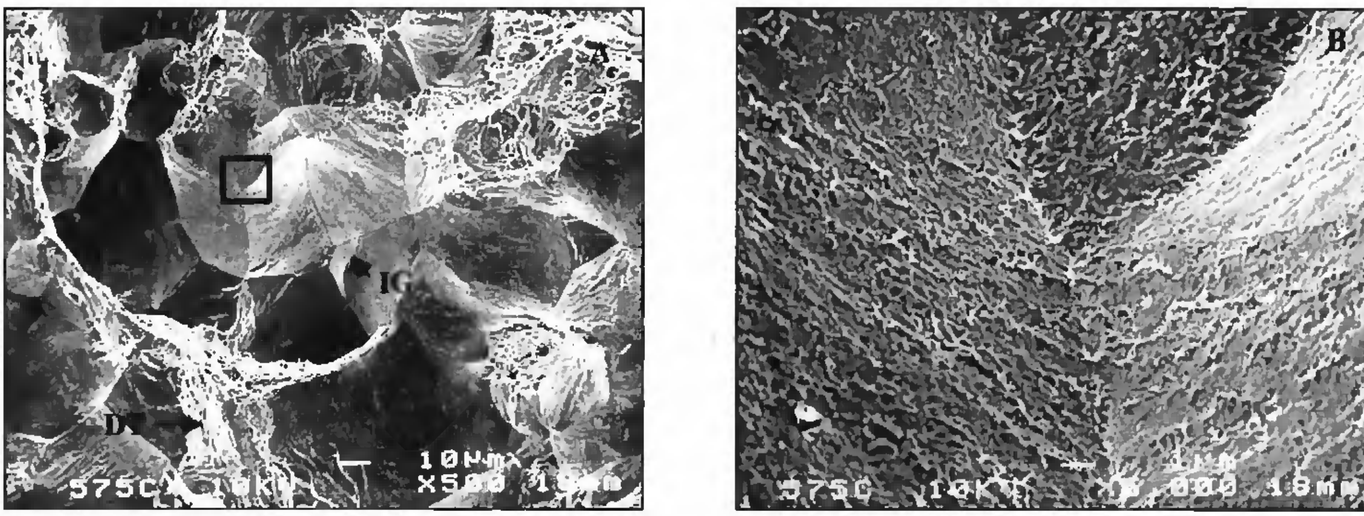

Fig. 3 — Representative SEM photomicrographs of the fracture surface of a sample that failed during testing at 575°C. IG = region of intergranular fracture; DT = region of ductile tearing.

mechanisms can operate simultaneously and the mechanism can change as a function of temperature.

The alloy HCM2S may be susceptible to stress-relief cracking from a compositional standpoint because it contains many strong carbide-forming elements and elements known to embrittle grain boundaries. Previous studies have confirmed HCM2S can be susceptible to stress-relief cracking (Ref. 6). Therefore, the objective of this research was to gain a fundamental understanding of the mechanism(s) of stress-relief cracking using HCM2S as the model system. Although HCM2S is a complicated system, such an alloy is necessary to explore each of the possible mechanisms of stress-relief cracking. Conclusions of this research will form a basis for heat treatment and welding processing variables necessary to avoid a microstructure susceptible to stress-relief cracking in ferritic alloy steels and other susceptible alloys.

Experimental Procedure

The chemical composition of the HCM2S used in this work, as determined using optical emission spectroscopy and wet chemical analysis, is shown in Table 2. Constant displacement, stress-relaxation tests were conducted to assess the stress-relief cracking susceptibility of the CGHAZ of HCM2S using round samples with a length of approximately 105 mm and a diameter of 10 mm with threaded ends. The samples had a reduced gauge-section approximately 10 mm in length and 5 mm in diameter. The CGHAZ was simulated and all testing was done using a Gleeble 1000 thermomechanical simulator. The thermal cycle to produce the CGHAZ was representative of the following weld parameters: 2 kJ/mm energy input, 93°C preheat temperature, and a peak temperature of 1350°C for a 12.7-mm steel plate (Refs. 19, 20). The samples were then cooled to room temperature and heated to the desired PWHT temperature at a rate of 200°C/s. The simulated CGHAZs were tensile tested at temperatures of 575, 625, 675, and 725°C to obtain the necessary data for the stress-relaxation tests. The 0.2% offset yield point was determined from the tensile tests using a dilatometer, which allowed only the CGHAZ to be monitored during tensile testing. The corresponding lengthwise displacement at the 0.2% yield point was determined from the acquired data and then used for the constant displacement stress-relaxation tests because the Gleeble could not be programmed to pull the sample to the required cross-wise displacement. Further details of the stress-relaxation test procedure can be found in (Ref. 21).

The stress-relaxation tests were done as follows: The CGHAZ was simulated as described above, cooled to room temperature and heated to a programmed PWHT temperature of 575, 625, 675, or 725°C. The samples were loaded in tension to the

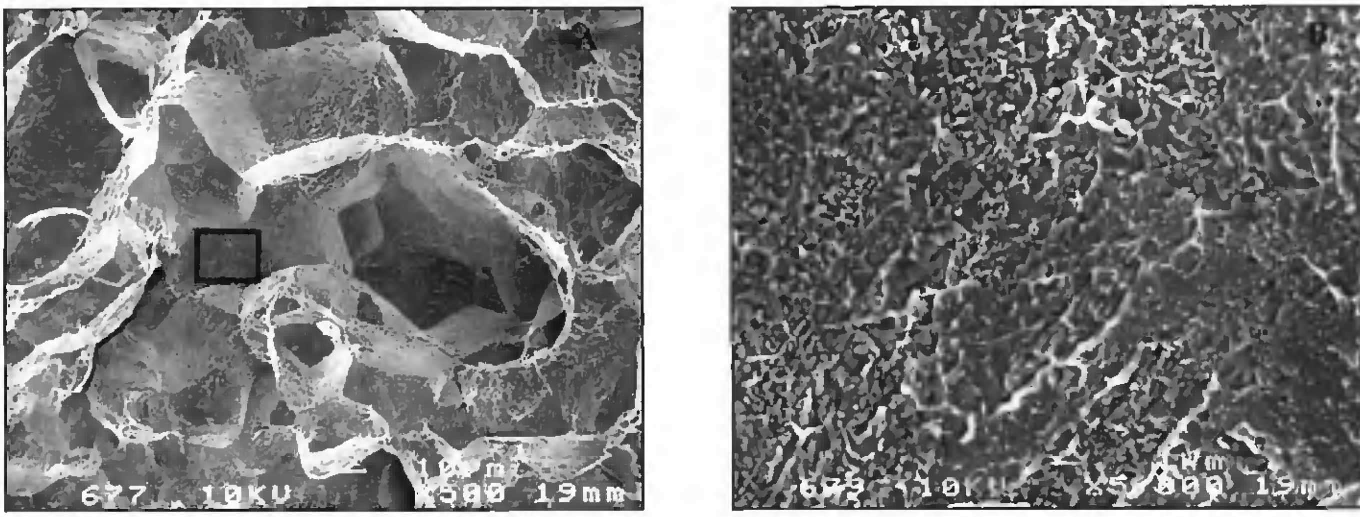

Fig. 4 — Representative SEM photomicrographs of the fracture surface of a sample that failed during testing at 675°C.

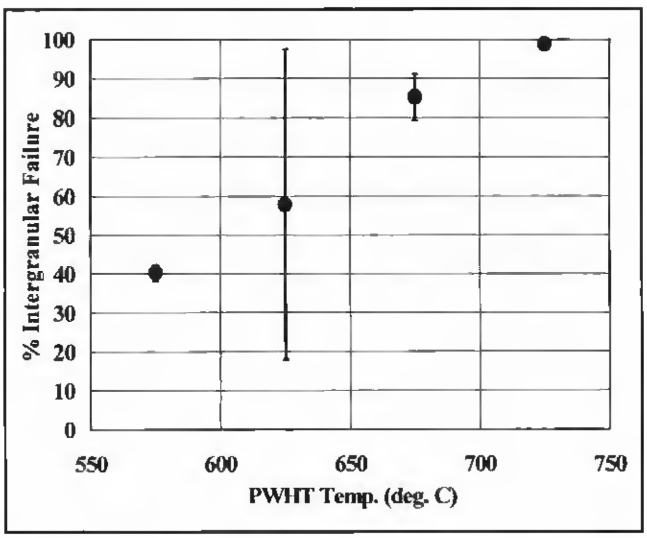

Fig. 5 — Amount of intergranular failure as a function of temperature.

displacement value corresponding to the 0.2% offset yield strength of the CGHAZ determined from tensile testing at temperature. The displacement was then held constant and the load was monitored as a function of time. This test method effectively simulates the residual stresses present in an actual weldment because the maximum residual stress that can be present is the yield strength (Ref. 22). Four to six stress-relaxation tests were performed per temperature and the times to failure obtained from the acquired data.

Failed samples were examined using light optical microscopy (LOM), scanning electron microscopy (SEM), and transmission electron microscopy (TEM). Samples were prepared using standard metallographic techniques and viewed in cross-section using light optical microscopy. The fracture surfaces were examined using a JEOL 6300f SEM operated at 10 kV. Thin foils were prepared by mechanically grinding 3-mm-diameter disks to ~50 µm followed by ion beam thinning to electron transparency. Elemental segregation was examined in thin foils by performing EDS linescans across prior austenite grain boundaries with a VG603 FEG STEM. The VG603 FEG STEM is a very unique instrument due to the very high beam current produced in a small area. The beam size is only ~1.5 nm and the accelerating voltage is 300 kV. These features allow very small areas of a sample to be analyzed without long counting times or sacrificing resolution. In addition, the small beam size allows the boundary to be analyzed with minimum interference from the matrix on either size of the boundary. Carbide precipitation was analyzed using carbon extraction replicas. The carbides were analyzed using EDS and convergent beam electron diffraction using both a JEOL 2000FX TEM operating at 200 kV and the previously mentioned VG603 FEG STEM. Secondary electron (SE) STEM imaging in the VG603 FEG STEM was used to resolve small precipitates on the carbon extraction replicas. These precipitates were unresolvable using conventional TEM and STEM techniques. Similar work, especially with regard to stress-relief cracking, had not been performed prior to this study.

Results and Discussion

Stress-Relaxation Tests

The stress-relief cracking susceptibility was measured by the time to failure during stress-relaxation testing. The time to failure as a function of temperature exhibited C-curve behavior as shown in Fig. 1. The nose of the C-curve, or shortest time to failure, occurred at 675°C. Typical light optical micrographs (cross-sectional view) of failed samples are shown in Fig. 2A and B. Many cracks are present behind the fracture edge. These cracks always occurred along prior austenite grain boundaries approximately normal to the tensile axis. Away from the fracture surface, cracks were never observed transgranularly or along packet boundaries. Cavities were also observed along the prior austenite grain boundaries, as illustrated in Fig. 2B. Thus, the general failure characteristics of the stress-relief cracking simulations are similar to those encountered in actual weldments.

The microscopic failure mode was further investigated using scanning electron microscopy to examine the fracture surfaces. The failure mode was strongly a function of test temperature. Figures 3 and 4 are representative scanning electron micrographs of the fracture surfaces of samples that failed during testing at 575 and 675°C, respectively. The samples tested at 575°C exhibited both intergranular failure (IG) and conventional macroscopic ductile tearing (DT), as shown in Fig. 3A. Examination of the areas of intergranular failure at higher magnification shows significant microductility (localized ductile failure comprised of microvoids) is present on the grain faces and possibly some small particles are also present on the grain faces — Fig. 3B. In contrast, the samples tested at 675°C failed almost completely intergranularly — Fig. 4A. The exposed grain surfaces were covered with microductility and small particles similar to the samples tested at 575°C — Fig. 4B. The amount of intergranular failure was measured from scanning electron photomicrographs using an image analysis system. In general, the amount of intergranular failure increased with increasing test temperature, as illustrated in Fig. 5. Samples tested at 575 and 625°C had only 40–60% intergranular failure, while those samples tested at 675 and 725°C exhibited 80–100% intergranular failure. These results imply the prior austenite grain boundary characteristics change with temperature and, therefore, further analysis of the grain boundaries was conducted.

Elemental Segregation

EDS linescans were done across prior austenite grain boundaries on thin foils prepared from samples that failed during stress-relaxation testing to determine if elemental segregation, in particular if known embrittling elements (S, P, Sn, As, Sb, and Mn), contributed to stress-relief cracking. Multiple boundaries (at least three) were analyzed in each sample and multiple linescans (at least two) were performed at different locations across a given boundary. Linescans were done by "stepping" the beam across prior austenite grain boundaries. Approximately 64 steps were done per linescan in increments of approximately 1 nm. The boundary could be analyzed with minimal interference from the matrix on either side of the boundary because the beam size was only ~1.5 nm. In addition, the beam current was high enough that a sufficient number of counts could be collected in a small amount of time, which minimized specimen drift. The results from typical EDS linescans are shown in Fig. 6, although not every element analyzed is shown. The STEM photomicrographs show the boundaries analyzed. The arrow on the photomicrograph indicates the direction of the EDS linescan (left to right on the graphs below the photomicrographs), and the "dotted" line to the left of the arrow on the photomicrograph shows, by virtue of the intense beam current, the path along which the beam traveled — Fig. 6A only. The graphs shown below the photomicrograph represent the number of X-ray counts as a function of distance or position for a given element. The prior austenite boundary position is

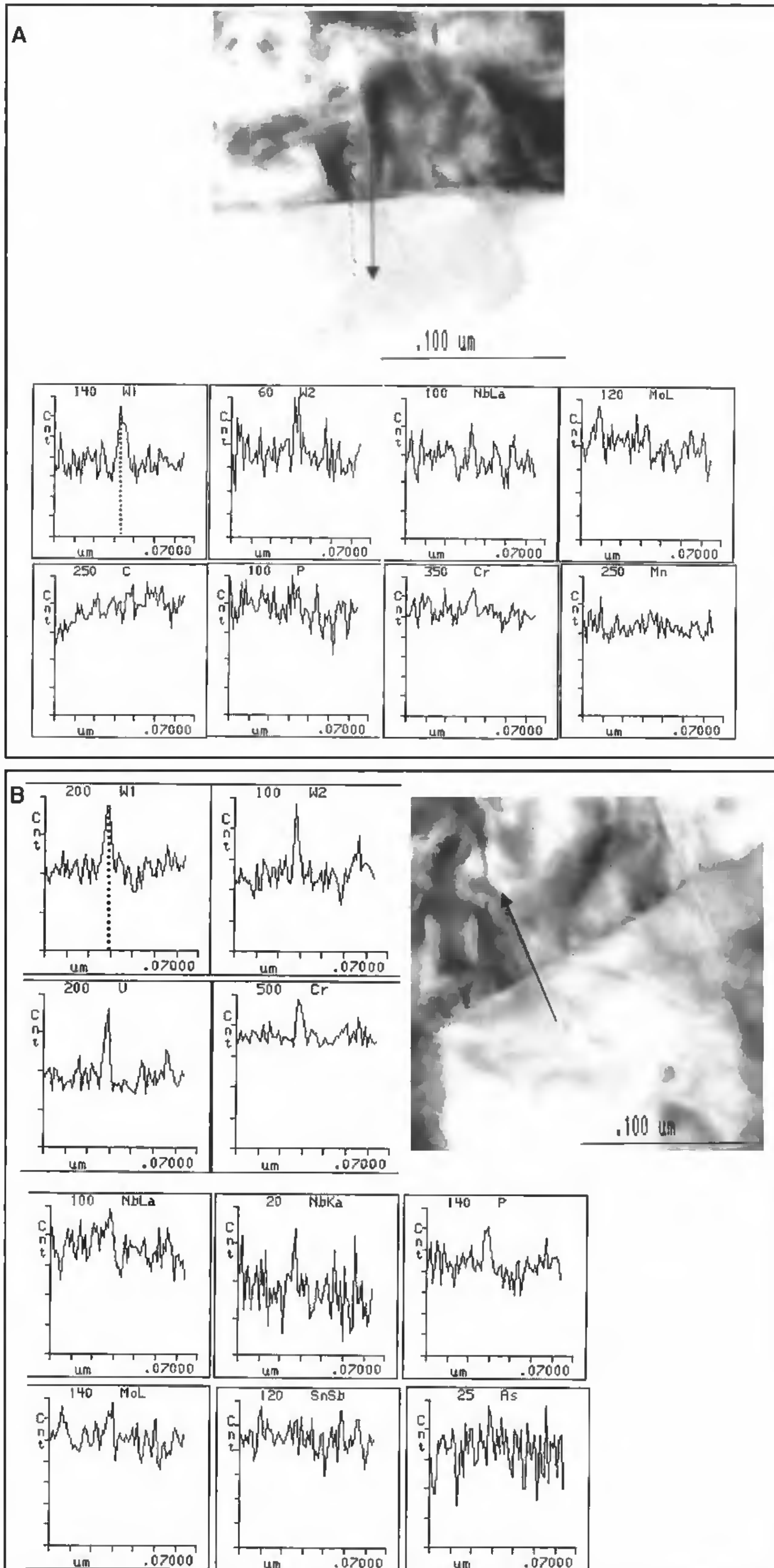

Fig. 6 — Typical EDS line scans done across prior austenite grain boundaries. Dotted line on W1 represents boundary position. A — Sample tested at 675°C; B — sample tested at 725°C.

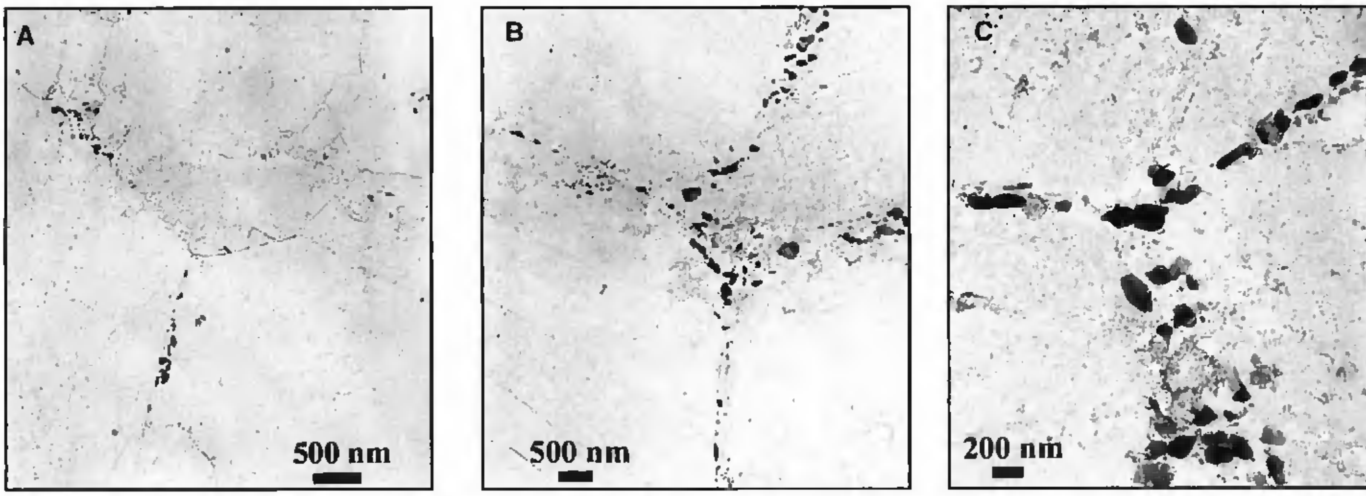

Fig. 7 — TEM photomicrographs of extraction replicas of typical prior austenite grain boundaries in a sample failed after testing. A — 575°; B — 675°C; C — 725°C.

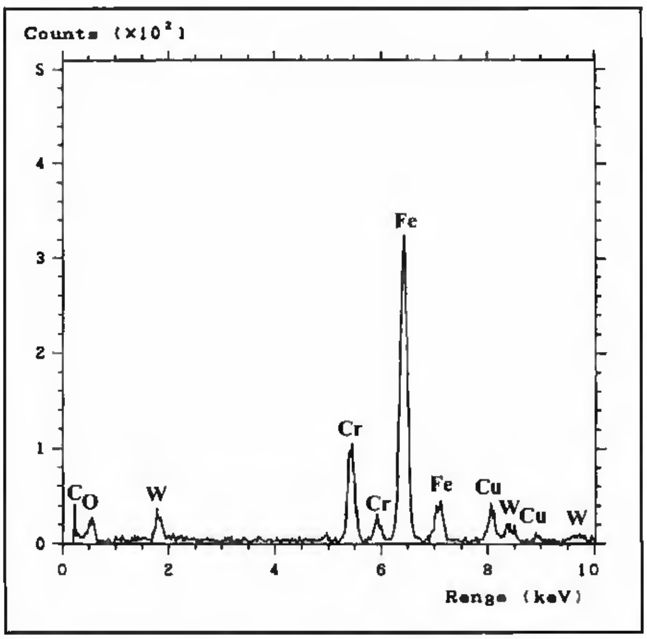

Fig. 8 — Representative EDS spectrum of Fe-rich M_3C found along prior austenite grain boundaries in the CGHAZ of failed stress relief cracking samples. Sample tested at 675°C.

Fig. 9 — TEM photomicrographs of extraction replicas of a typical prior austenite grain boundary triple point containing many course, incoherent M_3C carbides. Sample tested at 675°C.

indicated by the dotted line in the first graph of tungsten (W1). The only element enriched at the prior austenite grain boundary is W. Although it may appear an element such as Cr is also enriched at the prior austenite grain boundary (Fig. 6A), a calculation to indicate statistical significance (Ref. 23) shows W is the only statistically significant element enriched at the prior austenite grain boundary. Tungsten enrichment was found at almost every prior austenite grain boundary at each test temperature. Chromium and V segregation were occasionally observed, such as in Fig. 6B, but no tramp element segregation was detected at any prior austenite grain boundary. Again, it appears P is enriched at the prior austenite grain boundary, but the peak is statistically insignificant.

Tungsten has been shown to segregate to prior austenite grain boundaries in ferritic alloy steels (Ref. 24), but was found to de-embrittle the grain boundaries. In addition, much microductility was found on the areas of intergranular failure on the fracture surfaces. This characteristic fracture surface is not typical of failure due to tramp element segregation where the areas of intergranular failure have smooth and featureless fracture surfaces. It can be concluded from these results that elemental segregation did not contribute to stress-relief cracking in HCM2S. However, it should be noted boron segregation, which has been linked to stress-relief cracking in some alloys (Refs. 14, 15), couldn't be reliably detected by the analytical methods used here.

Carbide Precipitation

Transmission electron microscopy was used to further analyze the prior austenite grain boundaries. Carbides were identified using convergent beam electron diffraction patterns and from their characteristic EDS spectra (Refs. 25–27). Typical TEM extraction replica photomicrographs of prior austenite grain boundaries observed in samples tested at 575, 675, and 725°C are shown in Fig. 7. Carbides are visible along the prior austenite grain boundaries. These carbides ranged in size from about 50 to a few hundred nanometers and were identified as Fe-rich M_3C carbides with a representative EDS spectrum shown in Fig. 8. The samples tested at 575°C did not contain carbides at each prior austenite grain boundary — Fig. 7A. In contrast, the prior austenite grain boundaries of the samples tested at 675°C are more fully covered by the M_3C carbides (Fig. 7B), and the boundaries in Fig. 7C (725°C) are almost completely covered. The amount of grain boundary coverage as a function of temperature could not be quantified, but, in general, the amount of grain-boundary carbides (area fraction or % of grain boundary area covered) increased with increasing temperature. The varying coverage along a given grain boundary is probably due to orientation mismatch between adjacent grains. In general, increasing the degree of misorientation (less coincident sites) makes the site more energetically favorable to carbide precipitation because grain-boundary energy increases with misorientation (Ref. 28). As the temperature (or time) is increased, the degree of misorientation plays less of a role (Ref. 29). The varying degree of misorientation is presumably the reason almost every prior austenite grain boundary in the samples tested at 675°C were covered with carbides.

Further examination of the grain-boundary carbides explains their role in the stress-relief cracking failures. Figure 9 is a higher magnification view of a typical prior austenite grain boundary triple point containing many Fe-rich M_3C carbides. Most of these carbides have curved interfaces and are relatively coarse. In addition, M_3C car-

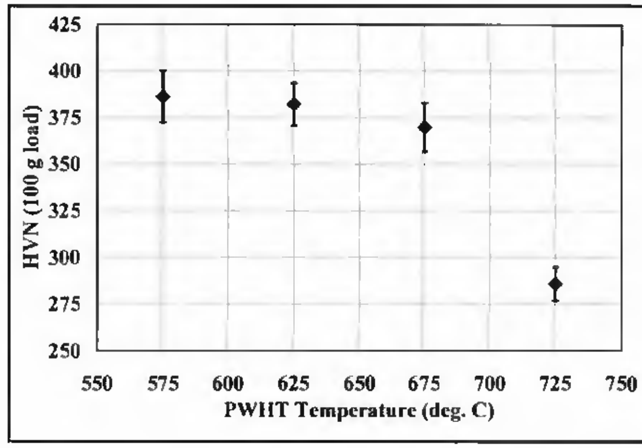

Fig. 10 — Intragranular hardness as a function test temperature.

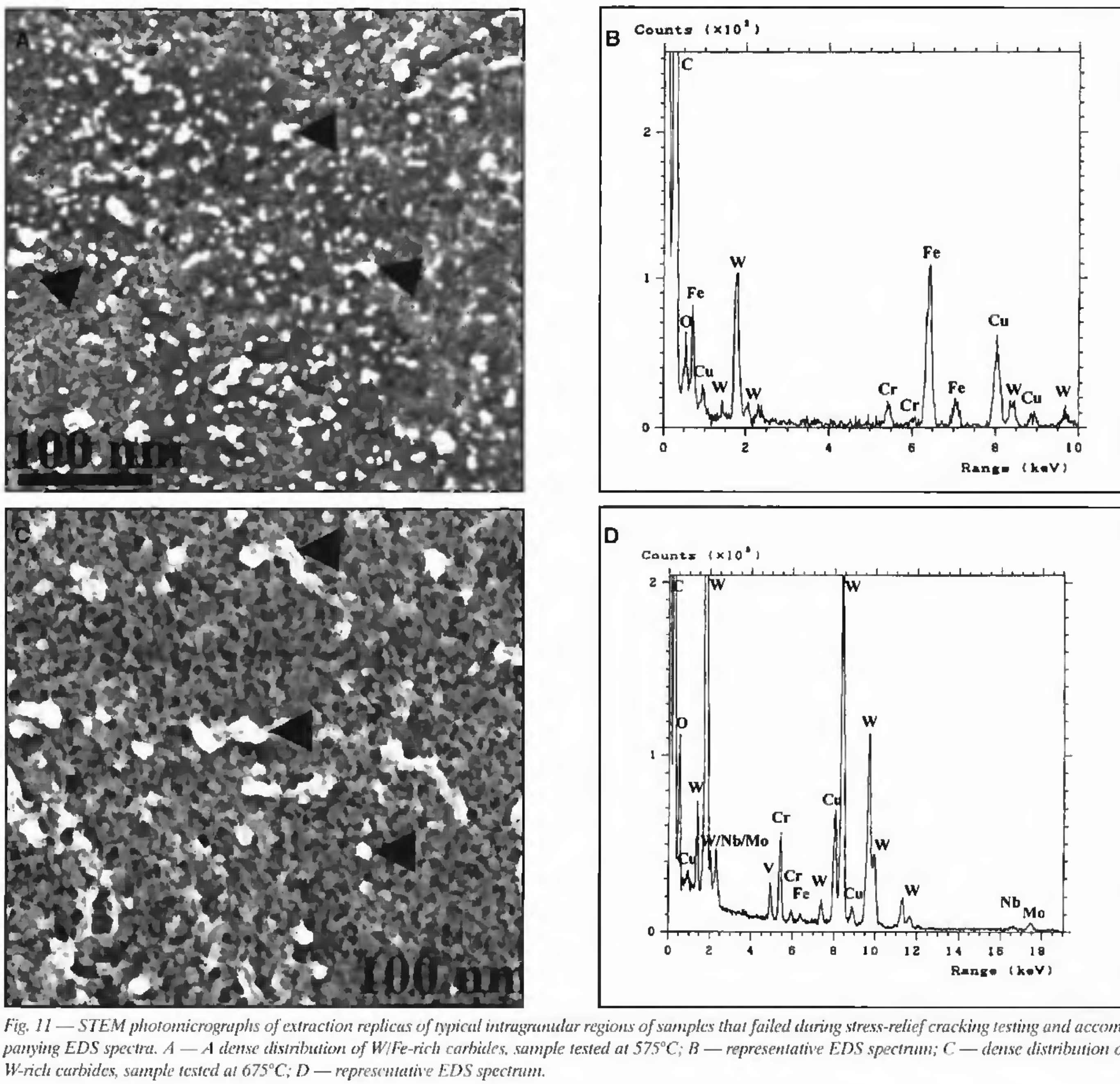

Fig. 11 — STEM photomicrographs of extraction replicas of typical intragranular regions of samples that failed during stress-relief cracking testing and accompanying EDS spectra. A — A dense distribution of W/Fe-rich carbides, sample tested at 575°C; B — representative EDS spectrum; C — dense distribution of W-rich carbides, sample tested at 675°C; D — representative EDS spectrum.

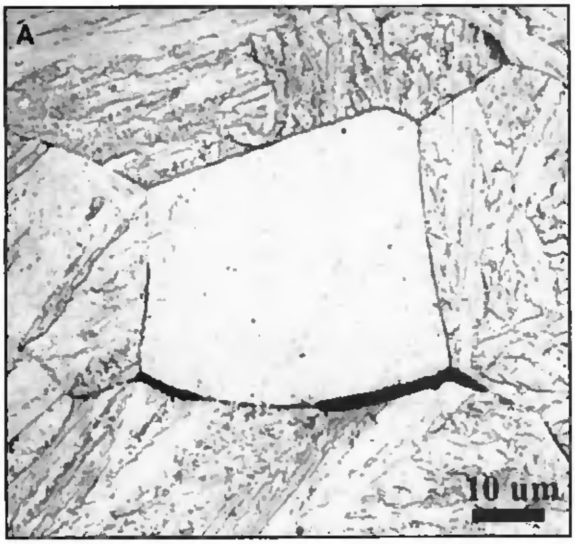

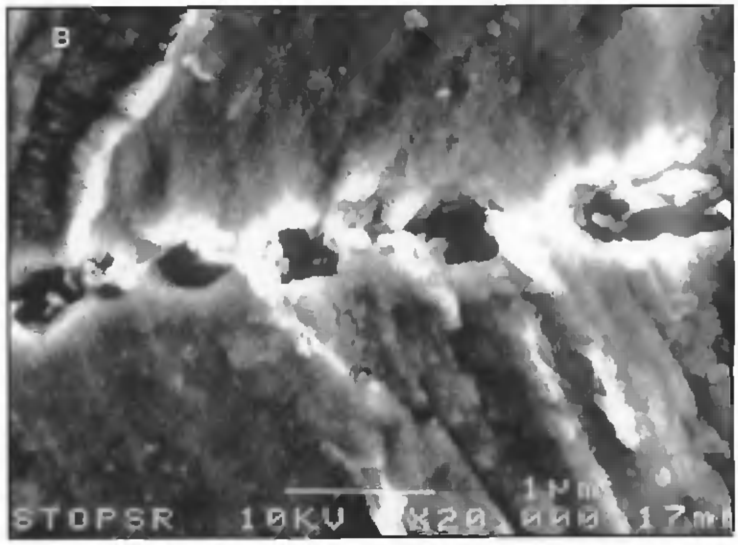

Fig. 12 — Example of crack and cavity formation at a prior austenite grain boundary. The cavities have nucleated on incoherent M_3C carbides. A — LOM photomicrograph; B and C — SEM photomicrographs.

bide has the orthorhombic crystal structure and, therefore, has little coherency with the bcc/bct ferrite matrix. The amount of intergranular failure increased with increasing temperature due to increasing amounts of intergranular M_3C carbides. However, if only grain- boundary carbides controlled stress-relief cracking, the time to failure would be expected to decrease with increasing temperature because the amount of grain-boundary carbides and intergranular failure increased with increasing temperature. However, the time to failure did not increase with temperature but exhibited C-curve behavior, as shown in Fig. 1. Thus, another factor is contributing to the stress-relief cracking failures.

Stress-relief cracking is a function of the material's ability to plastically deform to accommodate residual or service stresses. The strength of the prior austenite grain interiors largely governs the ability to plastically deform globally. Hardness measurements were taken on samples after stress-relaxation failure. The indents were placed only within the prior austenite grain interiors to minimize any contribution from the prior austenite grain boundaries and the results shown in Fig. 10. The hardness (resistance to plastic deformation) is approximately equal for the samples tested at 575, 625, and 675°C, but is significantly less in the sample tested at 725°C. It should be noted the use of a room temperature mechanical test to understand elevated temperature deformation is not entirely appropriate. These hardness tests were done at room temperature. The deformation mechanisms in most alloys differ between room temperature and elevated temperature. For instance, at elevated temperatures, dislocation climb and slip occur, but at room temperature, only slip typically occurs (Ref. 3). In addition, stress-relief cracking is a time-dependent failure, but hardness testing is time independent. Nevertheless, microstructural features such as precipitates, which provide obstacles to deformation, are likely to affect the deformation response in a qualitatively similar manner at high and low temperatures. Thus, the room-temperature hardness test should provide a reasonable representation of the relative strength of the grain interiors.

Carbide precipitation and, to a lesser extent, dislocation density, control the strength of the grain interiors. The morphology and coherency are the main factors that determine the strengthening potency of the precipitates. TEM and STEM techniques were used to examine intragranular precipitation as a function of test temperature. Figure 11A is a secondary electron (SE) STEM image of a carbon extraction replica of a typical intragranular region in a sample tested at 575°C. SE STEM imaging allows for the topography of a sample to be examined, and, therefore, small particles on a film are easily observed. These small particles were unobservable using conventional TEM imaging. A dense distribution of small precipitates is visible in Fig. 11A. These precipitates were found to be W and/or Fe-rich carbides that varied in size from approximately 5–20 nm with a representative EDS spectrum of an individual precipitate shown in Fig. 11B. Individual carbides were able to be analyzed using a VG603 FEG STEM because the beam size is only about 1.5 nm. These W/Fe-rich carbides provided significant precipitation strengthening that resulted in the relatively high hardness shown in Fig. 10. A SE STEM image of a typical intragranular region in a sample tested at 675°C is shown in Fig. 11C. A dense distribution of precipitates about 5–40 nm in size is present. These precipitates were found to be W-rich carbides with a representative EDS spectrum of an individual precipitate shown in Fig. 11D. Some V-rich carbides were also observed. The carbide distribution is relatively coarser than the samples tested at 575°C, but W and V-rich carbides are typically more coherent with the ferrite matrix than W/Fe-rich carbides. Therefore, it appears the differences in morphology are offset by the differences in composition, coherency, and morphology resulting in similar hardness values for the samples tested at 575 and 675°C.

Mechanism of Stress-Relief Cracking

The above results show that the stress-relief cracking response of HCM2S is a balance between intergranular and intragranular carbide precipitation kinetics and load relaxation. Examination of all the samples was done postfailure. Secondary cracks and cavities were present along the prior austenite grain boundaries away from the fracture surface in each sample and the exposed grain surfaces were covered with microvoids and small particles. From the microstructural characterization, it is known that large (50 to a few hundred nm) Fe-rich M_3C carbides are mainly present at the prior austenite grain boundaries. Therefore, the particles observed on the exposed grain surfaces can be assumed to be carbides. The fracture surfaces revealed varying amounts of macroscopic ductile tearing in addition to intergranular failure. It seems logical to conclude that because both the amount of grain boundary carbides and percentage of intergranular failure increased with increasing temperature, the two are directly related. However, the failure mechanism cannot be fully explained at this point.

A simple, yet critical experiment was done to isolate the role of grain boundary carbides in these stress-relief cracking failures. Since samples tested at 575°C exhibited significant amounts of both intergranular failure and macroscopic ductile rupture, 575°C was chosen as the test temperature for this experiment. An HCM2S sample was stress-relief tested as every previous sample. However, instead of allowing the test to continue until the sample failed, the test was stopped after 2000 seconds. This time was chosen because the average time to failure for HCM2S at 575°C was 2198 seconds. The intent was to stop the test at a point after cracking had initiated and close to failure. Although many of the cracks after 2000 seconds are probably in the propagation stage, examination of this sample still provides insight into crack initiation.

Examination of the sample using light optical microscopy revealed many cracks along prior austenite grain boundaries, as shown in Fig. 12A, but no evidence of ductile rupture. This indicates failure starts by microcracks along prior austenite grain boundaries, but it does not explain how cavities initiate. Scanning electron microscopy was then used to further examine the cracks. Figure 12B and C are SEM photomicrographs of a prior austenite grain boundary showing cavities that have formed in the vicinity of M_3C carbides. Although these particles were not analyzed on this sample, knowledge of the size and distribution of precipitates along prior austenite grain boundaries from TEM analysis indicates the small particles present on the exposed grain boundaries of the fracture surfaces must be Fe-rich M_3C carbides. No other particles were found at the prior austenite grain boundaries with the exception of small W/Fe-rich carbides or a random inclusion. These findings imply cracking initiates by cavity nucleation at prior austenite grain boundary carbides. These cavities then grow, coalesce, and form microcracks. Neither cavities nor microcracks were observed at prior austenite grain boundaries devoid of carbides.

Combining these results with the stress-relief cracking test results and microstructural characterization, the stress-relief cracking mechanism in the CGHAZ of HCM2S can be explained as schematically illustrated in Fig. 13. The mechanism is the same throughout the test temperature range, but the types of carbides and fraction of intergranular failure vary with temperature. During exposure to a PWHT temperature, Fe-rich M_3C carbides precipitate along the prior austenite grain boundaries and to a much lesser extent within the prior austenite grains. Some prior austenite grain boundaries are almost fully covered with these carbides, others are partially covered, and still others are completely devoid of these carbides. This is presumably due to the varying degree of misorientation from

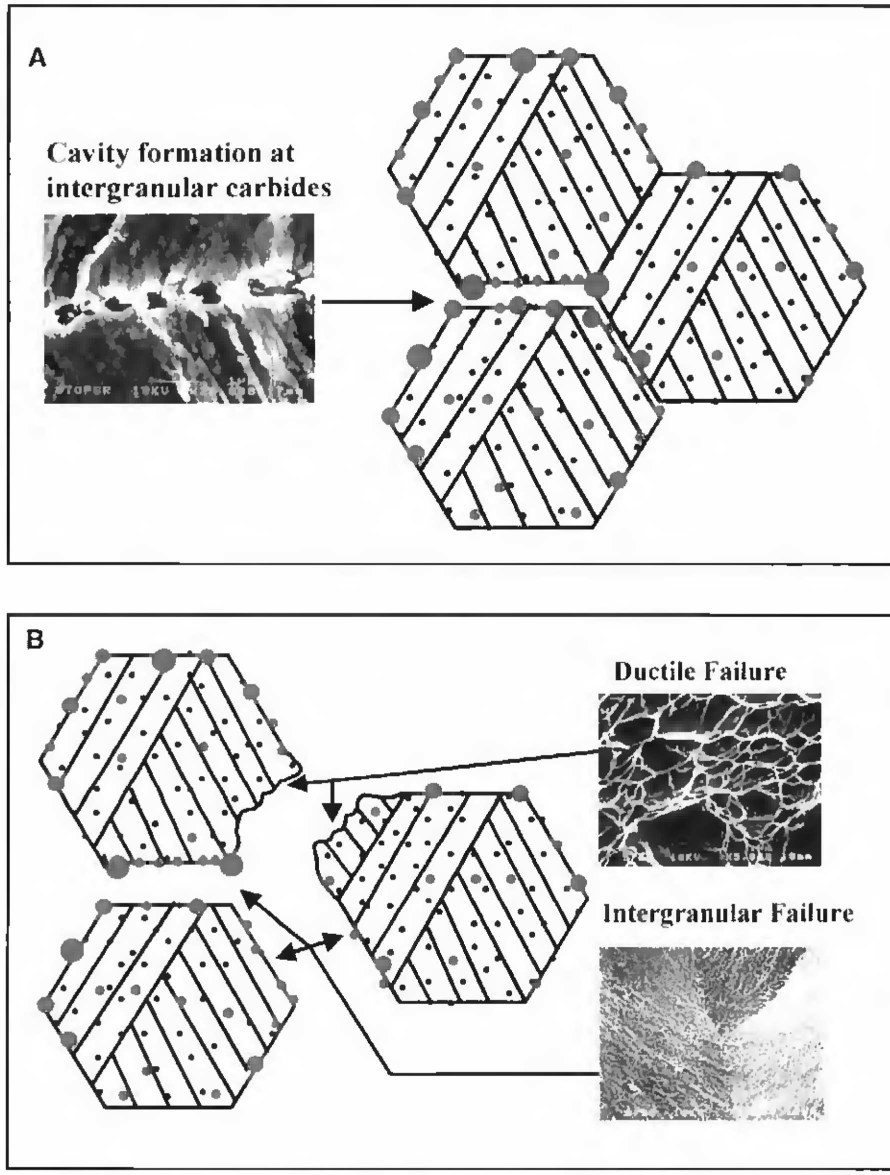

Fig. 13 — Mechanism of stress-relief cracking in the CGHAZ of HCM2S. A — During stress-relief relaxation; B — after failure.

boundary to boundary and along a given boundary. Some alloy carbides are also present along the prior austenite grain boundaries. These carbides also form a fine, uniform dispersion within the grain interiors both along lath boundaries and within laths. These alloy carbides provide significant precipitation strengthening. Simultaneously, the sample is held in tension at a constant displacement, which results in an applied load or stress that immediately begins to relax after the maximum load is reached. Carbide precipitation occurs simultaneously with the stress relaxation, and the rates of these two phenomena are functions of temperature.

Creep-like cavities formed during the load relaxation at M_3C/prior austenite grain boundary interfaces as illustrated in Figs. 12B and C and 13A. Eventually, these cavities linked to form microcracks along prior austenite grain boundaries. There were some grain boundaries that did not have any carbides present and therefore no cavities formed. Cavities continued to grow until enough microcracks formed and all the remaining stress was concentrated to the areas that were still intact. A point was eventually reached where the remaining uncracked areas could not sustain the stress and the material failed as conventional macroscopic ductile tearing simply due to being overstressed — Fig. 13B. This accounts for the ductile tearing shown in Fig. 3A. In addition, some grains that were only partially covered with carbides experienced both intergranular and macroscopically ductile failure at the same boundary.

The samples tested at 725°C experienced almost total intergranular failure because each prior austenite grain boundary contained many incoherent M_3C carbides. In general, these carbides were larger than those in the samples tested at 575°C. The coarser size leads to even greater incoherency because the carbides are becoming more spherical in order to minimize surface energy. Almost every prior austenite grain boundary cracked because almost every one was covered with incoherent carbides. However, the times to failure at 575, 625, and 725°C were comparable. The accelerated grain boundary weakening at 725°C relative to 575 and 625°C was offset by the increased ability of the grain interiors to plastically deform at 725°C relative to 575 and 625°C. This is the reason the times to failure were similar even though the resultant fracture surfaces were very different.

The nose of the temperature-time to failure curve occurred at 675°C. The times to failure were much shorter than any of the other test temperatures. These samples shared characteristics of both the low temperature samples (575 and 625°C) and the high temperature samples (725°C). Unfortunately, the shared characteristics were those that increase susceptibility to stress-relief cracking. Most of the prior austenite grain boundaries were covered with incoherent M_3C carbides, thus weakening the grain boundaries, as shown by the high amount of intergranular failure. The amount of intergranular failure in the samples tested at 675°C is only about 15% less than the samples tested at 725°C. A dense distribution of small intragranular W and V-rich carbides provided significant precipitation strengthening at 675°C. The intragranular hardness was approximately equal to that of the samples tested at 575 and 625°C. Therefore, the weak prior austenite grain boundary regions combined with a strong grain interior resulted in abrupt failure during the initial stages of stress-relaxation. The boundaries were covered with incoherent carbides and subsequent cavities because the grain interiors were precipitation strengthened before an appreciable fraction of the load could be relaxed. The load could then only relax through localized failure at prior austenite grain boundaries by precipitation-induced cavity initiation and propagation. This proposed mechanism explains both the C-curve behavior displayed in Fig. 1 and fracture characteristics (e.g., grain boundary cavities at precipitates and localized microvoid coalescence) of the CGHAZs of HCM2S.

Conclusions

The stress-relief cracking of a new ferritic alloy steel was investigated and a mechanism proposed based on stress-relaxation testing and detailed microstructural characterization. The coarse-grained, heat-affected zone of HCM2S was found to be susceptible to stress-relief cracking in the temperature range of 575–725°C. The stress-relief cracking susceptibility, as measured by the time to failure during stress-relaxation testing, exhibited C-curve behavior as a function of temperature when the nose of the C-curve was at 675°C. Stress-relief cracking was controlled by both intergranular and intragranular carbide precipitation. The amount of incoherent intergranular M_3C carbides increased with increasing temperature and resulted in an increase in intergranular failure. The grain interiors were resistant to plastic deformation due to precipitation strengthening by alloy carbides. Cracking initiated by cavity nucleation on incoherent, intergranular M_3C carbides. Eventually, these cavities linked to form microcracks. Complete failure occurred when the remaining uncracked areas could not sustain the load and failed due to conventional ductile tearing. Elemental segregation did not play a role in the stress-relief cracking failures. The results of this work provide a fundamental understanding of the underlying mechanisms of stress-relief cracking. In addition, this study can serve as a basis for the selection of heat treatment and welding processing variables necessary to avoid a microstructure prone to stress-relief cracking in susceptible alloys.

Acknowledgments

The authors would like to gratefully acknowledge Dave Ackland, Adam Papworth, and J. Alwyn Eades of Lehigh University for their contributions to this work.

References

1. Masuyama, F., Yokoyama, T., Sawaragi, Y., and Iseda, A. 1994. *Materials for Advanced Power Engineering*, Part I D. Coutsouradis et al., eds., Netherlands: Kluwer Academic Publishers, pp. 173–181.

2. Masuyama, F., Yokoyama, T., Sawaragi, Y., and Iseda, A. 1994. *Service Exposure and Reliability Improvement: Nuclear, Fossil, and Petrochemical Plants*. PVP, Vol. 288. ASME, pp. 141–146.

3. *Metals Handbook*, Vol. 1, 8th ed. Materials Park, Ohio: ASM International.

4. Prager, M., and Masuyama, F. 1994. *Proceedings Maintenance and Repair Welding in Power Plants V*. Orlando, Fla., pp. 16–30.

5. *Creep Rupture Data of HCM2S Steel Tubes, Pipes, Forgings, and Plates*. 1997. Sumitomo Metal Industries, Ltd., and Mitsubishi Heavy Industries, Ltd.

6. Nawrocki, J. G., DuPont, J. N., Robino, C. V., and Marder, A. R. 2000. *Welding Journal* 79(12): 355-s to 362-s.

7. Meitzner, C. F., and Pense, A. W. 1969. *Welding Journal* 48(10): 431-s to 440-s.

8. Swift, R. A., and Rogers, H. C. 1971. *Welding Journal* 50(8): 357-s to 373-s.

9. Edwards, R. H., Barbaro, F. J., and Gunn, K. W. 1982. *Metals Forum* 5(2): 119–129.

10. Irvine, K. J., Murray, J. D., and Pickering, F. B. 1960. *Journal of the Iron and Steel Institute* (10): 166–179.

11. Asbury, F. E., Mitchell, B., and Toft, L. H. 1960. *British Welding Journal* (11): 667–678.

12. Hughes, W. P., and Berry, T. F. 1967. *Welding Journal* 46(8): 361-s to 370-s.

13. Dix, A. W., and Savage, W. F. 1971. *Welding Journal* 50(6): 247-s to 252-s.

14. Dhooge, A., and Vinckier, A., 1986. *Welding in the World* 24: 104–126.

15. Meitzner, C. F. 1975. *WRC Bulletin* 211: 1–17.

16. McMahon, C. J. 1991. *Materials Characterization* 26: 269–287.

17. Dhooge, A., and Vinckier, A. 1992.

Welding in the World 30: 44–71.

18. Bika, D., Pfaendtner, J. A., Menyard, M., and McMahon, C. J. 1995. *Acta Metallurgica de Materialia* 43(5): 1895–1908.

19. Nippes, E. F., Merrill, L. L., and Savage, W. F. 1949. *Welding Journal* 28: 556-s to 564-s.

20. Nippes, E. F., and Nelson, E. C. 1958. *Welding Journal* 37: 289-s to 294-s.

21. Nawrocki, J. G. 2000. Ph.D. thesis. Lehigh University, Bethlehem, Pa.

22. *Welding Handbook*, Vol. 1, 8th ed. 1991. Miami, Fla.: American Welding Society.

23. Williams, D. B., and Carter, C. B. 1996. *Transmission Electron Microscopy*. New York, N.Y.: Plenum Press.

24. Lee, D. Y., Barrera, E. V., Stark, J. P., and Marcus, H. L. 1984. *Metallurgical and Materials Transactions* 15A: 1415–1430.

25. Titchmarsh, J. M. 1978. *Proc. 9th Inst. Congress on Electron Microscopy*, Vol I. Edited by J. M. Sturgess. Toronto, Canada: Microscopical Society of Canada, pp. 618–619.

26. Pilling, J., and Ridley, N. 1982. *Metallurgical Transactions A* 13A: 557–563.

27. Todd, J. A. 1986. *Scripta Metallurgica* 20: 269–274.

28. Read, W. T., Jr. 1953. *Dislocations in Crystals*. New York, N.Y.: McGraw-Hill Book Co., Inc.

29. Bennett, B. W., and Pickering, H. W. 1987. *Metallurgical Transactions* 18A: 1117–1122.

Preparation of Manuscripts for Submission to the *Welding Journal* Research Supplement

All authors should address themselves to the following questions when writing papers for submission to the Welding Research Supplement:

- ◆ Why was the work done?
- ◆ What was done?
- ◆ What was found?
- ◆ What is the significance of your results?
- ◆ What are your most important conclusions?

With those questions in mind, most authors can logically organize their material along the following lines, using suitable headings and subheadings to divide the paper.

1) **Abstract.** A concise summary of the major elements of the presentation, not exceeding 200 words, to help the reader decide if the information is for him or her.

2) **Introduction.** A short statement giving relevant background, purpose, and scope to help orient the reader. Do not duplicate the abstract.

3) **Experimental Procedure, Materials, Equipment.**

4) **Results, Discussion.** The facts or data obtained and their evaluation.

5) **Conclusion.** An evaluation and interpretation of your results. Most often, this is what the readers remember.

6) **Acknowledgment, References and Appendix.**

Keep in mind that proper use of terms, abbreviations, and symbols are important considerations in processing a manuscript for publication. For welding terminology, the *Welding Journal* adheres to AWS A3.0:2001, *Standard Welding Terms and Definitions.*

Papers submitted for consideration in the Welding Research Supplement are required to undergo Peer Review before acceptance for publication. Submit an original and one copy (double-spaced, with 1-in. margins on 8 ½ x 11-in. or A4 paper) of the manuscript. Submit the abstract only on a computer disk. The preferred format is from any Macintosh® word processor on a 3.5-in. double- or high-density disk. Other acceptable formats include ASCII text, Windows™, or DOS. A manuscript submission form should accompany the manuscript.

Tables and figures should be separate from the manuscript copy and only high-quality figures will be published. Figures should be original line art or glossy photos. Special instructions are required if figures are submitted by electronic means. To receive complete instructions and the manuscript submission form, please contact the Peer Review Coordinator, Doreen Kubish, at (305) 443-9353, ext. 275; FAX 305-443-7404; or write to the American Welding Society, 550 NW LeJeune Rd., Miami, FL 33126.

Do You Have Some News to Tell Us?

If you have a news item that might interest the readers of the *Welding Journal*, send it to the following address:
Welding Journal Dept.
Attn: Mary Ruth Johnsen
550 NW LeJeune Rd.
Miami, FL 33126.
Items can also be sent via FAX to (305) 443-7404 or by e-mail to *mjohnsen@aws.org*.

Influence of Reflected Arc Light on Vision Sensors for Automatic GTAW Systems

A model was developed to predict arc noise for various configurations of sensors, base metals, and welding arcs

BY J.-Y. YU, J.-I. KIM, AND S.-J. NA

ABSTRACT. Because of the difficulty in applying arc sensors to the welding of thin corrugated plates, vision sensors that provide three-dimensional geometry information by optical triangulation have been widely used for robot guidance in automatic welding of plates.

The reliability of vision sensors, however, is influenced considerably by arc light reflected from the base metal surface in spite of blocking the direct arc light with a light isolator. A reflectance model of a welding arc was developed to estimate arc noise for various configurations of sensors, base metals, and welding arcs in three-dimensional space by assuming the welding arc as a point and extended light source.

Various experiments were conducted to determine the bidirectional reflectance distribution function (BRDF) parameters of the model, and to verify the validity of the proposed model. Two proposed models, the point source model and the extended source model, were compared with the gray level of the reflected arc caught by a CCD camera. The experimental data of the gray level of the reflected arc generally agreed well with calculated results obtained by the two models, while the model with a point light source resulted in a greater discrepancy for short distances between the welding arc and reflecting surface of the base metal.

The proposed models and experimental results can be effectively used for optimal design of the configuration and the moving path of vision sensors according to base metal shape, which improves the measuring efficiency of vision sensors (Refs. 1, 2) and reduces the effect of arc noise on them (Ref. 3), thus enhancing the performance of the vision sensor in automatic joint tracking of the arc welding process.

J.-Y. YU and J.-I. KIM are with Mechanical Engineering Division, Advanced Reactor Development, Korea Atomic Energy Research Institute, Korea. S.-J. NA is with Department of Mechanical Engineering, Korea Advanced Institute of Science and Technology, Korea.

KEY WORDS

Vision Sensor
Joint Tracking
Light Reflectance
Arc Noise
Point Source
Extended Source

Introduction

Vision sensors are one of the most powerful forms of noncontact sensory feedback for monitoring and control of manufacturing processes such as welding. Machine vision applications in welding have included off-line determination of the locations of the workpieces to be welded (typically referred to as part finding); the in-process correction of robot paths to compensate for fixturing inaccuracies, part tolerances, or weld distortions during welding (joint tracking); the real-time sensing of weld joints, pool shape, and geometry for control of the welding process; and automated inspection of weld joints and bead surface shapes. However, welding poses particularly challenging problems to conventional optical sensing techniques. One of the major problems is the presence of the welding arc, which is not limited to a single spectral region (Refs. 4–8) and is thus difficult to filter optically. A novel vision sensing technique has been developed and is used to overcome the extreme variations in scene brightness created by the welding arc (Refs. 9–15). However, resolution and field of view were the primary considerations in the design of vision sensors, while sensor reliability was only rarely investigated. Lenef et al. (Ref. 16) measured the arc spectrum to find the wavelength range of the diode laser, which would minimize arc effect. In their experiments, the base metal shape was neglected and the diffuse reflection was assumed for the base metal surface. Nakata et al. (Ref. 17) studied the optimal configuration of optical components by varying the position and resolution of the camera and light source, camera exposure, and other factors. The results, however, were limited in practical application because the arc light was neglected and there was a lack of theoretical understanding in analyzing the experimental results. Various reflectance models have been used in the area of machine vision. Broadly speaking, these models can be classified into two categories: diffuse reflectance models and specular reflectance models. Until now, many applications have proven that the Lambertian model and the Torrance-Sparrow model adequately describe general diffuse and specular lobes in the vision research community (Refs. 18–20).

Because existing research (Refs. 21, 22) mostly deals with the arc light as a point source carried out in the same plane as the incident beam, those results should be applied only to the situation where vision sensors and the arc generated under the welding gun are positioned on the same plane. Wang has modeled the arc as a cylindrical shape in studies of arc light generated from an arc plasma (Ref. 23). Such a model should closely approximate the actual shape in order to precisely represent the intensity of the arc light in the short distance between the considered point on the base metal and the welding arc. It is important the arc shape is modeled sufficiently (Ref. 24); therefore, the shape of the arc light can be simplified as a half-hemisphere, which represents the

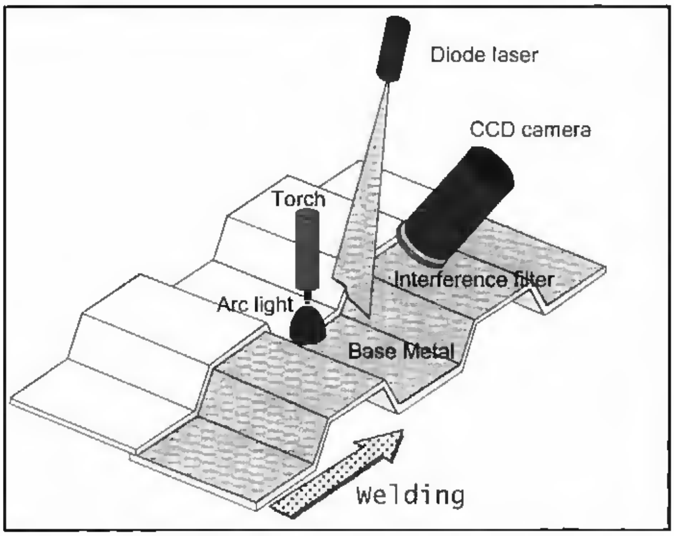

Fig. 1 — Schematic of an automatic welding system with vision sensor.

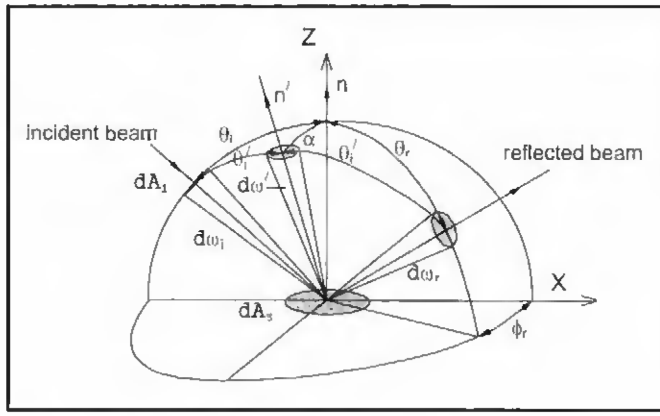

Fig. 2 — Coordinate system for defining BRDF.

arc shape in automatic welding (Ref. 25).

In order to improve the reliability of vision sensors in arc welding, the effect of arc light was investigated as to the geometrical configuration of the vision sensor and the welding arc in a three-dimensional space where various reflection properties of the base metal surface are considered. Base metal reflection was modeled in a three-dimensional (3-D) domain, and the intensity of the arc image was formulated by assuming the arc light as an extended light source.

Theoretical Formulation

Figure 1 shows the typical configuration of an automatic welding system with a visual joint tracking sensor, such as corrugated sheets used for inside walls of LNG tanks or shipping containers. The laser beam is reflected from the base metal surface in front of the welding arc, and the image pattern captured by the CCD camera is used to determine the shape of the weld joint. An interference filter in the camera allows only light with a wavelength range near the laser beam to pass through. At the same time, the arc light is also reflected from the base metal surface and captured by the CCD camera through the interference filter. The intensity of reflected arc from the base metal changes continuously, because the configuration of the vision sensor and torch must be varied according to the motion of the manipulator for joint tracking. In this study, only the arc noise reflected from the sensing area of the base metal surface covered by the CCD camera was considered in formulating the magnitude of the arc light in accordance with the three-dimensional configuration of the arc, base metal, and camera. The preview distance of the joint tracking vision sensor must also be considered because this parameter significantly contributes to the intensity variation of arc noise.

Reflectance Model of Surface

The local coordinates system was adopted to represent general reflectance characteristics. The angular distribution of the reflected radiant flux is conventionally expressed in terms of the bidirectional reflectance. Consider the geometry shown in Fig. 2. This coordinate system was used to derive the Torrance-Sparrow model. More detailed derivation is given in Refs. 19 and 20. The surface area dA_s is located at the origin of the coordinate frame, and its normal vector point in the direction of z axis. The surface is illuminated by a beam of light that lies in the x-z plane and is incident on the surface at the angle θ_i. The direction (θ_r, ϕ_r) determines the surface radiance for the viewing direction of the vision sensor, which is the direction of interest. Only those planar microfacets whose normal vectors lie within the solid angle $d\omega'$ are capable of specularly reflecting light into the infinitesimal solid angle $d\omega_r$.

The BRDF f_r is defined for the general expression of reflectance as follows:

$$f_r(\theta_i,\phi_i;\theta_r,\phi_r) = \frac{dL_r(\theta_i,\phi_i;\theta_r,\phi_r)}{dE_i(\theta_i,\phi_i)} \quad (1)$$

where $dE_i(\theta_i, \phi_i)$ is the irradiance in the direction of (θ_i, ϕ_i) and $dL_r(\theta_i, \phi_i; \theta_r, \phi_r)$ is the reflected radiance in the direction of (θ_r, ϕ_r) caused by $dE_i(\theta_i, \phi_i)$. The radiance of a Lambertian surface is proportional to its irradiance.

The surface irradiance dE_i produced by incident radiance dL_i is determined by dividing the radiant flux by surface area dA_s and expressed as follows:

$$dE_i(\theta_i,\phi_i) = L_i(\theta_i,\phi_i)\cos\theta_i d\omega_i \quad (2)$$

where $d\omega_i = \sin\theta_i d\theta_i d\phi_i$ is the infinitesimal solid angle. By integrating Equation 2 in all directions on the hemispherical surface, E_i is obtained as follows:

$$E_i(\theta_i,\phi_i) = \int_w L_i(\theta_i,\phi_i)\cos\theta_i d\omega_i \quad (3)$$

$L_r(\theta_r, \phi_r)$ is proportional to its irradiance $E_i(\theta_i, \phi_i)$. Thus, in a similar way, it can be obtained from Equations 1 and 3 with the following:

$$L_r(\theta_r,\phi_r) = \int_w f_r\, E_i(\theta_i,\phi_i)\cos\theta_i d\omega_i \quad (4)$$

It was considered that the BRDF f_r was composed of fractions of the diffused reflection f_{rd} and specular reflection f_{rs}. The polar plot of the three reflection components (diffuse lobe, specular lobe, and specular spike) is shown in Fig. 3.

$$f_r = f_{rd} + f_{rs} \quad (5)$$

The BRDF f_{rd} has a constant value κ_{diff}, which represents the level of diffused reflection. The BRDF f_{rs} is dependent on the surface of the workpiece, since different models are available according to the ratio between the *rms* value of the surface roughness R_q and light wavelength λ (Ref. 20). In the case of $R_q/\lambda << 1$, the specular reflection has the same property as on the mirror

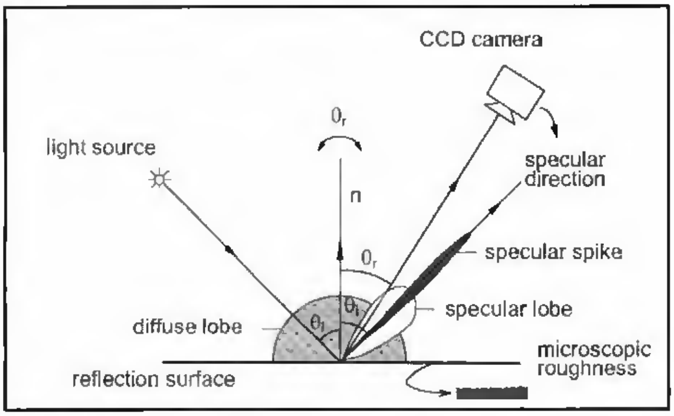

Fig. 3 — Schematic of three reflection components.

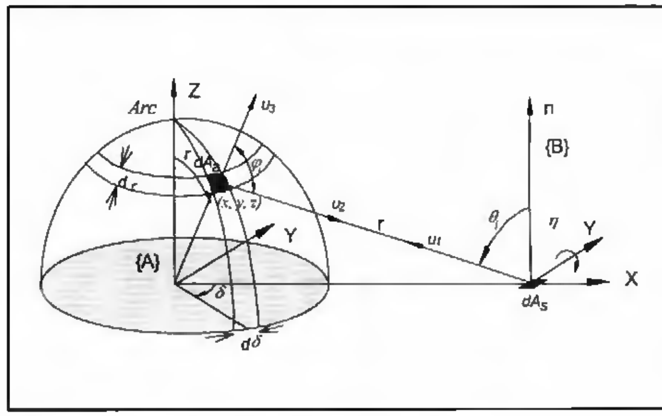

Fig. 4 — Coordinate system of arc shape and reflection point.

Fig. 5 — Apparatus for experiments of arc noise.

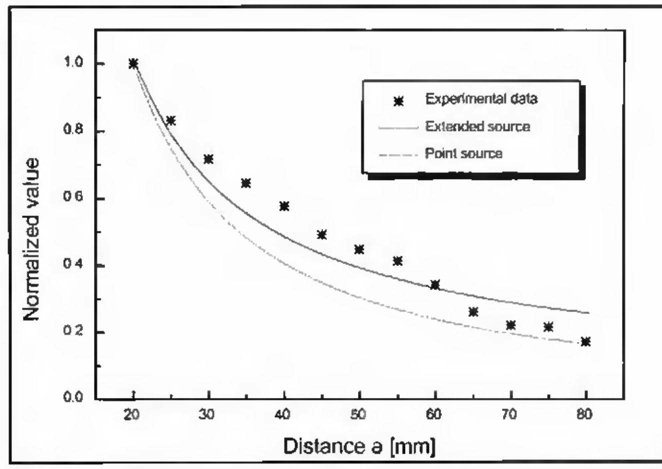

Fig. 6 — Intensity of gas tungsten arc reflected from mild steel with varying distance a (θ_i = 70 deg, θ_r = 20 deg, ϕ_r = 0 deg).

and is modeled in 3-D as follows:

$$f_{rs} = \delta(\theta_r - \theta_i)\delta(\phi_r - \phi_i - \pi) \quad (6)$$

where $\delta(\theta_r - \theta_i)\delta(\phi_r - \phi_i)$ is a function that satisfies the following:

$$\delta(\theta_r - \theta_i)\delta(\phi_r - \phi_i) = 1 \quad \text{for } \theta_r = \theta_i \text{ and } \phi_r - \phi_i = \pi$$

$$\delta(\theta_r - \theta_i)\delta(\phi_r - \phi_i) = 0 \quad \text{for } \theta_r \neq \theta_i \text{ or } \phi_r - \phi_i \neq \pi$$

In the case of $R_q/\lambda >> 1.5$, Torrance et al. established a model based on the assumption the rough surface was composed of specular elements arranged arbitrarily, and that Fresnel reflectance of a material has only a negligible effect on BRDF (Ref. 26). Ignoring the variation of the Fresnel reflectance in accordance to the angle change, the Torrance-Sparrow model can be expressed as follows:

$$f_{rs} = \kappa_{spec}\left[\frac{G(\theta_i,\phi_i,\theta_r,\phi_r)}{\cos\theta_r}\right]exp\left(-c^2\alpha^2\right) \quad (7)$$

where κ_{spec} is the fraction of specular reflection and c is the statistical distribution of the direction of specular elements. Using spherical trigonometry, the local angle of incidence θ'_i and slope α of the reflecting facets can be determined from angle θ_i, θ_r, and ϕ_r in Fig. 2. $G(\theta_i,\phi_i,\theta_r,\phi_r)$ was termed the geometrical attenuation factor, which included consideration of the effect of neighboring specular elements. A detailed derivation is given in Refs. 19, 20.

In the case of $R_q/\lambda \cong 1$, formulation of the specular reflection is quite complex and can be performed only by applying the physical model using wave optics. However, it has been shown that the Torrance-Sparrow model can very accurately predict specular reflection in this case, if no peak values occur. Furthermore, this case is only rarely encountered in applications of vision-aided welding systems, and thus was not formulated in the study.

Arc Noise Model

The welding arc is an electrically conductive gas called plasma, which is considered to be the fourth and most complex state of matter. The arc-column plasma is produced by the electrical breakdown of normally nonconducting gases between the electrode and the workpiece. Electrical breakdown of the gas occurs through ionization, the process of stripping electrons from atoms. The energy spectrum radiated from the welding arc is composed of characteristic spectral lines of the plasma elements and ions and the black body emission (Refs. 6, 17, 21). The position and intensity of the characteristic spectral lines are known to be strongly influenced by welding conditions, base metal, and shielding gas, while the black body emission of the arc spectral radiance $L_\lambda(\lambda)$ can be expressed by Planck's Law.

In general, configuration of the arc and the point measured by a vision sensor in joint tracking is shown in Fig. 3. If the effective area (A_{eff}) of the arc, which is defined as the part of the arc viewed from the center of the area of interest on the base metal, is relatively large compared to the square of the distance between the arc and base metal (a^2), the arc light must be assumed to be not a point light source, but an extended light source. The model of the arc shape should be close to its actual

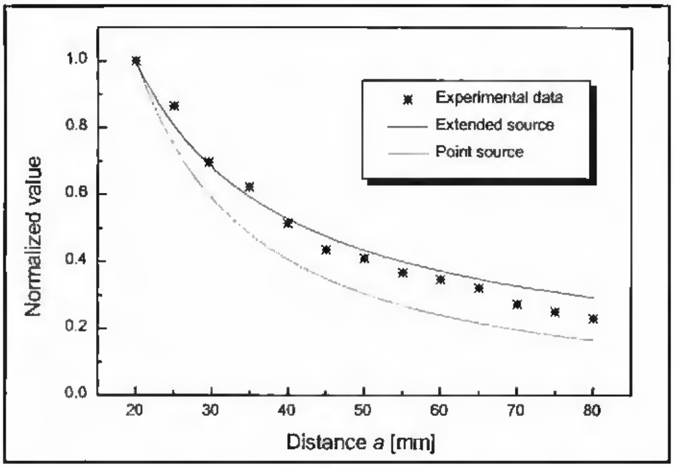

Fig. 7 — *Intensity of gas tungsten arc reflected from Zn-coated container panel with varying distance* a (θ_i = 30 deg, θ_r = 60 deg, ϕ_r = 0 deg).

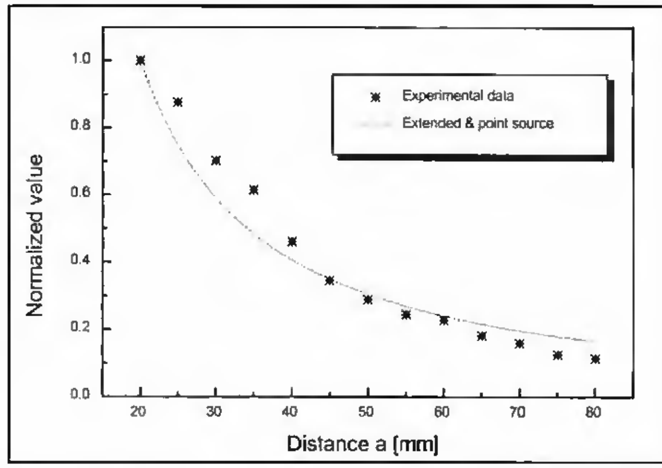

Fig. 8 — *Intensity of gas tungsten arc reflected from stainless steel with varying distance* a (θ_i = 50 deg, 0_r = 50 deg, ϕ_r = 0 deg).

shape because the arc shape affects the geometry in short distances between the point of consideration on the base metal and the welding arc. Thus, the shape of the arc is assumed to be half-spherical similar to the real arc.

Total irradiance on dA_s produced by the arc was obtained by integrating the effective area of the arc.

$$E_i = I_\lambda(\lambda)\int_{Arc}\frac{\cos\varphi_i\cos\theta_i}{r^2}dA_a \qquad (8)$$

where $I_\lambda(\lambda)$ means the spectral radiant intensity of the arc $(W/(sr\,\mathring{A}))$, which is assumed to be constant in this research because of a concern in formulation to define the influence and the geometrical relationship of the arc to the position of the vision sensor. Discussion continues about the problem of the optical thinness and thickness in the arc radiation, but this study dealt with the relative amount of radiation from the arc to the CCD camera, resulting from the complicated geometrical and reflective mechanism of the arc plasma.

Extended Light Source Model of the Arc

The effective area of arc is assumed to be a half-hemisphere, so Equation 8 can be expressed as follows:

$$E_i = I_\lambda(\lambda)\int_{-\pi/2}^{\pi/2}\int_{0}^{\pi/2}\frac{\cos\varphi_i\cos\theta_i}{r^2}dA_a \qquad (9)$$

The area dA_a is normal to the (τ, δ) direction, namely, vector u_3. It may be represented as $dA_a = a^2 \sin\tau d\tau d\delta$ for a spherical surface. Parameters r^2, $\cos\theta_i$, and $\cos\varphi_i$ vary according to points on the arc. Therefore, r^2 can be expressed as the two variables τ and δ. The distance between the arc and base metal is a and the radius of the welding arc is R.

$$r^2 = R^2 + a^2 - 2aR\sin\tau\cos\delta \qquad (10)$$

The polar angle of the incident beam can be determined by using surface normal vector n and direction vector u_1 from the following:

$$\cos\theta_i = \frac{n \bullet \vec{u}_1}{|n|\cdot|\vec{u}_1|} \qquad (11)$$

where η is the slope of the base metal at the corrugation; symbol • represents the inner product of vectors; and direction vector $\vec{u}_1$ lies on the line from the infinitesimal area dA_s on the base metal to an arbitrary point on the arc.

φ_i is the angle between the normal vector u_3 of the infinitesimal area of arc and its incident line. Therefore, $\cos\varphi_i$ can be obtained in the same manner as Equation 11:

$$\cos\varphi_i = \frac{\vec{u}_2 \bullet \vec{u}_3}{|\vec{u}_2|\cdot|\vec{u}_3|} \qquad (12)$$

If the coordinate frame of the base metal {B} is sloped as η, the azimuthal angle of the infinitesimal area of the arc about the coordinate frame of the sloped base metal is as follows:

$$\tan\phi_i = \frac{y}{(x-R)c\eta + zs\eta} \qquad (13)$$

The radiance of the reflected arc from the base metal $L_r(\lambda)$ can be modeled by assuming the arc as an extended source as follows:

$$L_r(\lambda) = I_\lambda(\lambda)\int_{-\pi/2}^{\pi/2}\int_{0}^{\pi/2} f_r(\theta_i,\phi_i;\theta_r,\phi_r)\frac{\cos\varphi_i\cos\theta_i}{r^2}a^2\sin\tau d\tau d\delta \qquad (14)$$

Point Light Source Model of Arc

If the arc is assumed to be a point light source, the general equation above can be simplified. The angle between the surface normal vector and the tangential plane of effective area are constant. If the effective lighting area of the arc concerns only the radiation, effective area can be expressed as follows:

$$dA_{eff} = \cos\varphi_i dA_a \qquad (15)$$

If the effective area on the arc is negligibly smaller than the square of the distance between the arc and concerned area dA_s on the base metal, namely $A_{eff} / a^2 << 1$, $\cos\theta_i/r^2$ can be assumed to be constant in the period of integration. Irradiance E_i can be modeled by assuming the arc as a point light source as follows:

$$E_i = A_{eff} I_\lambda(\lambda)\frac{\cos\theta_{io}}{a^2} \qquad (16)$$

The radiance of the reflected arc from the base metal $L_r(\lambda)$ can be modeled by assuming the arc as a point source as follows:

$$L_r(\lambda) = f_r(\theta_i,\phi_i;\theta_r,\phi_r) A_{eff} I(\lambda)\frac{\cos\theta_{io}}{a^2} \qquad (17)$$

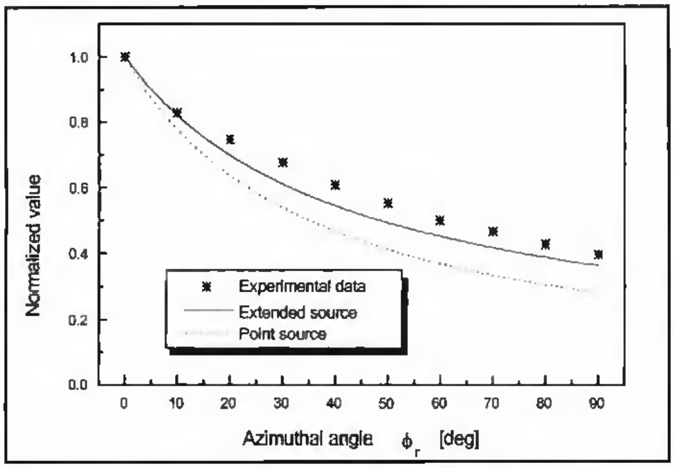

Fig. 9 — Intensity of gas tungsten arc reflected from mild steel with varying azimuthal angle ϕ_r (a = 30 mm, θ_i = 55 deg, θ_r = 45 deg).

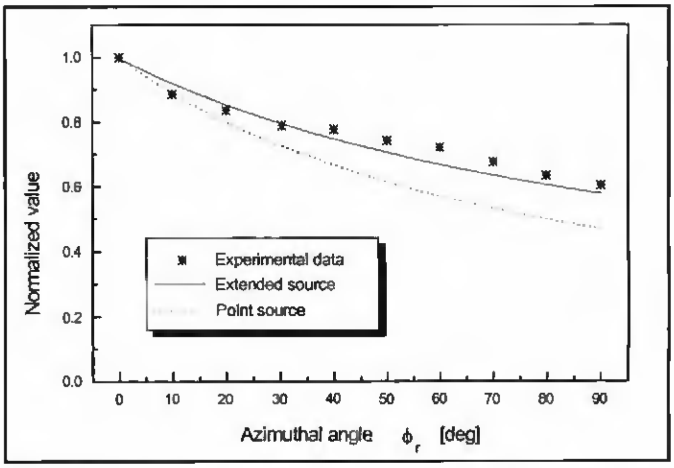

Fig. 10 — Intensity of gas tungsten arc reflected from Zn-coated container panel with varying azimuthal angle ϕ_r (a = 30 mm, θ_i = 55 deg, θ_r = 45 deg).

Image Forming Model

Arc light reflected from the base metal surface is filtered through the interference filter, condensed through the lens, and finally captured by the CCD camera to produce an image. The relationship between the spectral radiance $L_r(\lambda)$ caused by the reflection on a surface point and the corresponding irradiance E on the image plane is modeled by considering the pass band of the interference filter. Light power is concentrated in the image (if losses in the lens are ignored). Since no light from other areas reaches this image patch, the irradiance of the patch on the image plane corresponding to the patch on the object surface can be expressed as follows:

$$E = L\frac{\pi}{4}\left(\frac{d}{f}\right)^2 \cos^4 \varsigma \tag{18}$$

The above equation reveals that E is in a direct proportion to the radiance of the arc light through the lens. This is the fundamental relationship used to recover information about objects from their images. The factor of proportionality in the formula above contains the inverse square of the effective f-number of the CCD camera, f/d. It also includes a term that falls off with the cosine to the fourth power of the angle made by the ray from the image point to the center of the lens with the optical axis. In this study, this falloff in sensitivity is not important when the image covers only a narrow angle, and the sensing area of the pixels of the vision sensor is very small compared to the distance between the lens and measuring point.

Generally, vision sensors used in automatic welding systems have attached optical interference filters in order to reduce the influence of arc light in welding. The arc light reflected from the surface is filtered through the interference filter. The irradiance of the image due to reflected arc light from the base metal can be represented as follows, when the optical interference filter is attached to the front of the lens:

$$E\left(\lambda_c\right) = \left[\frac{\pi}{4}\left(\frac{d}{f}\right)^2 \cos^4 \varsigma\right] \int_0^{\infty} L_r\left(\lambda\right) F_G\left(\lambda - \lambda_c\right) d\lambda \tag{19}$$

where λ_c is the center wavelength of the optical interference filter. The value $F_G(\lambda)$ is the spectral response of the optical interference filter, and can be expressed in the Gaussian distribution. The image sensor converts irradiance E into gray level G_I, which is expressed as follows.

$$G_I = pE^{\gamma} \tag{20}$$

where the p is the proportional constant and γ is the characteristic that is normally 1 for measurements, resulting in a proportional relationship between G_I and E.

Simulation and Experiment

Experiments for BRDF Parameters

In order to determine the BRDF from the reflectance model of arc light for applicable materials used in height-varying weldments, the three BRDF parameters κ_{diff}, κ_{spec}, and c^2 must be obtained through experiments. A diode laser with a wavelength λ of 690 nm, which has been widely used in active vision sensors, was employed to determine these constants, because it can be easily suited to satisfy conditions of the reflectance model of the arc light passing through the optical interference filter of the vision sensor. The diode laser supplied the parallel light and the image it projects on the specimen is seen as a point, and the image is captured by a CCD camera with a γ characteristic value of 0.45 in order to expend the dynamic response range of a CCD camera about the high spectral intensity of the light source. A bandpass filter having the same wavelength as the laser and the FWHM of 10 nm was placed in front of the CCD camera to consider the actual configuration of the practical vision sensor used in automatic welding.

The specimens were prepared from hot-rolled mild steel, Zn-coated container panel, and 304 stainless steel, and their surface roughness was measured by atomic force measurement (AFM). The ratios R_q/λ of mild steel and Zn-coated container panel were larger than 1.5; therefore, the surface of these specimens had both diffuse and specular characteristics, which could be applied to Lambert and Torrance's BRDF model. However, the ratio R_q/λ of SUS304 stainless steel was less than 1; therefore, obtaining the BRDF parameter for this specimen was not possible.

The angle of reflection was varied in a wide range, while the angle of incidence was fixed at values between 10 deg and 80 deg. These gray level values obtained directly from the CCD camera were then normalized with regard to maximum gray level. As expected from the Torrance-Sparrow model, these results showed

Table 1 — Results of Nonlinear Regression for Mild Steel Plate and Zn-Coated Container Panel Using Gauss-Newton Method

Parameters	K_{diff}	K_{spec}	C^2	K_{spec}/K_{diff}
Mild steel plate	0.021	0.326	112	15.52
Zn-coated container panel	0.495	0.153	8.331	0.309

characteristics of a diffuse lobe, a specular lobe, and a specular spike. The characteristics of a specular lobe and a specular spike were especially dominant in the mild steel specimen, the other side, the characteristic of a diffuse lobe was mainly an effect of surface reflectance in the container panel specimen. These normalized data were used in the nonlinear regression with the Newton-Gaussian method to obtain three BRDF parameters of Equations 5 and 7. The resultant κ_{diff}, κ_{spec}, and c^2 values are shown in Table 1.

Experiments for Arc Noise Models

A photograph of the experimental apparatus is shown in Fig. 5, showing components such as the gas tungsten arc welding torch, water-cooled copper anode, CCD camera and optical band pass filter. The center wavelength of the optical band-pass filter is 690 nm with a bandwidth of 10 nm in front of CCD camera. In order to avoid the direct influence of arc light to CCD camera without reflectance of specimen, during the experiment the isolator was installed between the arc plasma and the CCD camera except the pass of arc light from arc plasma to specimen. And the concerned area in FOV (field of view) of CCD camera is 4 mm^2 (2 x 2 mm) at the center of the specimen. This experimental apparatus had devices with goniometers that could change the slope of the specimen, the azimuthal angle, the reflected angle, and the distance between the arc and reflected area. The experiments were performed with gas tungsten arc welding (GTAW) at 100 A; tungsten tip-to-workpiece distance was 5 mm. In order to generate a constant and stable arc, a water-cooled copper anode, which could not be melted during welding, was used in the experiments. The magnitude of the gray level of reflected arc light from each specimen was obtained by averaging 20 values measured every 0.2 s. To investigate the validity of the assumptions of considering the arc light as an extended light source and a point light source, the reflected arc light was first measured for various a values at fixed angles of incidence and reflection, then for various azimuthal angles of reflection and reflected angles under the fixed relatively short a. In two cases, the fixed distance a between the arc and reflection area was determined to be 30 mm, because too large a values would greatly decrease the assumption of an extended light source, which would be proved by the experiments by varying the distance a for the incident and reflected fixed angles.

Results and Discussion

Figures 6, 7, and 8 show the gray level of the arc in GTAW reflected from a hot-rolled mild steel plate, Zn-coated container panel, and SUS304 stainless steel with respect to the distance between the arc and reflection area. The experimental data were determined by normalizing the gray levels of the CCD camera with regard to the value at minimum R after compensating them with the gamma characteristic γ of the CCD camera. That is, *(measured gray level)*$^{1/\gamma}$ was divided by *(maximum gray level)*$^{1/\gamma}$ to take into account the spectral response of the CCD camera because its gamma characteristic γ was set as 0.45 in the experiments in order to expand its dynamic response range. The experimental results show a theoretical relationship in which normalized gray level is inversely proportional to the square of the distance. The theoretical results obtained by assuming the arc as a point source are in agreement with the experimental results in relative long distances, but not proper for relative short distances. On the other hand, the theoretical results that were obtained by assuming the arc as an extended source agree well with the experimental results in a wide range of distances between the arc and reflected area. The geometrical effect of arc shape plays a large role in the variation of intensity of the reflected arc light. The extended source, including the geometrical effect of the light source, should be considered in the examination of the arc light in relatively short distances. But the intensity variation of the reflected arc in long distances differed somewhat with the results of the extended source model on specular surfaces, such as mild steel, because the CCD camera has a limited dynamic response range. In Fig. 8, two theoretical results from each assumption show the same tendency because the surface reflectance model of SUS304 stainless steel is represented as a mirror.

From these experimental and theoretical results, it can be concluded that the welding arc can be assumed as a point light source for establishing the reflectance model of arc noise, especially with long distances between the arc and reflection surface. In actual welding with the vision sensor, however, the welding arc should be assumed to be an extended light source

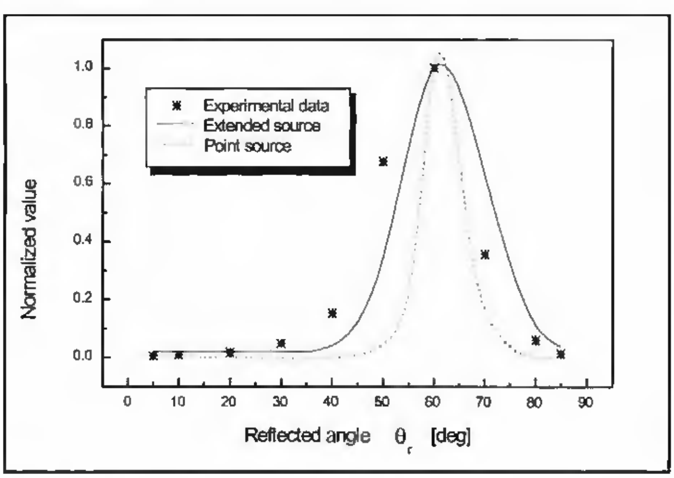

Fig. 11 — Intensity of gas tungsten arc reflected from mild steel with varying polar angle θ_r (a = 30 mm, θ_i = 60 deg, ϕ_r = 0 deg).

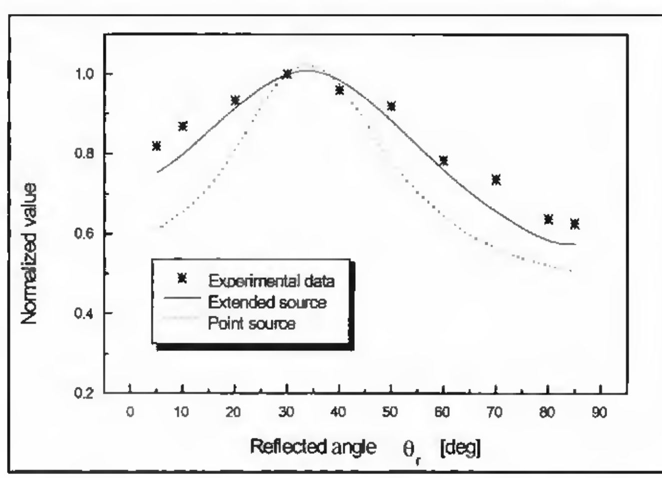

Fig. 12 — Intensity of gas tungsten arc reflected from Zn-coated container panel with varying polar angle θ_r (a = 30 mm, θ_i = 30 deg, ϕ_r = 0 deg).

because the arc is generally located a short distance from the viewing area of the vision sensor.

Figures 9 and 10 show the results of the experiment and the simulation for the arc in GTAW reflected from the hot-rolled mild steel surface and the Zn-coated container panel. The experiments were conducted for various azimuthal angles ϕ_r of reflection, while θ_i, θ_r, and a were fixed at 55 deg, 45 deg, and 30 mm, respectively. The specular characteristic was considerably higher around the same polar angle of reflection than around the incident polar angle; therefore, the experiments were carried out when each polar angle was different. This facilitated comparison of intensities corresponding to various azimuthal angles. By comparing the normalized data of the measured gray level with the simulated values, it was revealed that the extended source model with Torrance-Sparrow surface reflectance could adequately predict the reflectance behavior of the welding arc. The image pixel area was larger than the infinitesimal area of the theoretical model, which resulted in some difference between simulation and experiment. Thus, these results can be used effectively for designing visual joint tracking sensors for the arc welding process. Also, the influence of arc light in the vision sensor, which is at slightly tilting angle, can be decreased.

Figures 11 and 12 show the results of experiment and simulation for a GTAW arc reflected from a hot-rolled mild steel surface and a Zn-coated container panel. The experiments were carried out for various polar angles θ_r of reflection in the incident plane, while a was fixed at 30 mm. Peak values of the simulation results shifted somewhat more at the reflected angle than at the same angle of the incident beam; these results were caused by the characteristics of the geometrical attenuation factor in the surface reflectance model. But the peak gray levels of the reflected arc occurred around the polar angle of incident light, which could cause substantial noise in the image data. This effect appeared clearly with the reflection from mild steel, because its surface reflectance model largely represented the characteristics of the specular lobe and spike compared to the Zn-coated container panel. These phenomena were caused by their surface reflectance characteristics.

Conclusions

It was demonstrated that arc light should be assumed as an extended light source in the reflectance model for relatively short distances between the welding arc and base metal because the geometrical relationship of the arc shape has largely affected the reflected area in a relative short distance between the welding arc and the reflected area of the base metal.

In order to avoid the influence of the reflected arc light from the base metal, vision sensors must be designed using a little tilting angle and should be positioned as far out of the incident plane as possible. The proposed models and experimental results can be used effectively to design the configuration and moving path of vision sensors according to the base metal shape; they can thus reduce the effect of arc noise on vision sensors and consequently improve their reliability in automatic joint tracking in the arc welding process.

Acknowledgment

This work has been performed under the nuclear research and development program sponsored by the Ministry of Science and Technology, Korea.

References

1. Yu, J. Y., and Na, S. J. 1997. A study on vision sensors for automatic welding of height-varying weldment — Part 1: Mathematical model. *Mechatronics* 7(7): 599–612.

2. Yu, J. Y., and Na, S. J. 1998. A study on vision sensors for automatic welding of height-varying weldment — Part II: Application. *Mechatronics* 8(1): 21–36.

3. Yu, J. Y., Na, S. J., Kang, G. H., and Han, Y. S. 1995. Development of an automatic welding system for corrugated membranes of the LNG tank. *Proceedings of the International Conference on the Joining of Materials* (JOM-7), Helsinki, Denmark, pp. 519–525.

4. Shaw, C. B., Jr. 1975. Diagnostic studies of the GTAW arc: Part 1 — Observational studies. *Welding Journal* 54(2): 33-s to 44-s.

5. Shaw, C. B., Jr. 1975. Diagnostic studies of the GTAW arc: Part 2 — Mathematical model. *Welding Journal* 54(2): 81-s to 84-s.

6. Kim, E. W., Allemand, C., and Eagar, T. W. 1987. Visible light emissions during GTAW and its application to weld image improvement. *Welding Journal* 66(12): 369-s to 377-s.

7. Sliney, D. H., Moss, C. E., Miller, C. G., and Stephens, J. B. 1982. Transparent welding curtains. *Welding Journal* 61(3): 17-s to 24-s.

8. Yuuki, M., and Tejima, A. 1988. Development of visual welding sensors and feedback control of molten pool. *IHI Engineering Review* 21(3): 94–98.

9. Brzakovic, D., and Khani, D. T. 1991. Weld pool edge detection for automated control of welding. *IEEE Trans. on Robotics and Automation* 7(3): 397–403.

10. Voelkel, D. D., and Mazumder, J. 1990. A visualization of a laser melt pool. *Applied Optics* 29(12): 1718–1720.

11. Gorgon, S. S., Flanigan, L. A., and Dyer, G. E. 1987. Development of a CCTV system for welder training and monitoring of space shuttle main engine welds. *Welding Journal* 66(3): 47-s to 54-s.

12. Yen, L., Lin, W., and Dinghua, C. 1986. A study on direct vision sensor for welding visual sensing. *Proceedings of the 6th International Conference on Robot Vision and Sensory Controls*, Paris, France, pp. 245–248.

13. Cullison, A., and Irving, B. 1992. Where in the world is the weld? *Welding Journal* 71(8): 45–49.

14. Yoo, W. S., Yu, J. Y., and Na, S. J. 1999. Application of vision sensor for welding automation. *2nd Joint Korea-Australia Workshop on Manufacturing Technology on Steel Processing*, Postech, Pohang, Korea, pp. 42–46.

15. Yu, J. Y., Na, S. J, Kang, G. H., and Han, Y. S. 1996. A study on development of automatic welding system for corrugated membranes of the LNG tank. *Journal of KWS* 14(1): 62–69.

16. Lenef, L., and Gardner, C. S. 1985. Optical emissions from weld arcs and their effects on the performance of welding robot vision systems. *Applied Optics* 24(16): 2587–2595.

17. Nakata, S., Jie, H., Tsuruha, Y., Noguchi, N., and Kobashiri, T. 1989. Determination on geometrical arrangement of optical equipment and photographic parameters for construction of visual sensing system. *Quarterly Journal of the Japan Welding Society* 17(3): 358–362.

18. Lambert, J. H. 1760. *Photometria, sive de mensura et gratibus luminis, colorum et umbrae*, Augsburg, Germany, Eberhard Klett.

19. Torrance, K. E., and Sparrow, E. M. 1966. Off-specular peaks in the directional distribution of reflected thermal. *Journal of Heat Transfer-Trans. of ASME*(C) 88(2): 223–230.

20. Nayar, S. K., Ikeuchi, K., and Kanade, T. 1991. Surface reflection: physical and geometrical perspectives. *IEEE Trans. Pattern Analysis and Machine Intelligence* 13(7): 611–634.

21. Inoue, K. 1981. Image processing for on-line detection of welding process (Rep. 3) — improvement of image quality by incorporation of spectrum of arc. *Trans. of Japan Welding Research Institute* 10(1): 13–18.

22. Lee, C. W., and Na, S. J. 1996. A study on the influence of reflected arc light on vision sensors for welding automation. *Welding Journal* 75(12): 379-s to 387-s.

23. Wang, Q. L., and Li, P. J. 1997. Arc light sensing of droplet transfer and its analysis in pulsed GMAW process. *Welding Journal* 76(11): 458-s to 469-s.

24. Li, P. J., and Zhang, Y. M., 2000. Analysis of arc light mechanism and its application in sensing of GTAW process. *Welding Journal* 79(9): 252-s to 260-s.

25. Lee, S. Y., and Na, S. J., 1996. A numerical analysis of stationary TIG welding arc considering various electrode angles. *Welding Journal* 75(9): 269-s to 279-s.

26. Torrance, K. E., and Sparrow, E. M. 1967. Theory for off-specular reflection from roughened surface. *Journal of the Optical Society of America* 57(9): 1105–1114.

Improved Ferrite Number Prediction Model that Accounts for Cooling Rate Effects – Part 2: Model Results

Results of a prediction model based on a neural network system of analysis are described

BY J. M. VITEK, S. A. DAVID, AND C. R. HINMAN

ABSTRACT. A new Ferrite Number prediction model, ORFN (Oak Ridge Ferrite Number), was developed in Part 1 of this study (*Welding Journal*, January 2003) and, in this contribution, the model predictions are evaluated and compared with predictions of other models. The ORFN quantitatively takes account of cooling rate effects on the Ferrite Number for the first time. It is shown the new ORFN model presents very good agreement with experimental data and is significantly more accurate than existing constitution diagrams or recently developed composition-only neural network models. The model is equally valid for austenitic stainless steels and duplex stainless steels. Furthermore, the model is applicable to both conventional arc welding conditions as well as high cooling rate conditions prevalent during high energy beam welding, such as laser beam welding, and high-speed arc welding.

Introduction

Stainless steel welds typically contain a two-phase microstructure with anywhere from a few percent to more than 50% ferrite in an austenite matrix. Numerous models have been proposed over the years to predict ferrite content (or Ferrite Number[1]) in stainless steel welds (Refs. 2–12; see Ref. 6 for a review of earlier models). In all these models, the predicted ferrite content is based on the alloy composition alone. This applies for both traditional constitution diagrams as well as more recently developed models, including neural network models. However, it is well known cooling rate can have a significant effect on the Ferrite Number (FN), especially for laser beam welds, high-speed arc welds, and duplex stainless steel welds. In Part 1 of this paper, the basis for the cooling rate effect was reviewed and the need for a better predictive model outlined (Ref. 13). Also in Part 1, the details and procedures for developing an improved predictive model that includes cooling rate were described, including the generation of the dataset required for the new model development. In this portion of the two-part study, after a very brief overview of some of the features of the dataset generation and model development, the results of the model are presented. The predictability of the new Oak Ridge Ferrite Number (ORFN) model, which includes consideration of cooling rate, is evaluated and the model results are compared with existing composition-only models.

Model Development

The new ORFN model is based on a neural network analysis. This type of analysis is nonlinear in nature and thereby allows for identification of complex elemental interaction effects missed in more traditional models based on a regression analysis. It was shown in earlier neural network models based only on alloy composition that the predictions were significantly more accurate than those using other approaches (Refs. 10–12). The optimum neural network architecture for ORFN was identified by a procedure described in Refs. 10 and 13. Using this optimum architecture, several hundred networks were trained and the best of these was chosen as the final model, ORFN (Ref. 13). The best network consisted of 6 hidden nodes, along with the fixed 14 input nodes and the single output node. The network architecture is shown in Fig. 1. The two square nodes in the input and hidden layers in Fig. 1 represent the bias, which corresponds to a constant in the weighted sums over all nodes in a layer. In this figure, the line types and line thicknesses schematically represent the sign and magnitude of the weights between nodes, as described in the figure caption. The actual parameters for the model are given in the appendix.

Several hurdles had to be overcome when generating the database for training and testing the neural network model. First, many welds were made with a pulsed laser, and the small size of the welds prohibited the direct measurement of FN. Consequently, a conversion routine was needed to convert volume percent ferrite to FN so all the data were consistent. Second, a simple and consistent means for calculating the cooling rate, both for 2-D and 3-D heat flow conditions, was required. Third, in order to use the large dataset that was the basis of earlier composition-only models, cooling rates had to be "assigned" to all those data. Fourth, some consistent approach was needed to address data that were missing chemical analyses for some of the elements considered in the model. Finally, new data were generated to supplement the data in the

KEY WORDS

Ferrite Number
Neural Network
Duplex Stainless Steel
Austenitic Stainless Steel
Ferrite Content
Cooling Rate
Alloy Composition
Constitution Diagram

J. M. VITEK and S. A. DAVID are with Oak Ridge National Laboratory, Oak Ridge, Tenn. C. R. HINMAN, formerly an intern at Oak Ridge, is now at Syracuse University, Syracuse, N.Y.

Paper presented at the AWS Annual Meeting, March 4–7, 2002, Chicago, Ill.

1. Ferrite Number rather than volume-percent ferrite is the preferred measure of ferrite content (Ref. 1).

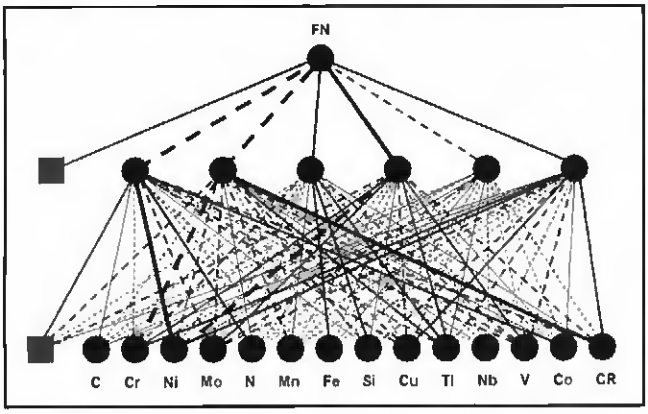

Fig. 1 — Final ORFN neural network model structure. The square nodes represent bias nodes corresponding to a constant input. Dashed lines represent negative weights between nodes while solid lines signify positive weights. Line thicknesses correspond to different ranges for the absolute values for the connecting weights: thin lines correspond to weights (absolute values) of 0 to <1.0; medium thickness lines represent weights from 1 to <4.0; thick lines correspond to weights ≥ 4.0.

literature and enhance the model with regard to its applicability to duplex stainless steels. All of these issues are described in detail in earlier publications and the reader is referred to those articles for further information (Refs. 10, 13). The final ORFN neural network model was developed on a dataset containing 1196 points. This complete dataset was comprised of three parts: the WRC dataset used to develop the WRC-1992 constitution diagram (Ref. 8) and FNN-1999 composition-only model (Refs. 10, 11); the "DVH" dataset that consists of data from an earlier investigation into cooling rate effects in stainless steel welds (Ref. 14); and the "NEW" dataset with data generated in this study (Ref. 13). The ranges of variables (composition, cooling rate) included in the complete training dataset are listed in Table 1.

Results

The predicted FN values for the entire dataset of 1196 points are plotted against the experimental values in Fig. 2A. For such a plot, the degree to which the predicted values agree with the experimental values is an indication of the accuracy with which the data are fitted in the model since the data were used to train the neural network.

Comparison of New ORFN Model with Other Models

The results from the new cooling-rate-inclusive neural network model (ORFN) can be compared with predictions of other models to see how well the models fit the experimental data. In Fig. 2B, the predicted FN using the FNN-1999 model are plotted against the experimental values, and a similar plot is presented in Fig. 2C for predictions using the WRC-1992 model. These plots include the data generated under higher cooling rate conditions and the superiority of the new model is unmistakable. Both the FNN-1999 and the WRC-1992 models (Fig. 2B and C) show significant errors. Although the new ORFN model was trained on the entire dataset, including the DVH and NEW datasets, and therefore some improvement in the overall fit is expected, the primary reason for the significantly better performance of the ORFN model is based on the fact the new model allows for a cooling rate contribution to the determination of the FN, while this is totally absent in the other two models. Thus, the

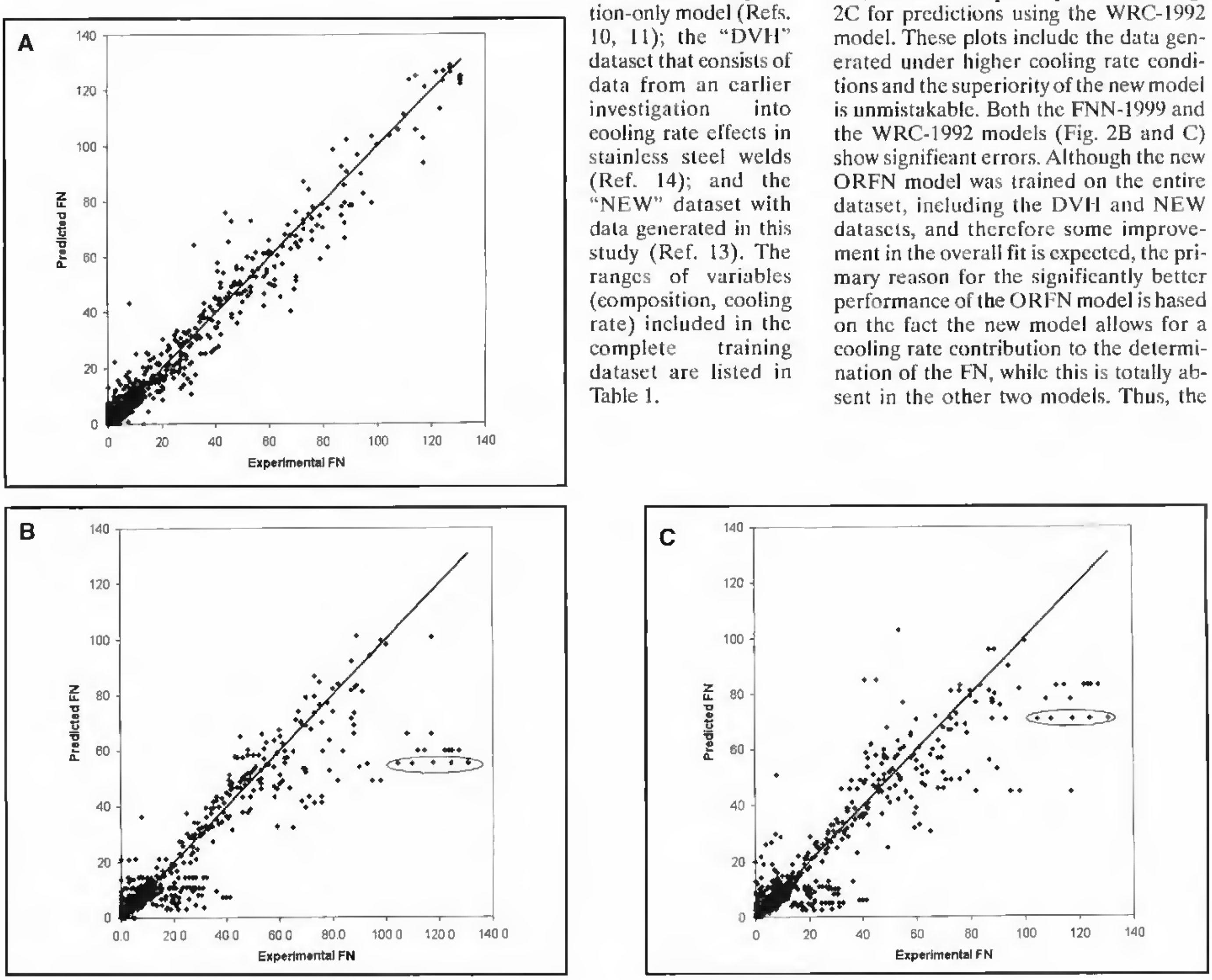

Fig. 2 — Plot of experimental vs. predicted FN using the entire training dataset (WRC + DVH + NEW) for three different models: A — ORFN; B — FNN-1999; and C — WRC-1992.

Table 1 — Composition and Cooling Rate Ranges in Dataset Used for Training ORFN

Input data		min.	max
Concentration (wt-%)	Fe	45.60	72.52
	Cr	14.74	32
	Ni	4.61	33.5
	C	0.008	0.2
	N	0.01	0.33
	Mo	0.01	6.85
	Mn	0.35	12.67
	Si	0.03	1.3
	Cu	0.0	3.04
	Ti	0.0	0.54
	Nb	0.0	0.88
	V	0.0	0.23
	Co	0.0	0.45
	Log Cooling Rate (°C/s)	1.00	6.54

Table 2 — Comparison of RMS Errors for Three FN Prediction Models (Smaller RMS Represents Better Fit to Data)

Model	RMS using entire dataset, with high cooling rate data (1196 points)	RMS using WRC dataset only (961 points)
ORFN	4.70	3.88
FNN-1999	11.00	3.52
WRC-1992	9.92	5.84

Table 3 — Compositions of Alloys Evaluated in Fig. 3 (wt-%)

Alloy	Fe	Cr	Ni	C	N	Mo	Mn	Si	Cu	Ti	Nb	V	Co
304B	70.258	18.29	8.7	0.066	0.018	0.15	1.31	0.74	0.15	0[a]	0.01	0.05	0.22
312B	59.09	29.72	8.78	0.11	0.01[a]	0.2	1.68	0.39	0[a]	0[a]	0[a]	0[a]	0[a]
316A	66.488	17.01	11.44	0.04	0.022	2.3	1.95	0.3	0.19	0[a]	0.01	0.04	0.17

(a) Value assigned in neural network analysis since chemical analysis was not available.

ORFN model can predict different FN values for the same alloy composition when the weld conditions are changed, whereas the other models predict only one FN for a given alloy regardless of the weld conditions and corresponding cooling rate. This effect of cooling rate is readily demonstrated. Consider, for example, the data within the circled regions in Fig. 2B and C. These data were generated for the same alloy composition and, consequently, the two earlier models predict the same FN for all conditions, even though the measurements show an unmistakable and substantial variation due to different weld conditions and cooling rates. In contrast, the new ORFN model takes the cooling rate into account and predicts different FNs for the same alloy when the cooling rates are different. As shown in Fig. 2A, the new neural network model fits the data quite well, covering a wide range of cooling rates (10 to > 3×10^6 °C/s) and FN (0 to 131) (Table 1). A quantitative comparison can be made with the use of the root mean square (RMS) error values[2], which are listed in Table 2 (discussion of the RMS values for the WRC-only dataset, also listed in Table 2, is in a later section). The errors for the ORFN model are considerably lower than those for either the FNN-1999 or the WRC-1992 models when the high cooling rate data are included; a drop in RMS of more than 50% is found. The somewhat lower RMS for the WRC-1992 model compared to FNN-1999 is meaningless because both RMS values are unacceptably high.

The differences in predictions using the three models (ORFN, FNN-1999, and WRC-1992) are examined in greater detail in Fig. 3. The figure shows the predicted FN versus cooling rate for three of the alloys used to generate the NEW dataset (Ref. 13): 304B (Fig. 3A), 316A (Fig. 3B), and 312B (Fig. 3C). The alloy compositions are listed in Table 3. These alloys were chosen because they were among the few alloys for which experimental data covering a large range in cooling rate were available. The experimental measurements are superimposed on the figures. The experimental data show a strong variation in FN with cooling rate, and only the new ORFN model has the ability to describe this behavior since the other models are independent of cooling rate. It can be seen the ORFN model fits the experimental data reasonably well. This is true for both the austenitic stainless steel alloys such as 304 and 316, where the FN increases and then decreases with cooling rate, and the duplex stainless steel alloy 312, where the FN increases monotonically with cooling rate until a maximum FN corresponding to 100% ferrite is reached. It is also worth noting all three models predict nearly the same FN at the lowest cooling rate, especially for Alloys 304 and 316. This is an indication all three models do a reasonable job fitting the data for low cooling rate conditions.

A fair amount of scatter is evident in the experimental data plotted in Fig. 3 and in data for other alloys as well. There are two primary sources for this scatter: the cooling rate calculations are of limited accuracy, and the experimental measurements may be in error. In most cases, the different cooling rates correspond to systematic changes in welding speed or laser power. Therefore, the absolute cooling rates may not be accurate but the sequence of the data points in terms of increasing cooling rate is likely to be correct. Nevertheless, some irregularities may exist when cooling conditions changed from a 2-D condition at high heat input to a 3-D condition at low heat input. The larger instances of scatter and erratic data behavior are more likely due to inaccuracy of the FN measurements themselves. For high cooling rate welds, the measurements were made by metallographic identification of volume-percent ferrite and potential sources of error in this technique are well documented. Furthermore, the conversion from volume-percent ferrite to FN has some uncertainty as well. Given that the data are somewhat stochastic in nature, the predicted curves seem to show a reasonably smooth variation that duplicates the overall alloy behavior. The plots in Fig. 3 indicate the new ORFN model will properly predict overall trends, but some degree of uncertainty must be accepted with the predictions.

True Predictability Assessment

The preceding plots comparing predicted FN with experimental results are an indication of how well the models fit the data on which they were trained. However,

2. $RMS = \sqrt{(\Sigma(Experimental\ FN - Predicted\ FN)^2)/1196}$

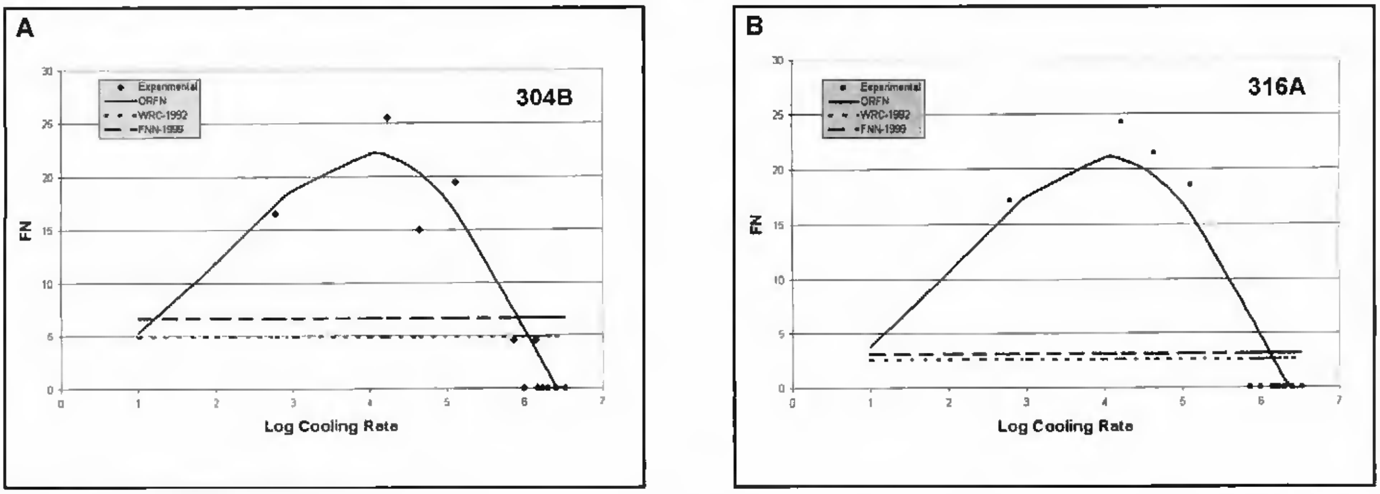

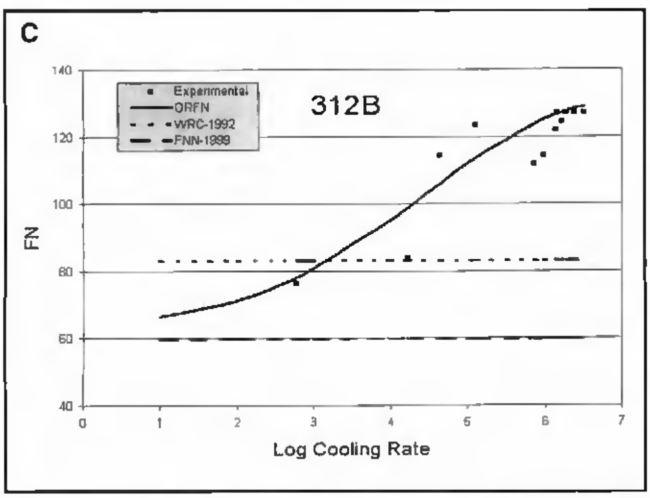

Fig. 3 — Plots showing predicted FN vs. cooling rate for three specific alloys (Table 3). Experimental data points are superimposed. Predictions for three models (ORFN, FNN-1999, WRC-1992) are shown as solid lines. A — Alloy 304B (austenitic stainless steel); B — Alloy 316A (austenitic stainless steel);, and C — Alloy 312B (duplex stainless steel).

there is a need to assess the true predictability of the ORFN model. This was done as follows. Nine separate tests were conducted in which a single data point was removed from the entire training dataset and new neural networks were calculated. In each case, many networks were calculated using the same single-point-depleted datasets in order to arrive at a "best" network. As was the case for the models trained on all the data, the use of different starting weights and data sequences produced slightly different final networks and the best among these was chosen (Ref. 13). These networks were then used to predict the FN for the data point that was purposely left out. In this way, the calculated FN values are true predictions.

Before examining the results of this predictability test, some discussion of the data points that were purposely removed is appropriate. Nine different cases were examined. In many cases, the data represented values where a maximum FN is expected or where a reversal in the FN variation with cooling rate takes place (see Fig. 1, Ref. 13). Thus, the omitted data points represented critical points in the FN vs. cooling rate behavior. In other cases, the removed data point was one where the experimental value showed considerable scatter or was inconsistent with data at lower and higher cooling rates. Only in case #9 was a data point removed where data existed at cooling rates below and above the removed point and where the data were very consistent.

The prediction results are shown in Table 4, where the predicted values for the nine tests are compared with the experimental FN as well as the predictions from the three best neural networks that were trained on the entire dataset (including the data that were omitted in the prediction runs). A few points are worth noting from the listing in Table 4. First, the true "predicted" FNs are very close to the values derived from the other networks, where the data points were included in the training. Thus, the predictability of the networks is comparable to the ability of the networks to fit the data. This same conclusion was reached for the composition-only FNN-1999 model (Refs. 10, 11) and is confirmed by the comparable RMS errors determined for the group of nine predictions. It is interesting that the RMS errors in Table 4 are noticeably higher than the errors over the entire dataset (compare Tables 2 and 4). This is due to the fact the RMS errors are calculated over a small set of data and that many of the data points used in this series of predictability tests were "critical" data points, or inconsistent data points, as noted above. Therefore, the nine test cases are especially severe tests for evaluating prediction accuracy, and larger RMS values can be expected.

As an example, the predicted FN is plotted along with the experimental data in Fig. 4 for Alloy 309A (Ref. 13), which was the alloy used in test cases #6 and #8. It can be seen the predicted values are quite consistent with the experimental data. In fact, for case #6, not only does the predicted curve fit the overall experimental data very well, it appears the prediction at a log cooling rate of 4.65 (corresponding to the omitted data point, open triangle) is more consistent with the other data than the actual experimental data point. Furthermore, both predicted curves show the same trend, indicating the predicted behavior is consistent and does not vary significantly with the inclusion or exclusion of a specific data point. Thus, in spite of the relatively large differences between the measured (14.3, 7.8) and predicted (25.7, 18.4) values for cases #6 and #8, respectively, the trends identified by the neural network appear to be correct. Data scatter also was significant for cases #4 and #5, where the predictions and experimental results are not in good agreement and the discrepancy may be more of a reflection of the scatter in the experimental data rather than the inaccuracy of the neural network prediction. It is noteworthy that in all nine cases shown in Table 4, when the network predictions are quite close to the experimental values (tests 1, 2, 9), they are close for all the network models, and when the network predictions show larger errors (tests 3–8), they show larger errors for all four networks. Thus, the inclusion of the data for training did not result in improved models. This observation implies that when significant prediction errors are found, the cause may be unreliable experimental data more than inaccurate predictions.

Discussion

It was shown in the earlier, composition-only neural network model (FNN-1999) that a significant improvement in FN prediction accuracy could be achieved with the neural network compared to the traditional constitution diagram model (WRC-1992). It is important when expanding the predictive model to include cooling rate and, in particular, high cooling rates, the prediction accuracy for low cooling rate conditions corresponding to conventional arc welding is not sacrificed. To confirm the predictive accuracy for low cooling rates is not compromised in the ORFN model, two comparisons can be made. First, the new, cooling-rate-inclusive ORFN model can be compared to the earlier FNN-1999 and WRC-1992 models when considering only the WRC dataset (which has no high cooling rate data). Plots of predicted versus experimentally measured FN are shown in Fig. 5. It can be seen the accuracy of the ORFN model is comparable to the FNN-1999 model for this limited dataset and is considerably better than the WRC-1992 model. The comparison is quantified in Table 2. A very small increase in RMS error is found for the ORFN model compared to FNN-1999, while the improvement over the WRC-1992 model is still large (≈ 34%). In this comparison, the ability of the three models to fit the data is assessed and it must be remembered that the FNN-1999 and WRC-1992 models were trained on this dataset alone, whereas the ORFN model was trained on a 25% larger dataset covering many different alloys and cooling rates.

A second, more severe test of the models can be made by comparing predicted vs. experimental FN values for a totally independent dataset. Such a dataset was compiled by Ornig (Ref. 15) and was used in other studies as a test dataset (Refs. 11, 16). It is referred to as the supplemental dataset and is described in greater detail in Ref. 11. It consists of 265 points produced under conventional (low cooling rate) conditions by arc welding. It also has a more restricted range of compositions than the entire training dataset, as noted in Ref. 11. Plots of predicted versus measured FN are shown in Fig. 6 for all three models, and corresponding RMS values are listed in Table 5. In this case, the ORFN model shows a smaller RMS than the other two models and the better fit is apparent in Fig. 6. Based on these comparisons, it can be concluded the predictive accuracy for low cooling rate conditions is not sacrificed in the new ORFN model, which is designed to cover a broader range of conditions.

The variation in predicted FN as a function of cooling rate shown in Fig. 3 is exactly what is expected from a theoretical viewpoint and shown schematically in Part 1 (Fig. 1, Ref. 13). The new model predicts an initial increase in FN for austenitic stainless steels with increasing cooling rate, and this corresponds to the inhibition of the solid-state ferrite-to-austenite transformation. At the highest cooling rates, the predicted FN decreases with cooling rate, in accord with the transition to a primary austenitic solidification mode. In contrast, the model predicts a monotonic increase in FN with cooling rate for duplex stainless steels, corresponding to the suppression of any transformation of ferrite upon cooling. In these steels, the primary solidification of austenite is not possible and so a reversal in behavior is not expected and the model does not predict it.

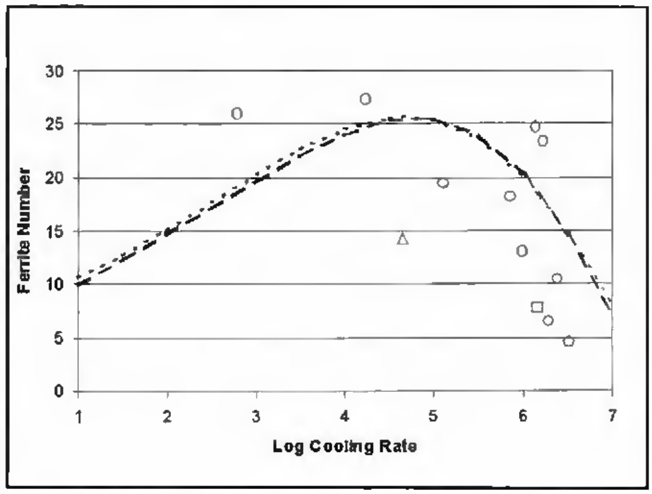

Fig. 4 — FN vs. cooling rate for Alloy 309A showing scatter in the data and the ability of the predictions to follow trends in spite of apparent large discrepancies between experiment and prediction. Data points represent experimental data. The triangle represents the experimental value for prediction case #6 and the square represents the value for prediction case #8. The short-dash line is the predicted FN vs. cooling rate for case #6 and the long-dash line is the predicted behavior for case #8.

With the inclusion of data for several duplex stainless steel alloys in the NEW dataset, the applicability of the ORFN ferrite prediction model to duplex stainless steels is more reliable and accurate. This is a significant extension of the earlier FNN-1999 neural network model, even for low cooling rate conditions. Furthermore, the inclusion of cooling rate effects is especially important when considering duplex stainless steels since their microstructures are very sensitive to cooling

Table 4 — Comparison of FN Values and RMS Errors for Prediction Tests (Network Trained on All but One Data Point) and Three Best Networks (Networks Trained on All Data Points)

Test Number	Experimental FN	Predicted FN	FN from Best Network (ORFN)	FN from 2nd Best Network	FN from 3rd Best Network
1	70	66.8	67.6	66.4	67.9
2	59	58.1	55.5	54.6	55.9
3	90	74	78.4	71.5	70.9
4	38.4	22.5	25.8	25.5	24.6
5	31.1	6.4	10.7	10.7	9.3
6	14.3	25.7	25.5	23.7	25.9
7	28.2	21	17.8	16	17.5
8	7.8	18.4	18.8	18.6	20.5
9	124.2	123.8	123.4	125.3	124.2
RMS error		12.6	11.0	12.1	12.7

Table 5 — Comparison of RMS Errors on the Supplemental Dataset for Three FN Prediction Models (Smaller RMS Represents Better Fit to Data)

Model	RMS using supplemental dataset, with no variation in cooling rate (265 points)
ORFN	1.84
FNN-1999	2.24
WRC-1992	2.59

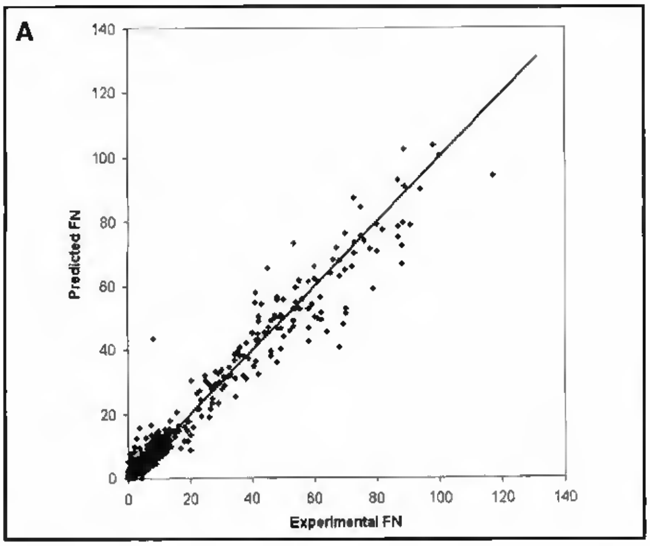

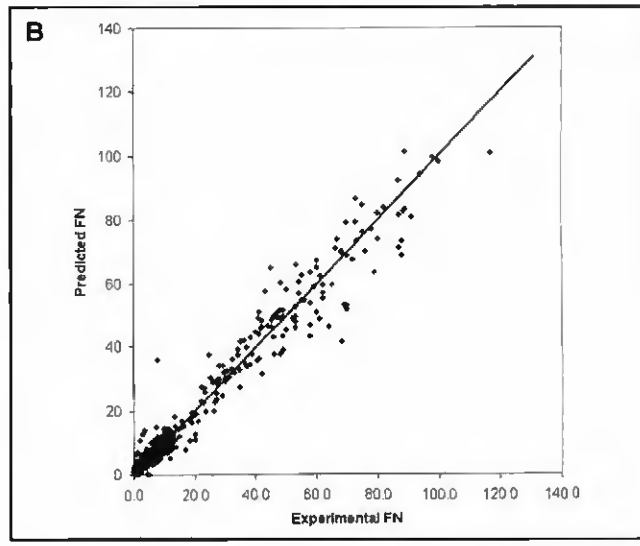

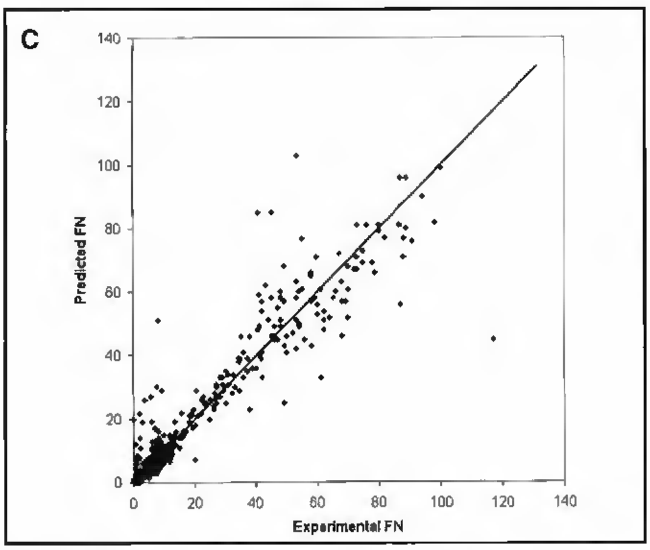

Fig. 5 — Plot of experimental vs. predicted FN for the WRC dataset (no high cooling rate data) for three different models: A — ORFN, B — FNN-1999, and C — WRC-1992.

rates. Although these steels do not exhibit any change in solidification mode when welded under high cooling rate conditions, the austenite formation during cooling after solidification can be readily suppressed. Thus, even at modest cooling rates, they may contain widely different levels of austenite, and, consequently, their properties at room temperature may vary considerably. Such effects are taken into account by the ORFN model.

The ORFN model can also be used to predict the propensity of an alloy to change solidification mode. The critical cooling rate for a given alloy can be easily calculated. In addition, the effect of changes in composition on the tendency to change solidification mode can be readily determined. Similarly, the model can determine how sensitive the ferrite content in duplex stainless steels will be to changes in composition. This ability to take both cooling rate and composition into account in predicting ferrite content has been totally absent until now.

The inclusion of cooling rate effects when predicting ferrite content is a major advance in predictive modeling. Experimental studies have shown such a sensitivity to cooling rate effects, but they have been ignored up to now in predictive models. Thus, the ORFN model is a much more robust tool for welding and weld microstructure prediction. Limited example calculations and information on obtaining the model can be found at our Web site: *engm01.ms.ornl.gov*. All of the parameters needed to calculate the predicted FN are given in the appendix. The recommended composition range for the model is the same as the composition range for the training data set given in Table 1.

There are, however, several areas in which improvements to the model can be made. The cooling rate calculations can be improved so that variations in material properties are taken into account. In addition, the extension to other welding processes, such as continuous wave laser welding, CO_2 laser welding, or electron beam welding, must be investigated. The critical issue is that the calculated cooling rates must be consistent across all processes and process conditions so that the relative cooling rates between two weld conditions are properly determined. This could be accomplished, for example, for continuous wave (CW) laser welding as follows. Conditions in CW welding could be varied and the conditions that yield comparable microstructures to those found in pulsed Nd:YAG welds could be identified. Then, the absorptivity factor for CW welding could be optimized so that comparable cooling rates are calculated for comparable microstructures. With such a procedure, the necessary parameters for calculating consistent cooling rates for processes not used in training ORFN could be identified and the applicability of the model could be extended.

There are other factors that may affect the final ferrite content in a weld. For example, minor alloying additions may alter the fluid flow conditions within the weld, resulting in a significant change in weld pool shape and corresponding weld cooling rate. It is unlikely any model can accurately take all such factors into account. Therefore, under the best of conditions, a predictive model must be considered as an estimator with limited accuracy.

Recent advances in heat and fluid flow modeling, solidification modeling, and kinetics modeling suggest that in the future one may be able to model the entire transformation behavior directly. Up to now, however, such models are of limited accuracy. For example, kinetic modeling of the solidification and ferrite-to-austenite transformation during cooling consistently overpredict the final ferrite content (Refs. 17–19). Improvements in such models are to be expected in the future. Thus, it is possible theoretical models will be able to predict behavior more accurately without resorting to empirical methods. However, such modeling re-

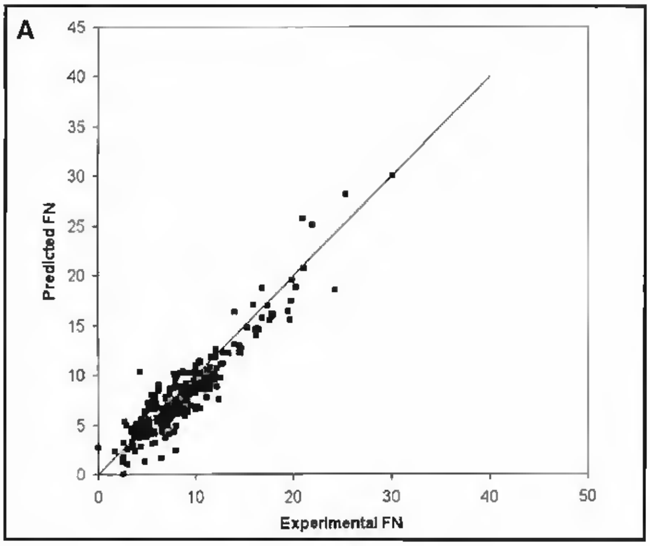

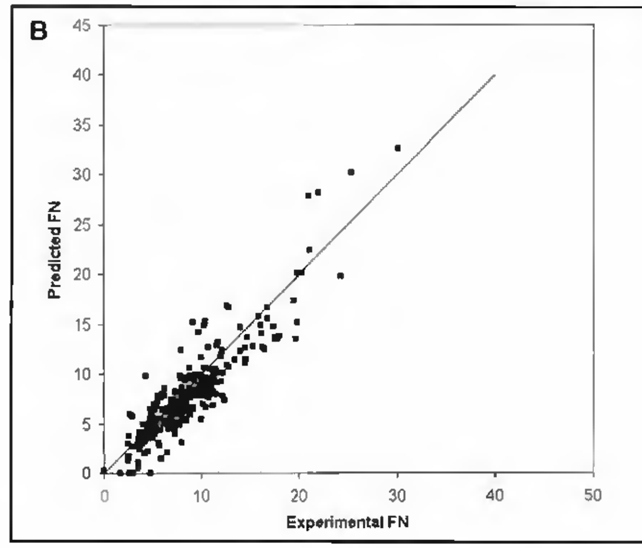

quires intensive computation, especially if it is extended to cover a wide range of compositions and is combined with computationally intensive heat and fluid flow models. When all of these models are developed to the point where they are accurate and reliable, they may be ideal for use in generating data for training a more user-friendly and computationally less demanding neural network model. Such artificial data would also eliminate the uncertainty and error in experimental data due to FN measurement, chemical analysis, etc. Under such conditions, gaps in the training database due to limited experimental data or difficult experimental conditions can be eliminated and the resultant model should be significantly more accurate.

Summary and Conclusions

A neural network model has been developed for predicting Ferrite Number (FN) in stainless steels welds as a function of cooling rate and composition. This new model, called ORFN (Oak Ridge Ferrite Number), allows, for the first time, the prediction of FN as a function of composition and weld process conditions (weld speed, welding power, material thickness) for both conventional arc welding and more rapid cooling rate processes such as laser beam welding. The significant effects of cooling rate on final ferrite content have been well documented and this new model takes these effects into account. It is shown that the extension of the neural network analysis to include cooling rate has not sacrificed the accuracy of the earlier, composition-only model for low cooling rate conditions. The new ORFN model takes account of changes in ferrite content due to suppression of the solid-state ferrite-to-austenite transformation, as well as changes in the primary solidification mode that are found in austenitic stainless steels at high cooling rates. The accuracy of the model was tested by various means and the results showed the present ORFN model is far superior to any other predictive model. In the development of the model, several assumptions and simplifications had to be made. These are described and possible avenues for further research and improvements to the model have been identified.

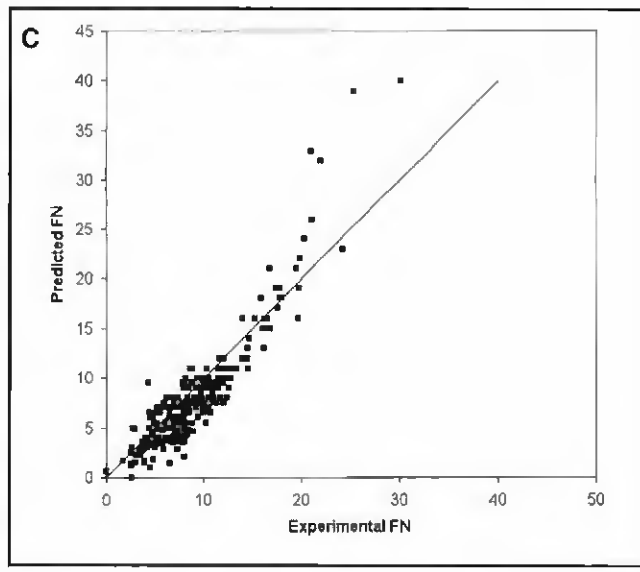

Fig. 6 — Plot of experimental vs. predicted FN using the supplemental dataset (that was not used in the training of any of the models) for three different models: A — ORFN; B — FNN-1999, and C — WRC-1992.

Acknowledgments

The authors would like to thank Y. Iskander for help with the neural network development in the early stages of this program. R. Reed, Oak Ridge National Laboratory, is thanked for preparing many of the welds in this study. The authors would like to thank the following people for providing materials for generating new data: D. Kotecki, The Lincoln Electric Co., Cleveland, Ohio; F. Lake, ESAB Welding and Cutting Products, Hanover, Pa.; S. Jana, Hobart Brothers, Troy, Ohio; and R. Gower, Carpenter Technology Corp., Reading, Pa. The authors would like to acknowledge the ERULF program of the U.S. Department of Energy, administered by Oak Ridge Associated Universities, Oak Ridge, Tenn., for providing the means for one of the authors (C.R.H.) to participate in this research. This research was sponsored by the Division of Materials Sciences and Engineering, U.S. Department of Energy, and the Office of Science, Laboratory Technology Research Program, U.S. Department of Energy, under contract DE-AC05-00OR22725 with UT-Battelle, LLC.

References

1. Kotecki, D. J. 1997. Ferrite determination in stainless steel welds – advances since 1974. *Welding Journal* 76(1): 24-s to 37-s.

2. Schaeffler, A. 1949. Constitution diagram for stainless steel weld metal. *Metal Progress* 56: 680–680B.

3. Hull, F. C. 1973. Delta ferrite and martensite formation in stainless steels. *Welding Journal* 52(5): 193-s to 203-s.

4. DeLong, W. T. 1974. Ferrite in austenitic stainless steel weld metal. *Welding Journal* 53: 273-s to 286-s.

5. Kakhovskii, N. I., Lipodaev, V. N., and Fadeeva, G. V. 1985. The arc welding of stable austenitic corrosion-resisting steels and alloys. *Avt. Svarka* 5: 55–57.

6. Olson, D. L. 1985. Prediction of austenitic weld metal microstructure and properties. *Welding Journal* 64(10): 281-s to 295-s.

7. Siewert, T. A., McCowan, C. N., and Olson, D. L. 1988. Ferrite Number prediction to 100 FN in stainless steel weld metal. *Welding Journal* 67(12): 289-s to 298-s.

8. Kotecki, D. J., and Siewert, T. A. 1992. WRC-1992 constitution diagram for stainless steel weld metals: a modification of the WRC-1988 diagram. *Welding Journal* 71: 171-s to 178-s.

9. Babu, S. S., Vitek, J. M., Iskander, Y. S., and David, S. A. 1997. New model for prediction of ferrite number of stainless steel welds. *Science and Technology of Welding and Joining* 2(6): 279–285.

10. Vitek, J. M., Iskander, Y. S., and Oblow, E. M. 2000. Improved ferrite number prediction in stainless steel arc welds using artificial neural networks — Part 1: neural network development. *Welding Journal* 79(2): 33-s to 40-s.

11. Vitek, J. M., Iskander, Y. S., and Oblow, E. M. 2000. Improved ferrite number prediction in stainless steel arc welds using artificial neural networks — Part 2: neural network results. *Welding Journal* 79(2): 41-s to 50-s.

12. Vasudevan, M., Murugananth, M., and Bhaduri, A. K. 2002. Application of Bayesian neural network for modelling and prediction of ferrite number in austenitic stainless steel welds. 6, ed. H. Cerjak, *Mathematical Modelling of Weld Phenomena*. London, U.K.:Institute of Materials, pp. 1079–1099.

13. Vitek, J. M., David, S. A., and Hinman, C. R. 2003. Improved ferrite number prediction model that accounts for cooling rate effects — Part 1: model development. *Welding Journal* 82: 10-s to 17-s.

14. David, S. A., Vitek, J. M., and Hebble, T. L. 1987. Effect of rapid solidification on stainless steel weld metal microstructures and its implications on the Schaeffler diagram. *Welding Journal* 66: 289-s to 300-s.

15. Ornig, H. 1988. *Proceedings International Institute of Welding 41st Annual Assembly and International Conference*. Vienna, Austria.

16. Kotecki, D. J. 1988. Verification of the NBS-CSM ferrite diagram. *International Institute of Welding Document* II-C-834-88.

17. Lee, H. M., Bae, J. S., Soh, J. R., Kim, S. K., and Lee, Y. D. 1998. Diffusional solidification behavior in 304 stainless steel. *Mater. Trans.* JIM 39(6): 633–639.

18. Hillert, M. and Höglund, L. 1999. Simulation of the peritectic reaction in 304 stainless steel. *Mater. Trans.* JIM 40(6): 567–570.

19. Vitek, J. M. 2000. Unpublished research. Oak Ridge National Laboratory, Oak Ridge, Tenn.

Appendix

Parameters for the ORFN model

In a neural network, a weighted sum of the input values is transferred to the hidden layer via a transfer function, and, in a similar manner, a weighted sum of the hidden node values is transferred to the final, output layer. In addition, the inputs and outputs are normalized with a simple linear function. Thus, the entire model can be described by the weights, normalization parameters, and the transfer function. The weights and normalization parameters are given in Tables A1, A2, and A3. The specific equations that apply, as well as the transfer functions that were used, are described in detail in Ref. 10. The equations and parameters used to calculate cooling rate are given in Part 1 (Ref. 13).

Table A1 — Normalization Parameters for Input and Output Quantities for ORFN

Data		Node	Normalization Parameters min.	max
Concentration (wt-%)	C	Input #1	0.008	0.2
	Cr	Input #2	14.74	32
	Ni	Input #3	4.61	33.5
	Mo	Input #4	0.01	6.85
	N	Input #5	0.01	0.33
	Mn	Input #6	0.35	12.67
	Fe	Input #7	45.599	72.51
	Si	Input #8	0.03	1.3
	Cu	Input #9	0.0	12.16(a)
	Ti	Input #10	0.0	2.16(a)
	Nb	Input #11	0.0	3.52(a)
	V	Input #12	0.0	0.92(a)
	Co	Input #13	0.0	1.28(a)
Log Cooling Rate (°C/s)		Input #14	1.00	6.54
Ferrite Number		Output	0	130.8

(a) "Artificial" maximum used in manner described in Ref. 10.

Table A2 — ORFN Neural Network Weight Parameters from Input Layer to Hidden Layer

Input Node #, Variable	Hidden Layer Node Number 1	2	3	4	5	6
1, C	+0.3208	–0.1134	–0.5135	–0.3222	+0.0663	+0.1241
2, Cr	–0.4786	–4.0781	–1.9866	+2.6729	–0.5038	+1.7295
3, Ni	+6.6912	–1.8838	–0.244	–6.1962	+0.1143	+2.7736
4, Mo	–1.792	–1.7971	–0.9168	+1.6175	–2.8306	–2.3327
5, N	+1.234	+0.0401	–0.095	–0.4997	–0.6155	–0.4854
6, Mn	–0.1341	–1.0444	+0.8119	–0.8526	–0.4334	–0.8806
7, Fe	–0.7731	–0.2389	+1.2479	–0.1887	+0.3862	–0.9014
8, Si	+0.1879	–1.112	+1.5089	+0.2254	–0.6211	–2.1438
9, Cu	–1.8901	–1.8028	–0.9316	–2.028	–0.8074	+2.0734
10, Ti	–1.827	+3.2775	+0.9634	+3.4904	+0.1944	–1.0833
11, Nb	–0.3184	+0.8096	–0.0322	–0.2077	–0.793	+0.0176
12, V	–2.0183	–1.3638	–1.1225	+3.2879	–0.2907	–3.3708
13, Co	+1.3447	+0.1086	–0.29	+0.4406	–0.1279	+0.4791
14, Log $\dot{T}$	–3.0779	+4.4439	+0.19	–1.0471	–0.5851	+1.2418
Bias	+2.5039	–2.0016	–0.3467	–1.9938	–0.1546	+0.9367

Table A3 — ORFN Neural Network Weight Parameters from Hidden Layer to Output Layer

Bias	Hidden Layer Node Numbver 1	2	3	4	5	6
+1.1759	–4.4588	–5.5929	+2.1049	+4.9924	–2.2004	+2.1616

PowerCut™ 1500
PowerCut™ 1250
PowerCut™ 875
Durability
VALUE
PLASMARC™
ESAB
Think of Us First for Plasma Cutting
From the innovators of plasma arc cutting comes PowerCut™, a new line of plasma cutting packages combining superior cutting performance with a new durable, weatherproof casing designed to handle the toughest work environments.
Portable, easy to use, and incorporating ESAB's exceptional plasma cutting technology, PowerCut™ provides outstanding value in a "go anywhere" machine.
ESAB
ESAB
Circle No. 23 on Reader Info-Card
ESAB®
Your Partner in Welding & Cutting
For powerful plasma cutting capabilities, and to find your local distributor, visit www.esabna.com